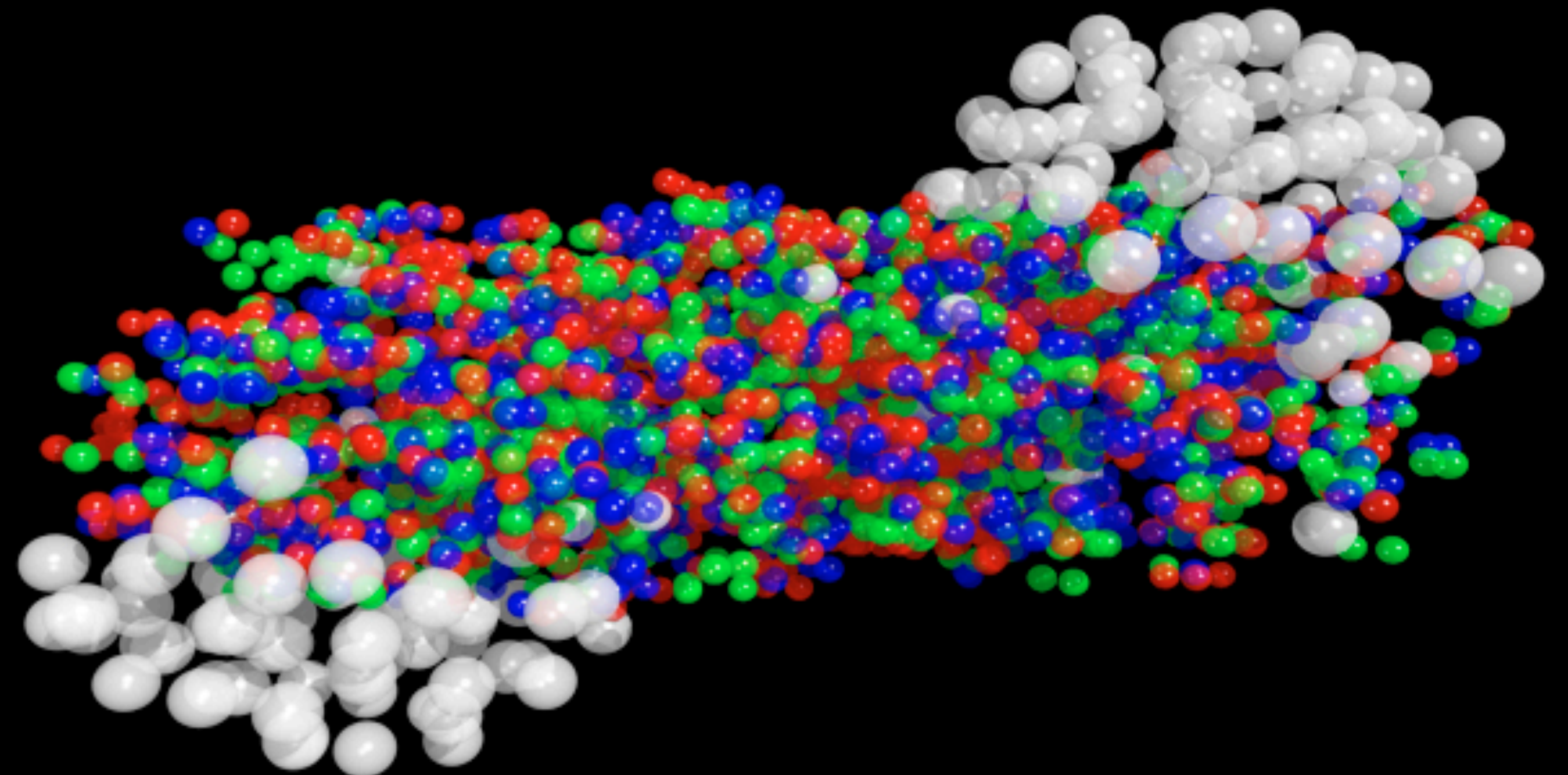




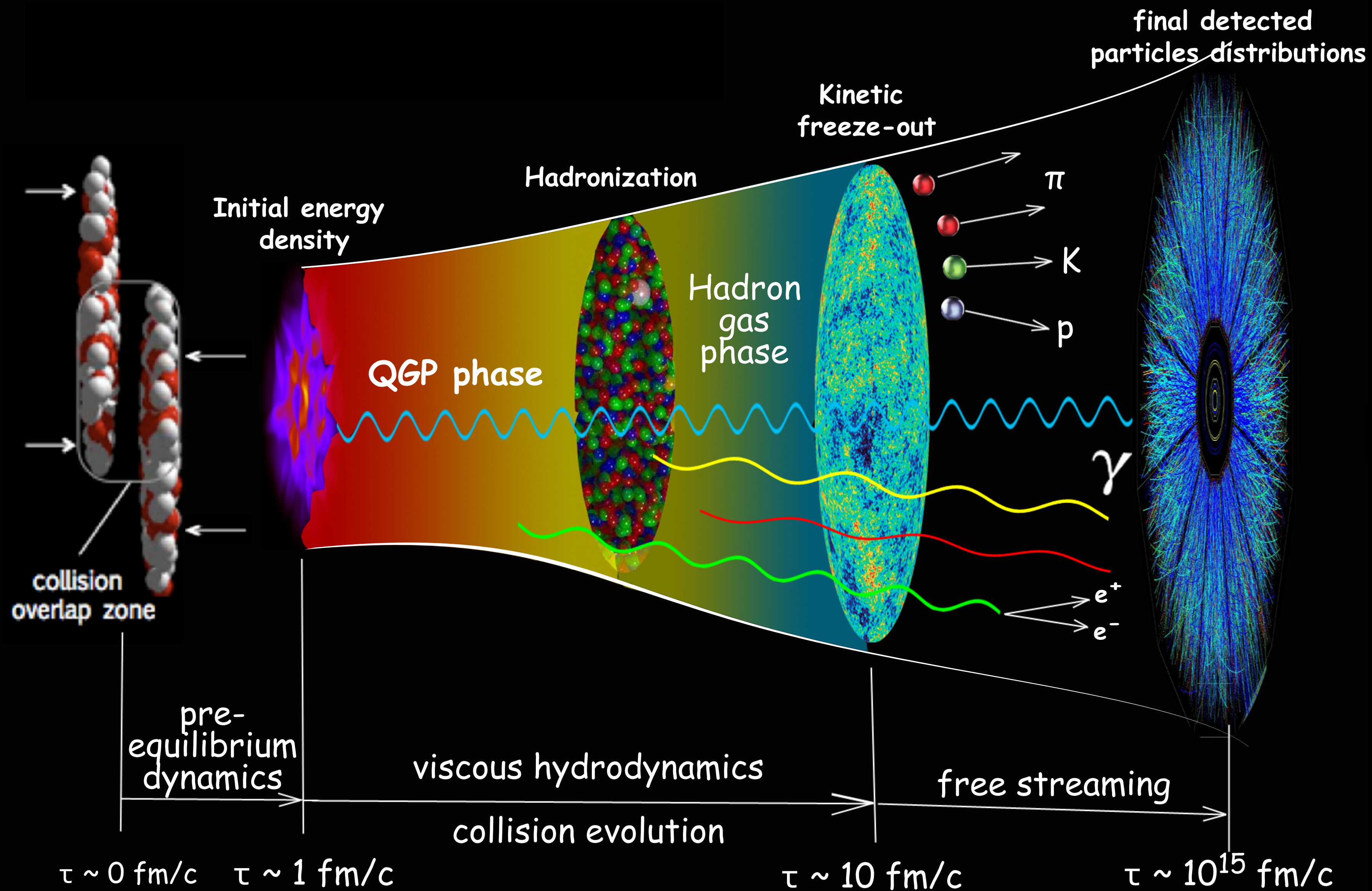
DYNAMICAL MODELING OF RELATIVISTIC HEAVY-ION COLLISIONS AT BEAM ENERGY SCAN ENERGIES

CHUN SHEN

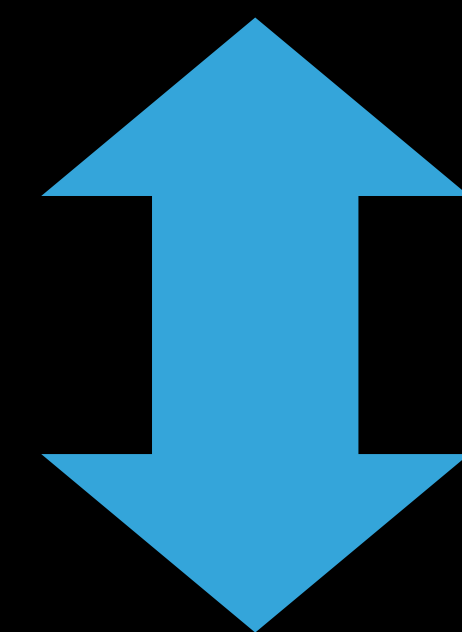
The 4th RHIC-BES Theory and
Experiment Online Seminar
Aug. 25, 2020



RELATIVISTIC HEAVY-ION COLLISIONS



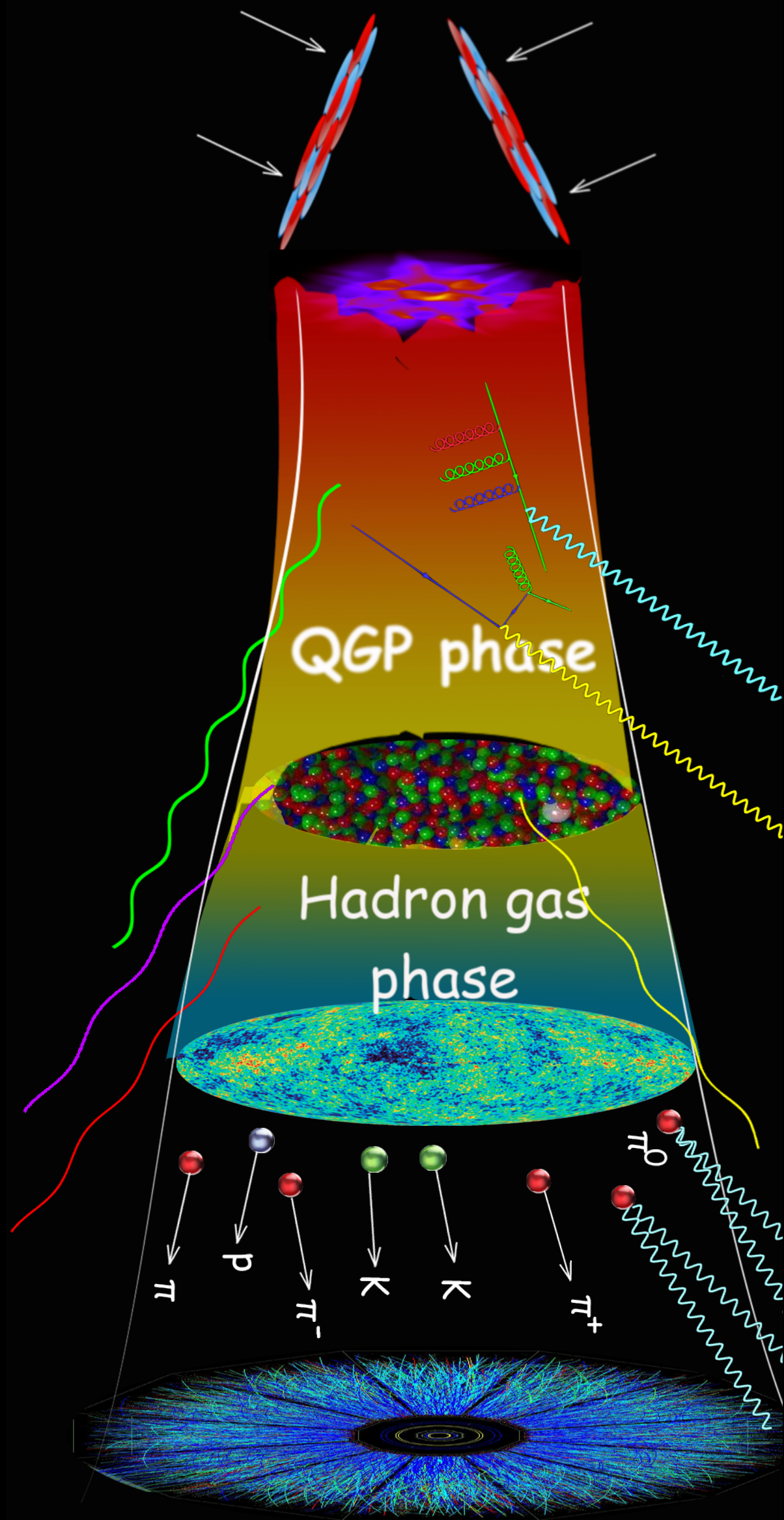
Complex dynamics driven by multiple length scales



Hybrid multi-stage modeling with event-by-event fluctuations

DEFINING THE QUARK-GLUON PLASMA

Which **properties of hot QCD matter** can we determine from relativistic heavy ion data (LHC, RHIC, and future FAIR/NICA/JPAC)?



Equation of State

$$e(T, \{\mu_q\}), P(T, \{\mu_q\}), c_s^2(T, \{\mu_q\})$$

Critical point & 1st order PT

Initial Fluctuation spectrum & baryon stopping $T^{\mu\nu}(\tau, \mathbf{r}), J^\mu(\tau, \mathbf{r})$

Shear and bulk viscosities $(\eta/s)(T, \{\mu_q\}), (\zeta/s)(T, \{\mu_q\})$

Charge diffusion D_B, D_Q, D_S

Electromagnetic emissivity

Spectra, collective flow, femtoscopy, light-nuclei production, net-proton fluctuations

Net particle distributions

Anisotropic flow v_n

Flow correlations

Balance functions

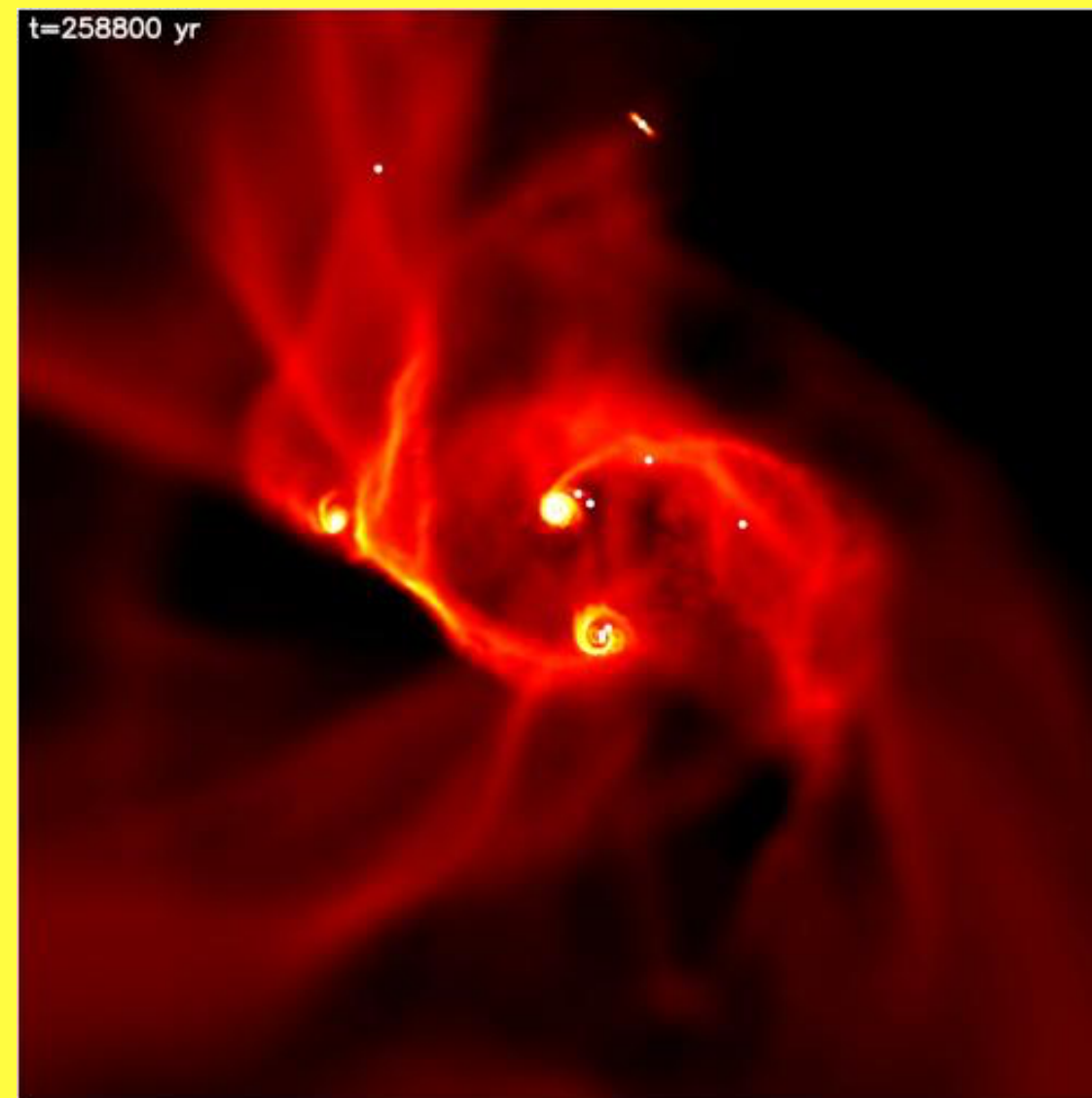
Photons and dileptons

COLLECTIVITY & HYDRODYNAMICS

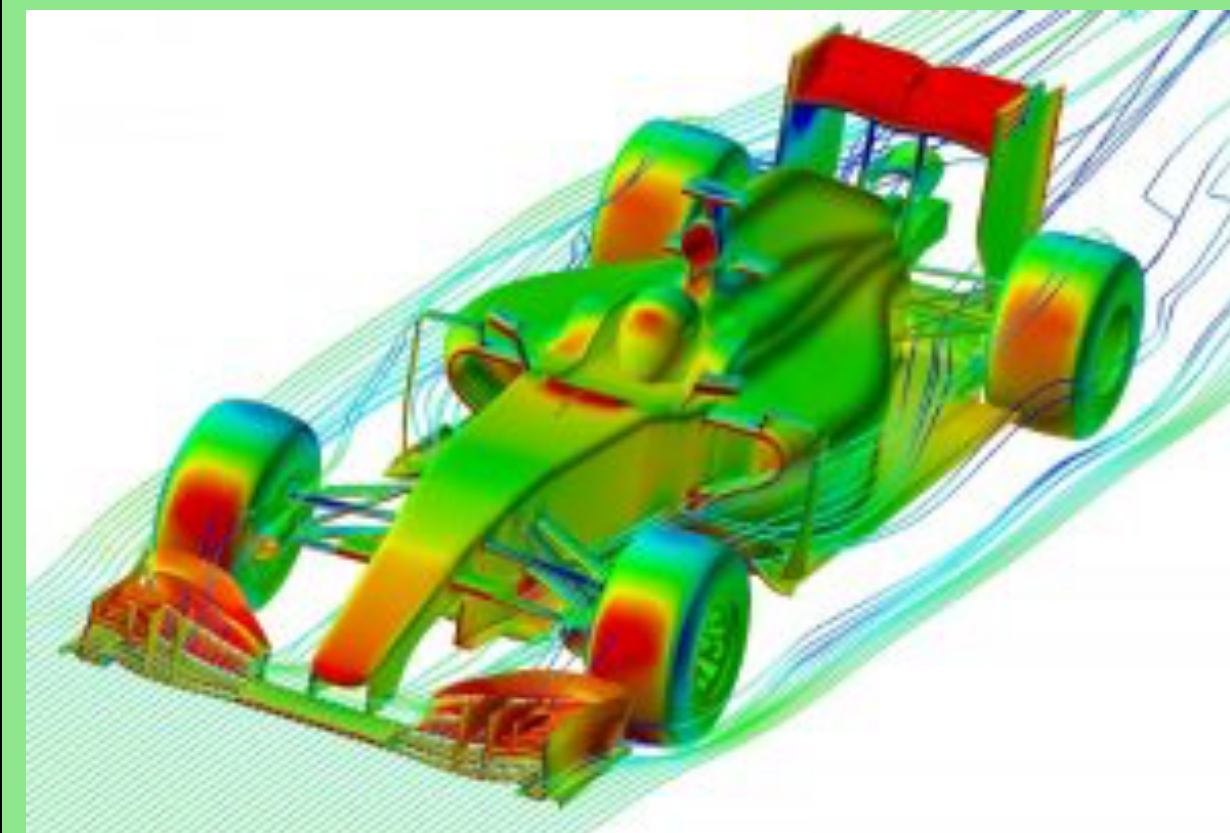
A long wavelength effective description of interacting systems

Conservation
laws
+
Equation of
State

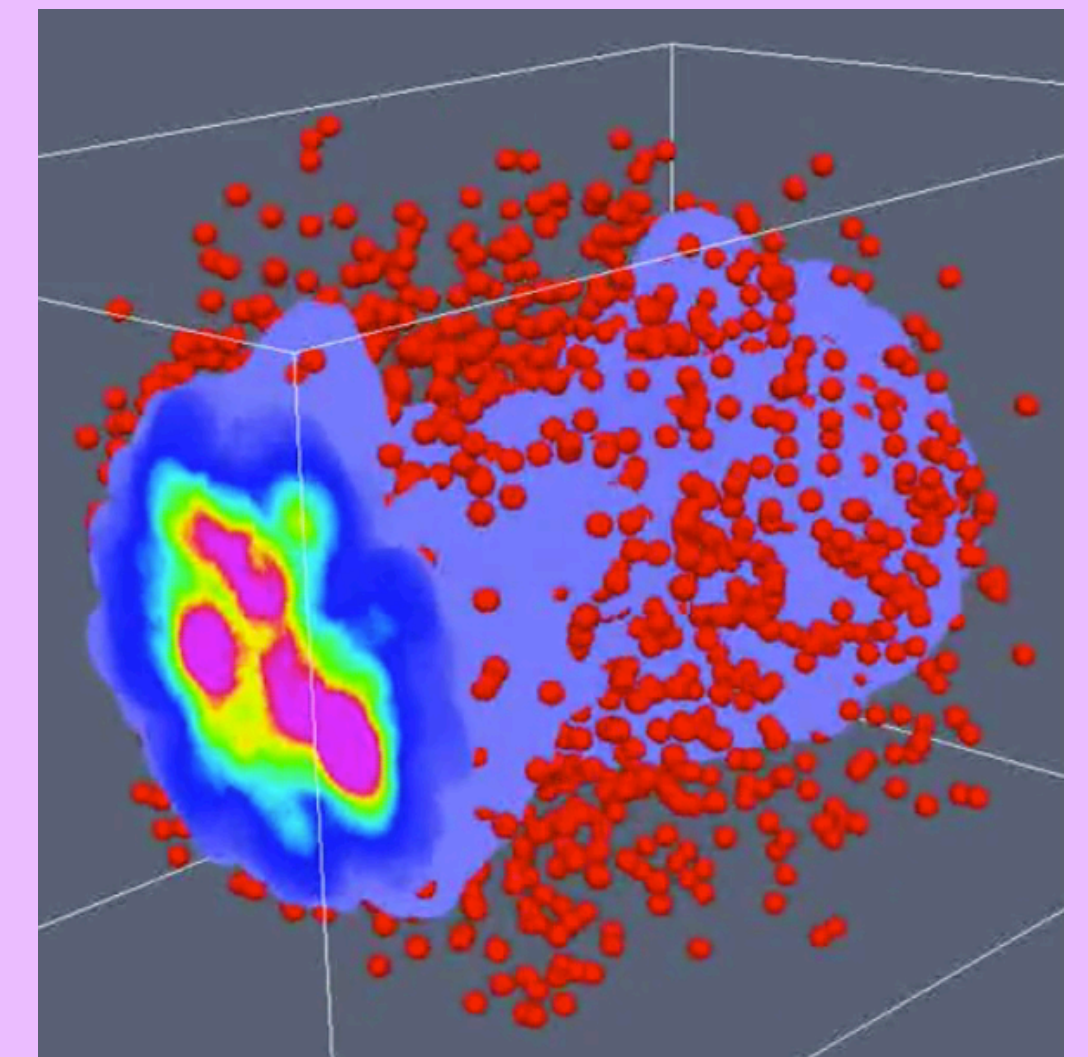
Star formation



Air dynamics of
race car



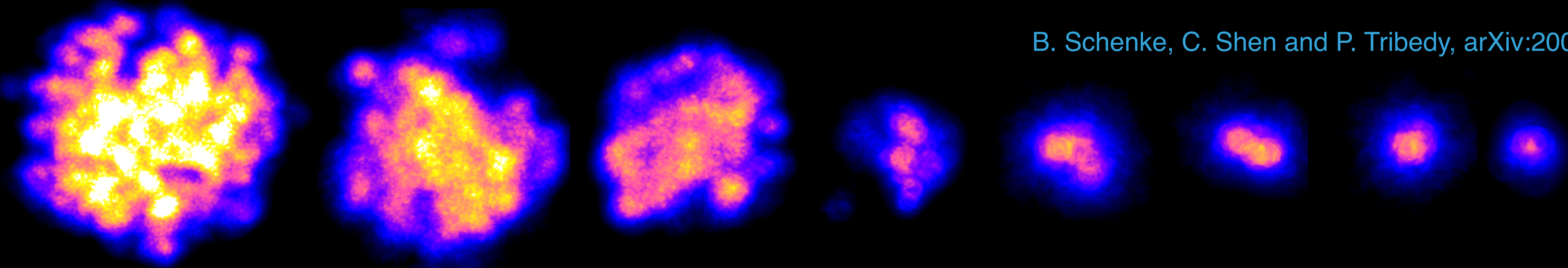
Quark-Gluon
Plasma



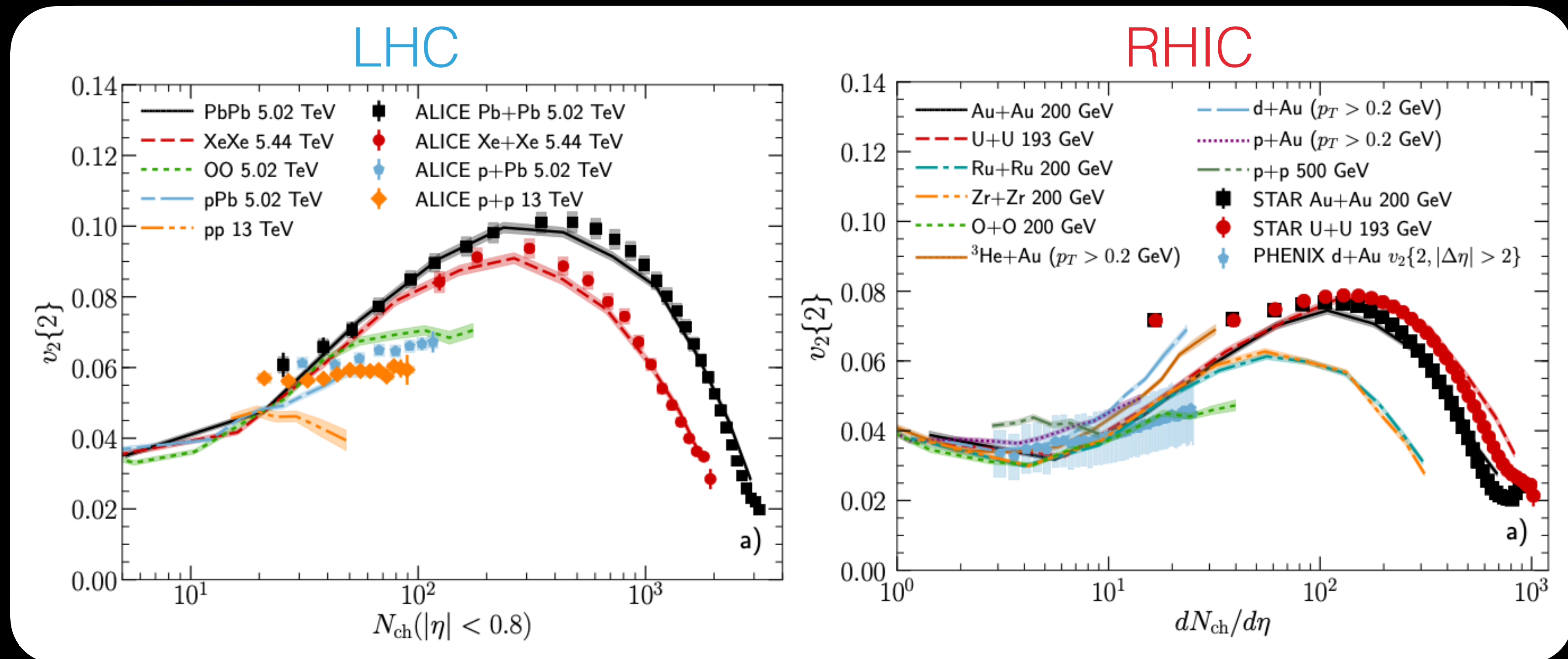
Studying collective phenomena in heavy-ion collisions has been **leading** the theory frontier of developing causal viscous relativistic hydrodynamics

RUNNING THE GAMUT OF HIGH ENERGY NUCLEAR COLLISIONS

B. Schenke, C. Shen and P. Tribedy, arXiv:2005.14682 [nucl-th]



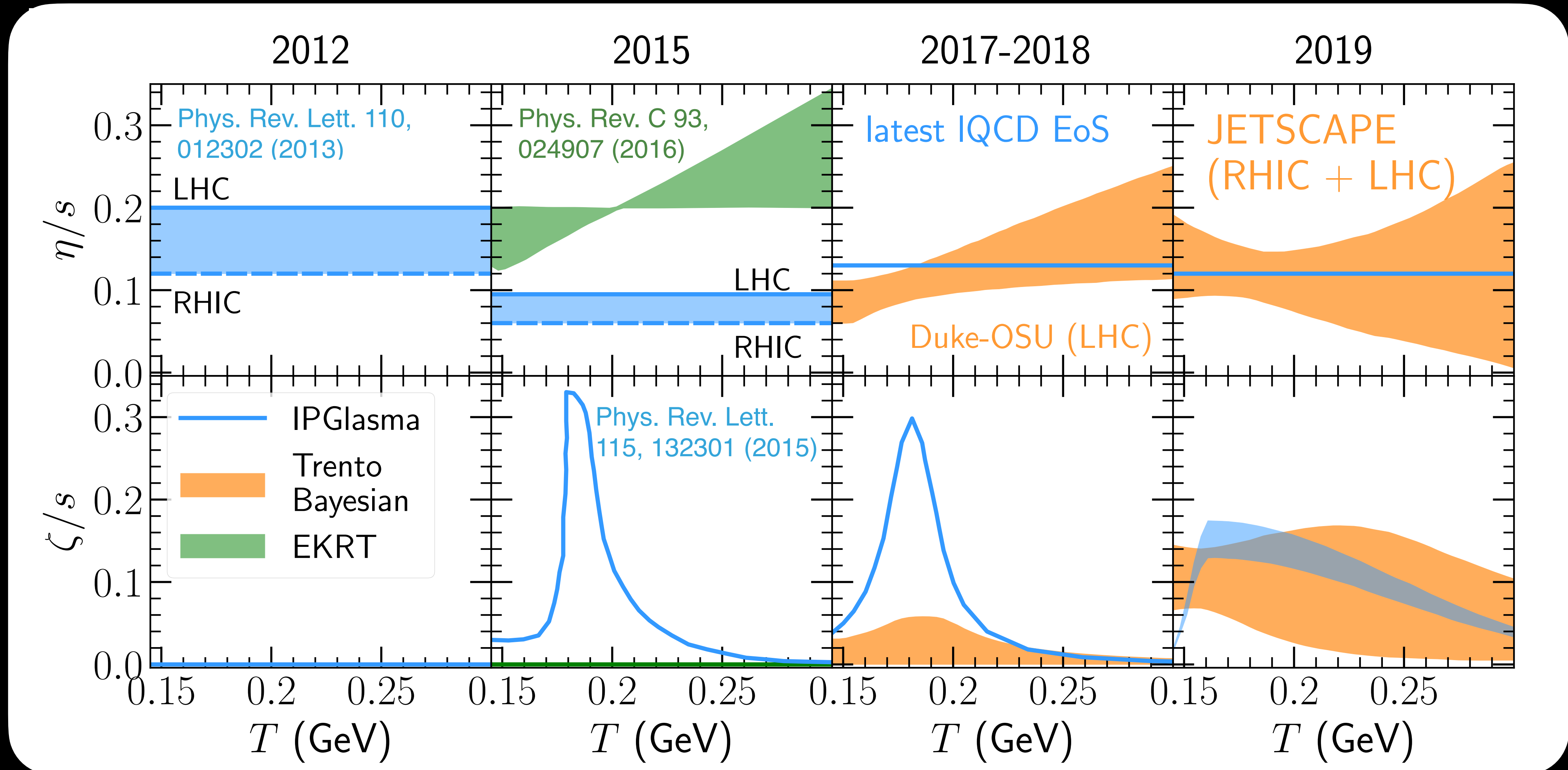
- One single set of model parameters for all types of collisions at the top RHIC and LHC energies



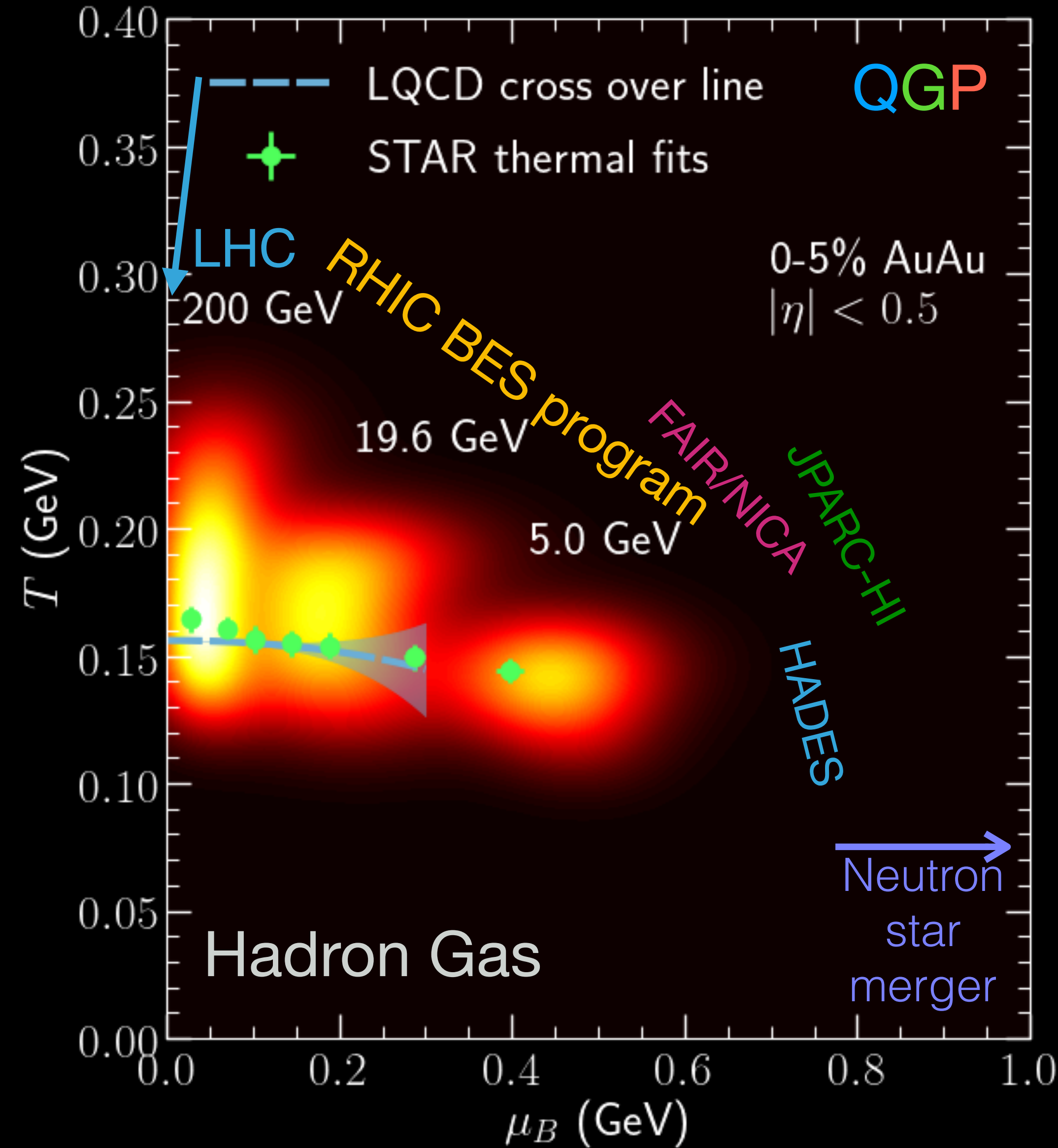
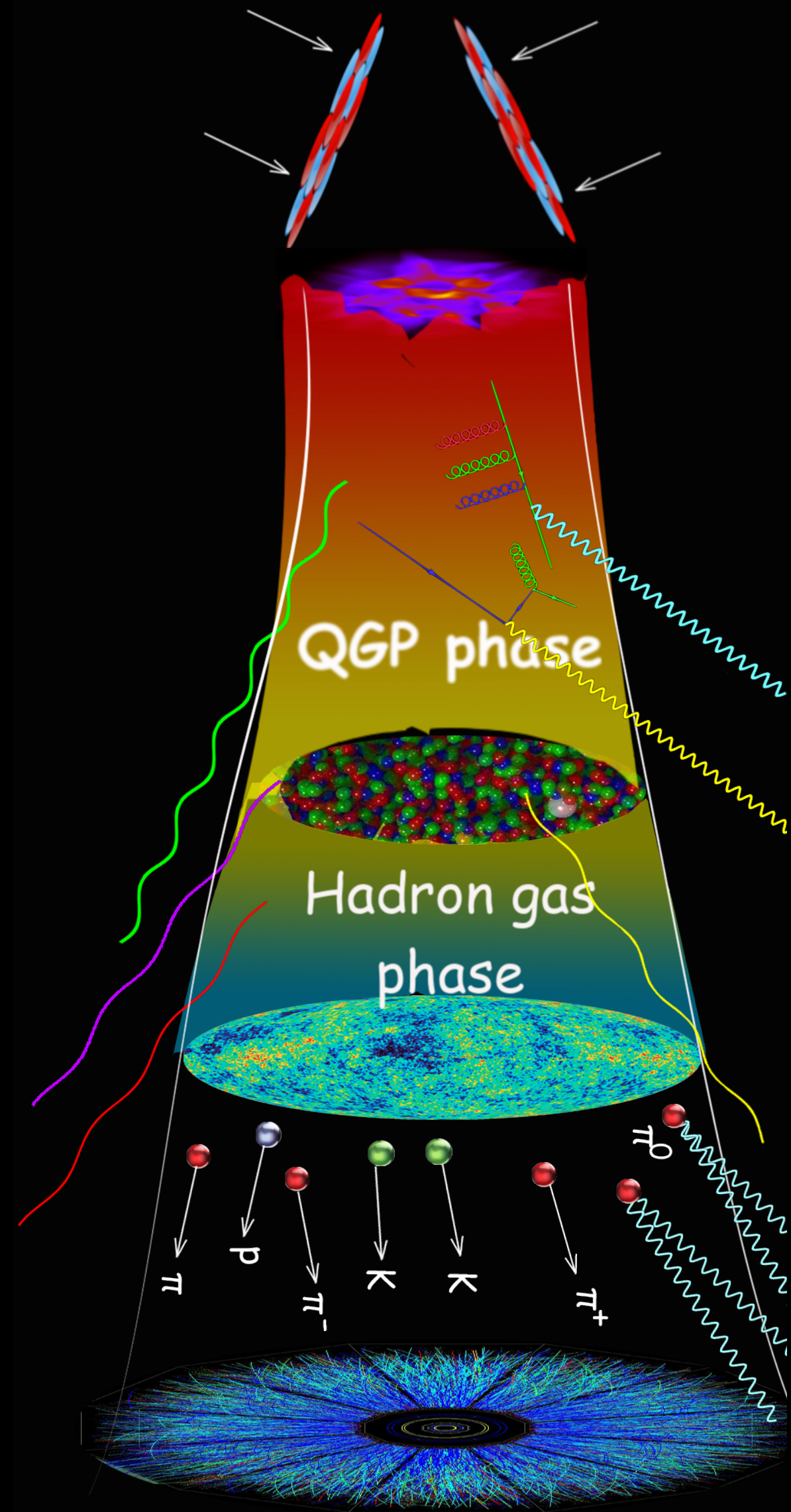
QUANTITATIVE CHARACTERIZATION OF QGP

C. Shen, arXiv:2001.11858 [nucl-th]

Phenomenological constraints from top RHIC and LHC data



PROBING THE NUCLEAR MATTER PHASE DIAGRAM



- Search for a critical point & 1st order phase transition

- How does the QGP transport property change with baryon doping?

$$(\eta/s)(T, \{\mu_q\}), (\zeta/s)(T, \{\mu_q\})$$

- Access to new transport phenomena
Charge diffusion

QCD EQUATION OF STATE AT FINITE DENSITIES

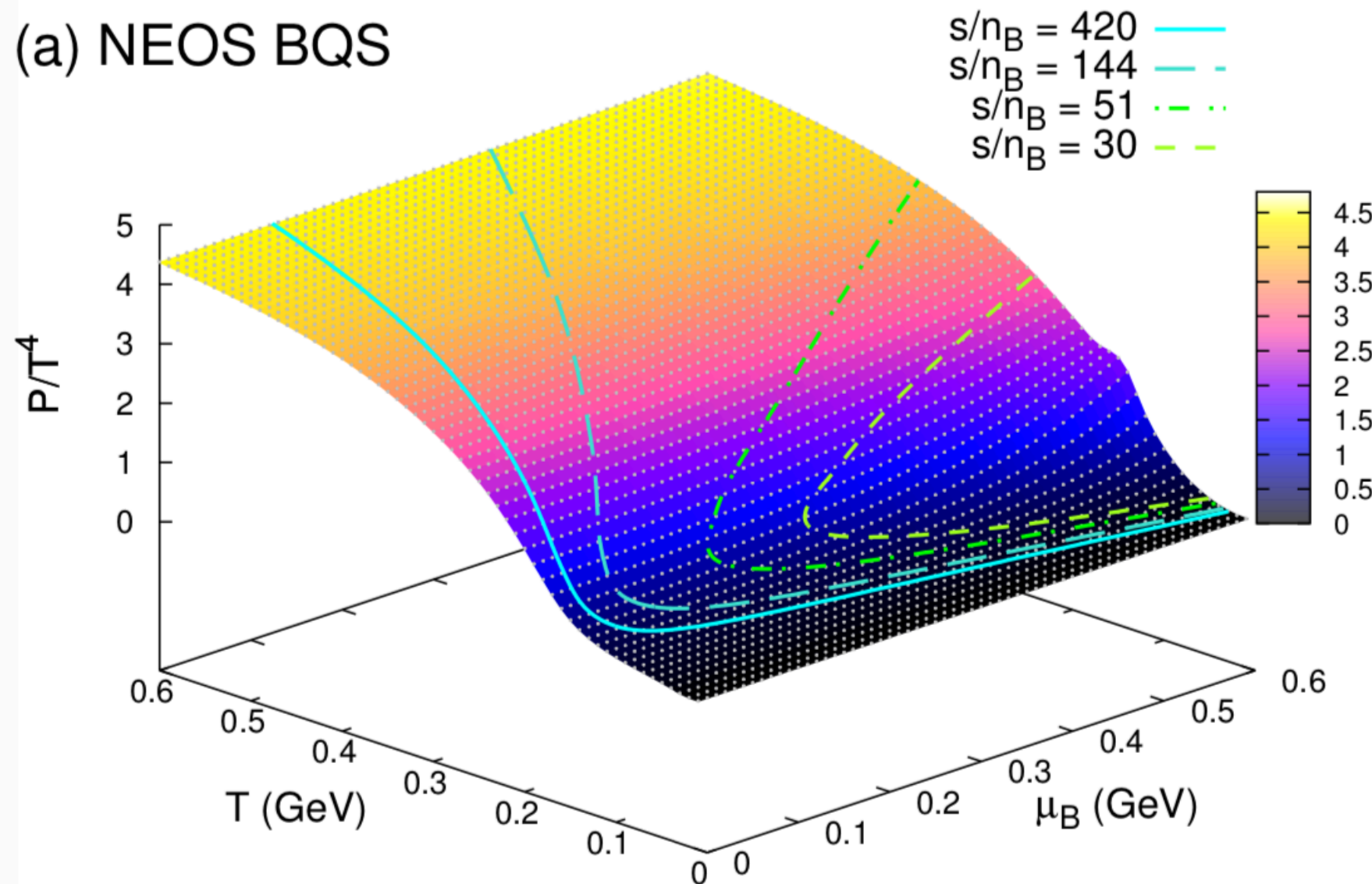
M. Albright, J. Kapusta and C. Young, Phys. Rev. C90, 024915 (2014)

A. Monnai, B. Schenke and C. Shen, Phys. Rev. C100, 024907 (2019)

J. Noronha-Hostler, P. Parotto, C. Ratti and J. M. Stafford, Phys. Rev. C100, 064910 (2019)

$$n_s = 0 \quad n_Q = 0.4n_B$$

(a) NEOS BQS



Lattice QCD: Taylor expansion up to the 4th order

$$\frac{P}{T^4} = \frac{P_0}{T^4} + \sum_{l,m,n} \frac{\chi_{l,m,n}^{B,Q,S}}{l!m!n!} \left(\frac{\mu_B}{T}\right)^l \left(\frac{\mu_Q}{T}\right)^m \left(\frac{\mu_S}{T}\right)^n$$

Match to Hadron Resonance Gas model at low T

$$\frac{P}{T^4} = \frac{1}{2} [1 - f(T, \mu_J)] \frac{P_{\text{had}}(T, \mu_J)}{T^4} + \frac{1}{2} [1 + f(T, \mu_J)] \frac{P_{\text{lat}}(T, \mu_J)}{T^4}$$

$$f(T, \mu_B) = \tanh[(T - T_c(\mu_B))/\Delta T_c]$$

$$T_c(\mu_B) = 0.16 \text{ GeV} - 0.4(0.139 \text{ GeV}^{-1} \mu_B^2 + 0.053 \text{ GeV}^{-3} \mu_B^4)$$

$$\Delta T_c = 0.1 T_c(\mu_B = 0)$$

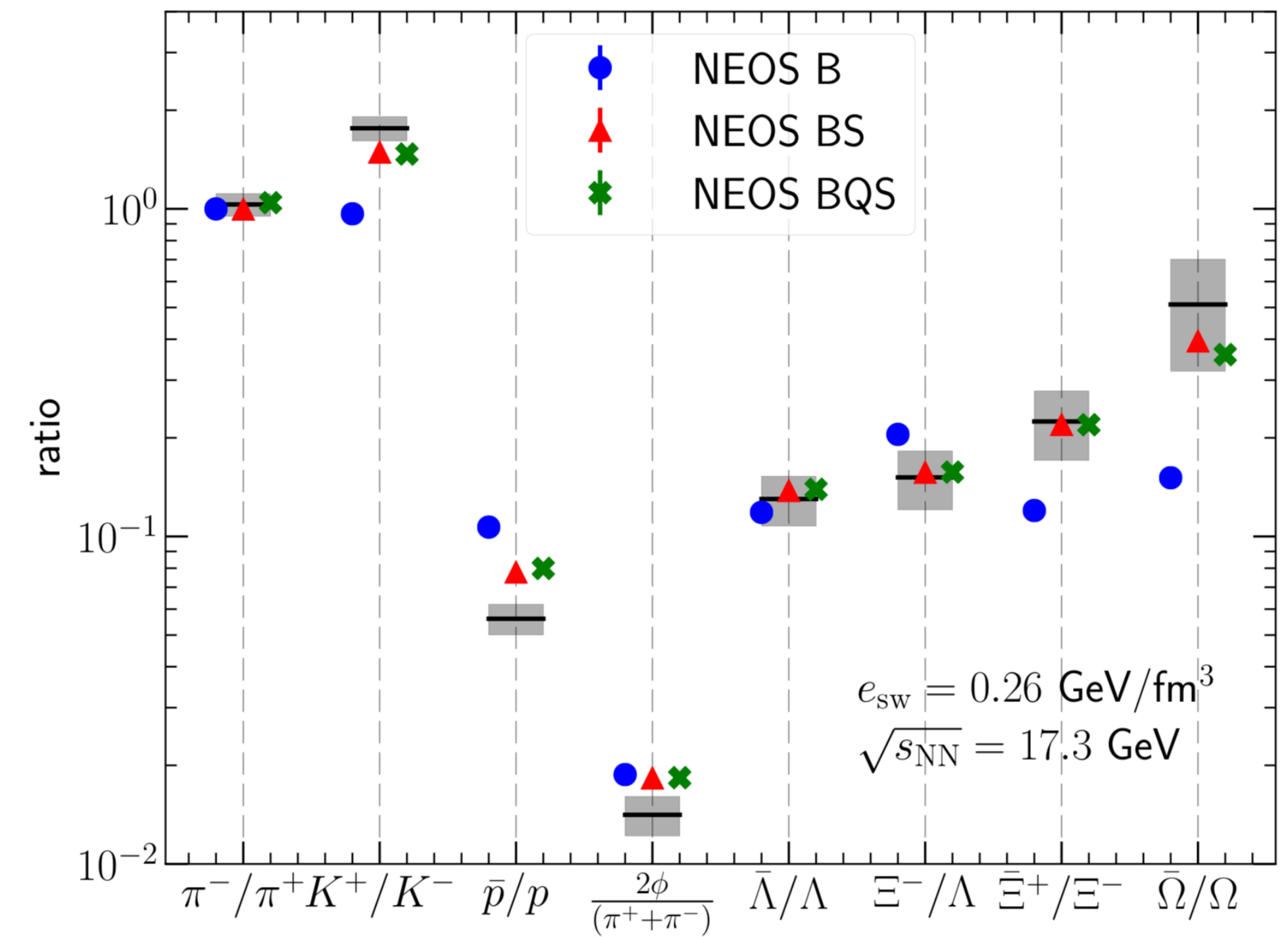
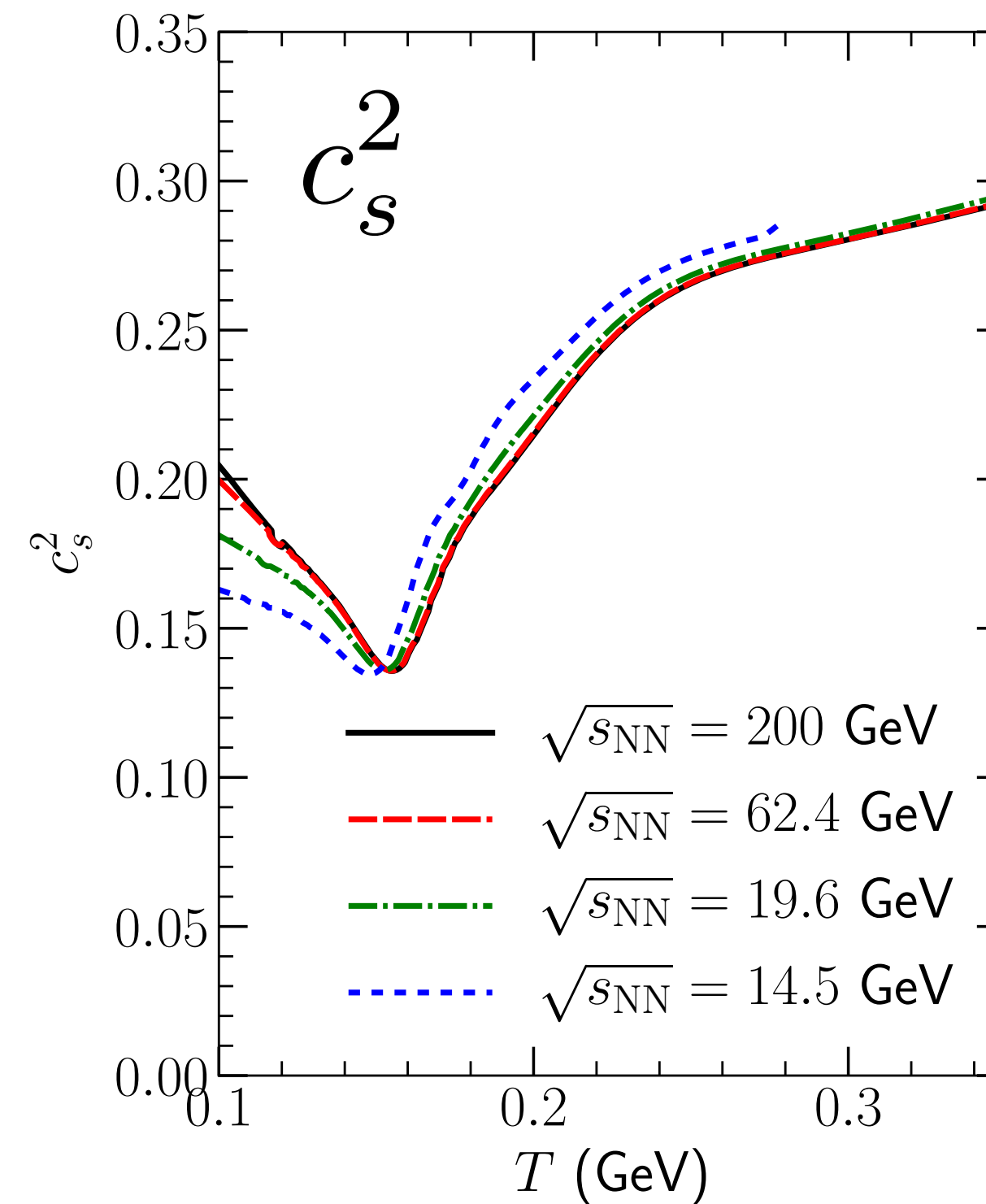
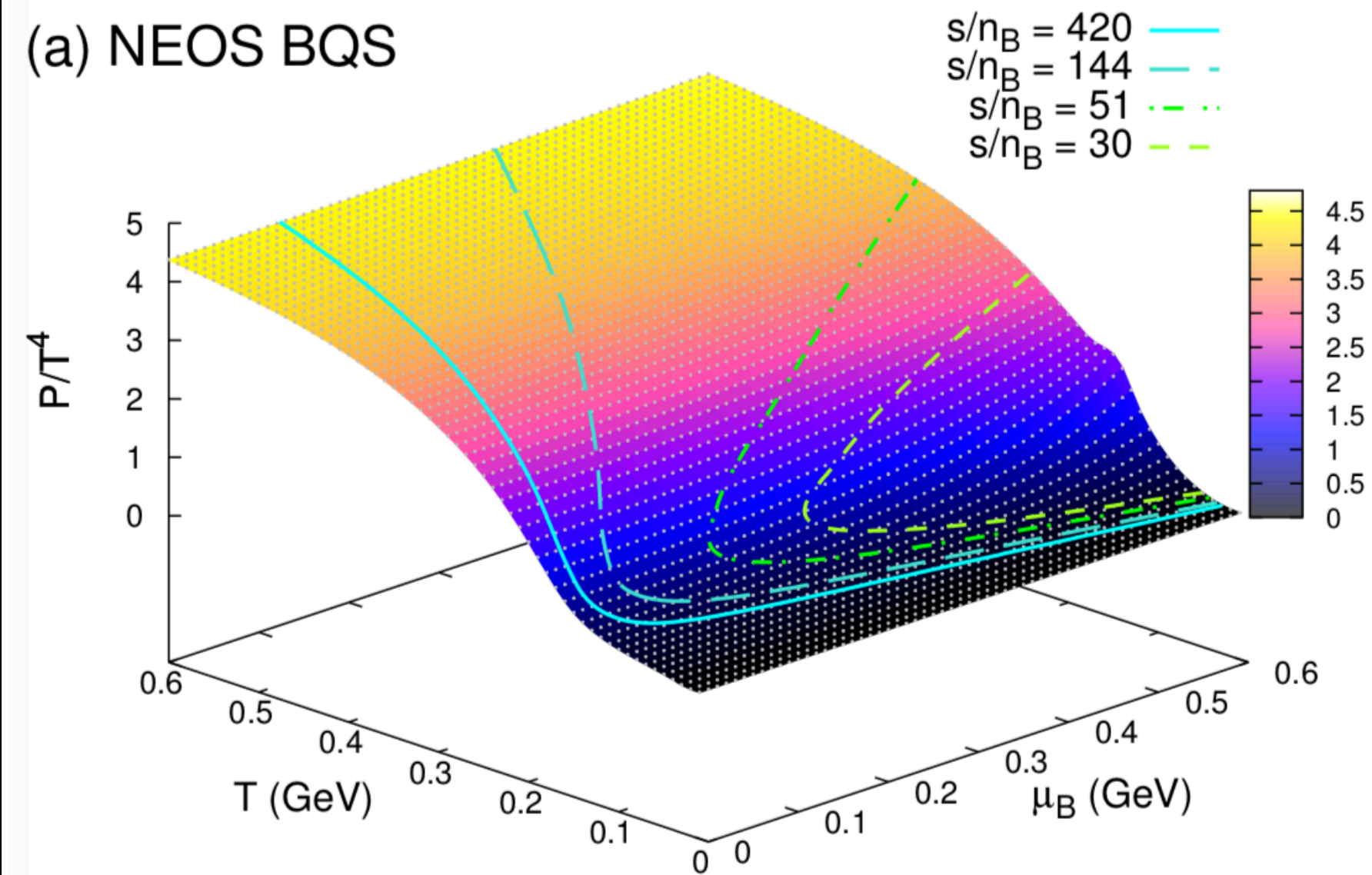
QCD EQUATION OF STATE AT FINITE DENSITIES

A. Monnai, B. Schenke and C. Shen, Phys. Rev. C100, 024907 (2019)

<https://sites.google.com/view/qcdneos/>

$$n_s = 0 \quad n_Q = 0.4n_B$$

(a) NEOS BQS



- Strangeness neutrality improves the hadronic chemistry in the hybrid dynamic framework

Enabled hydrodynamic simulations at finite μ

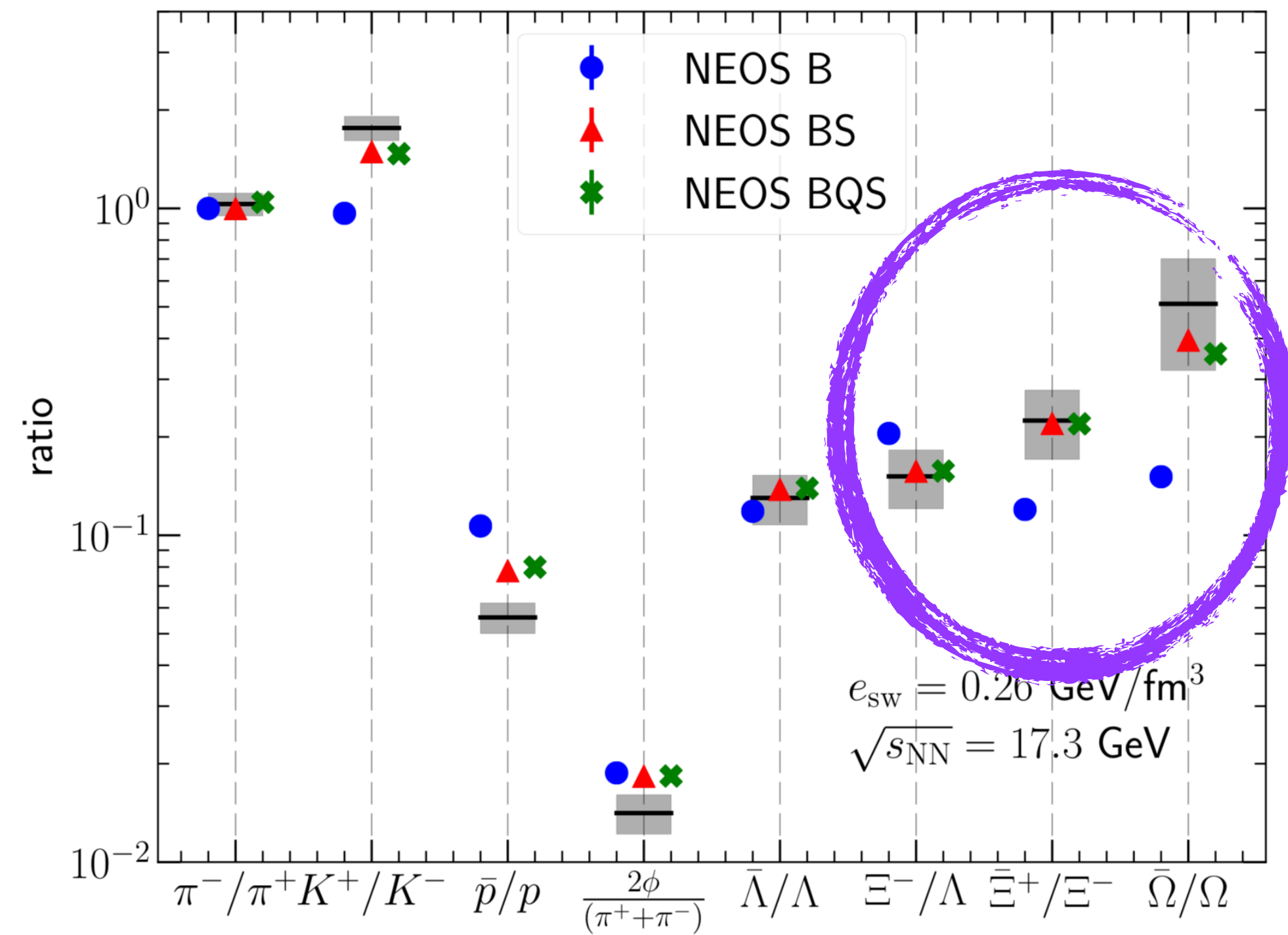
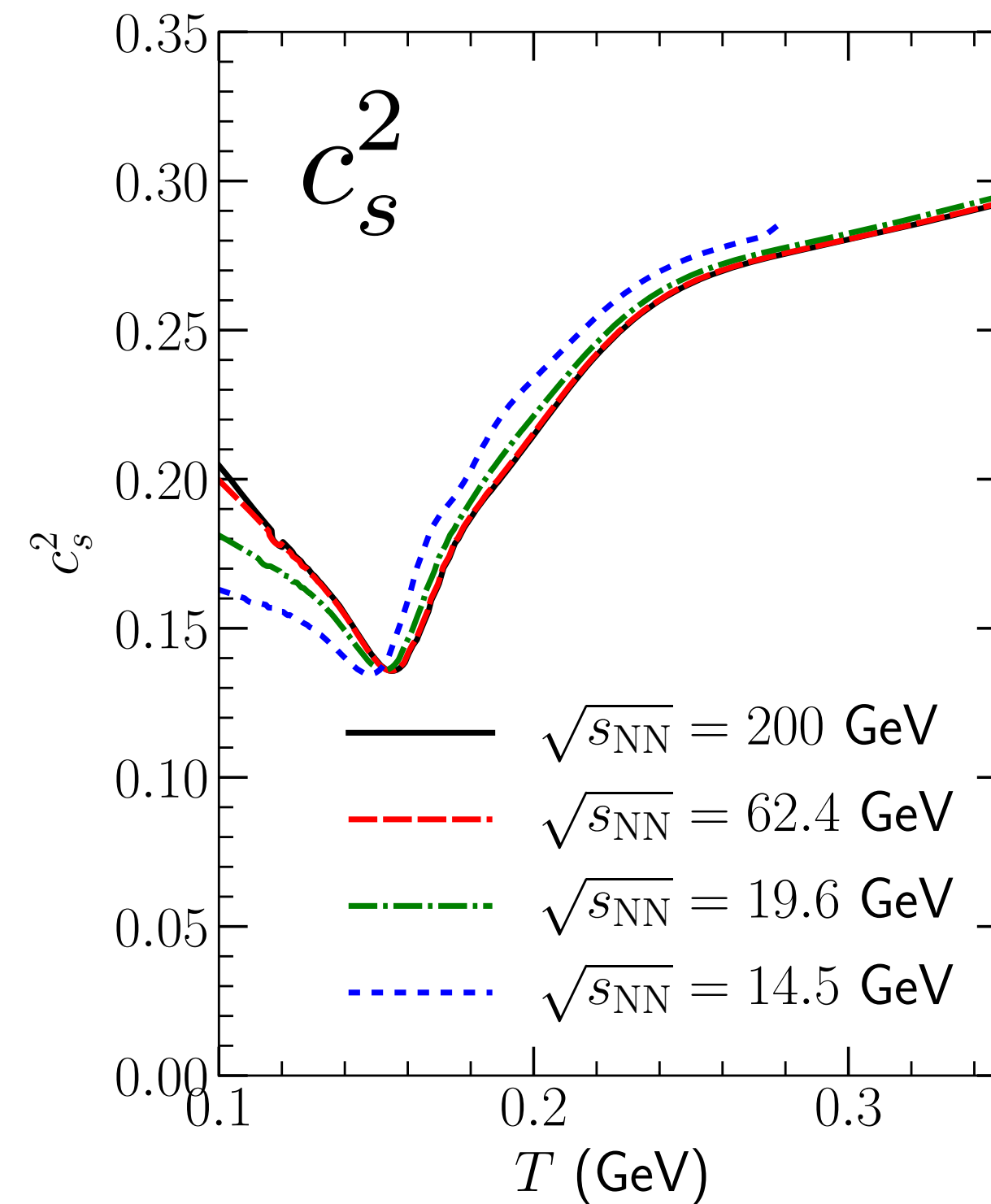
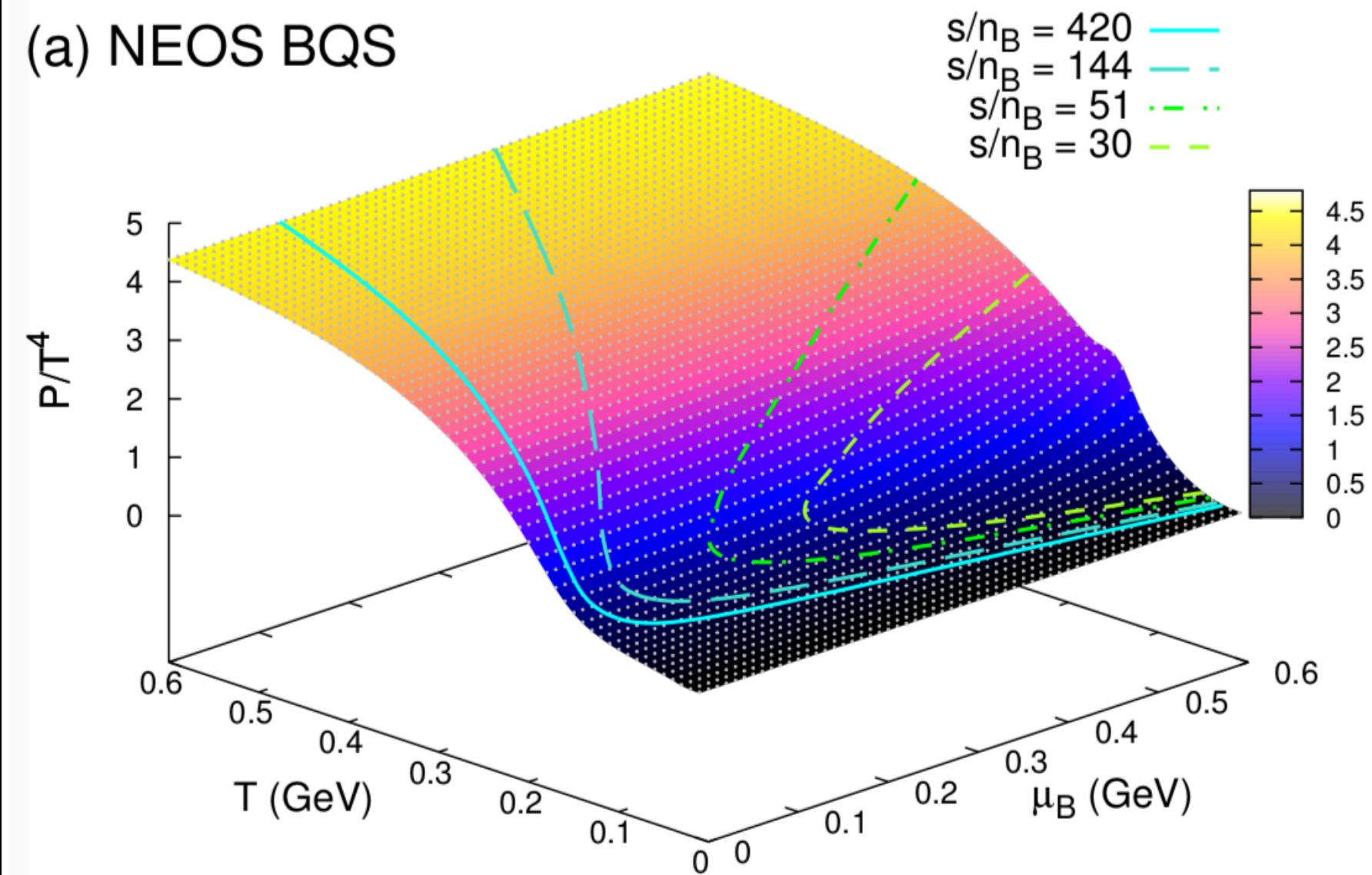
QCD EQUATION OF STATE AT FINITE DENSITIES

A. Monnai, B. Schenke and C. Shen, Phys. Rev. C100, 024907 (2019)

<https://sites.google.com/view/qcdneos/>

$$n_s = 0 \quad n_Q = 0.4n_B$$

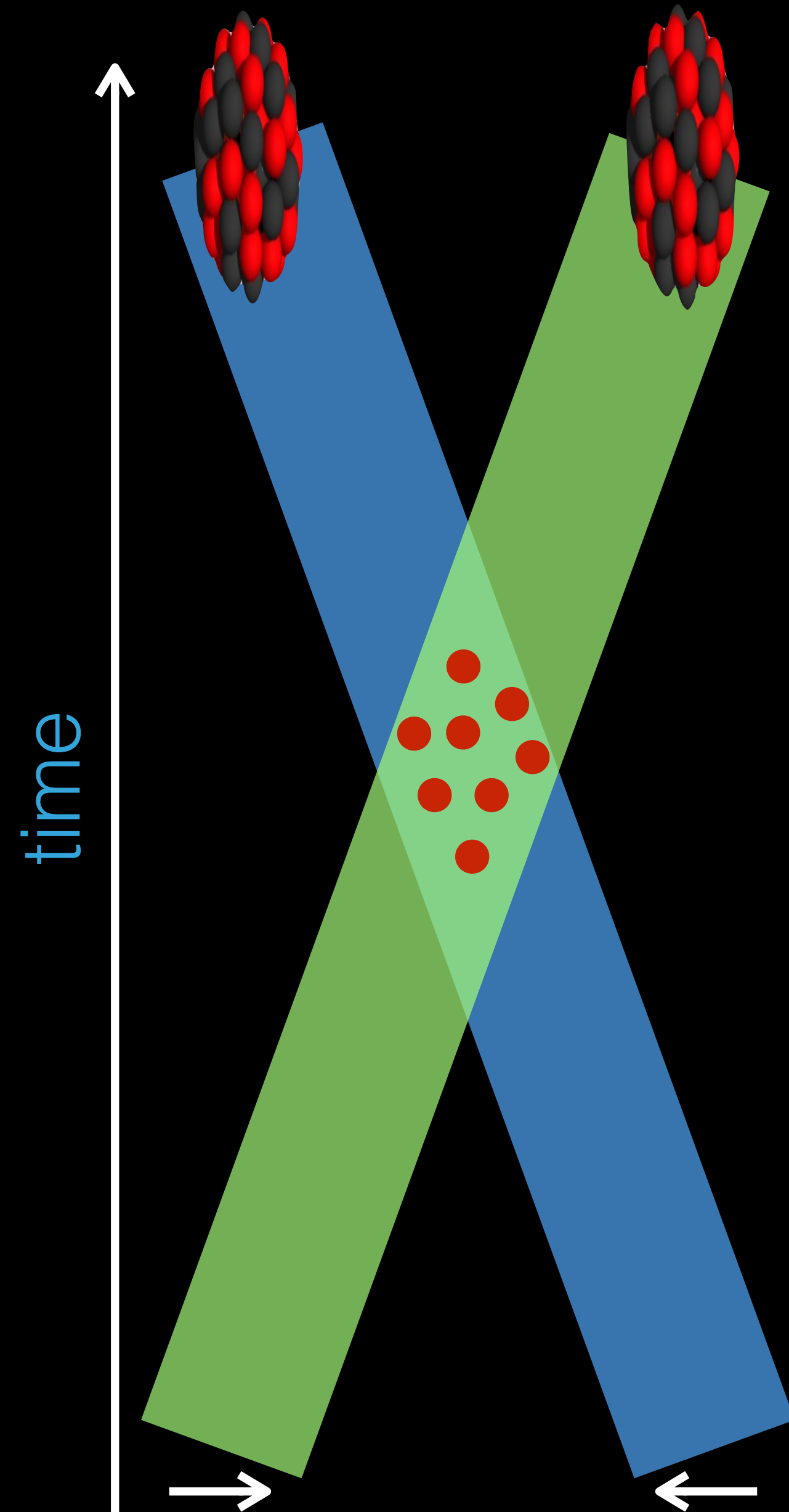
(a) NEOS BQS



- Strangeness neutrality improves the hadronic chemistry in the hybrid dynamic framework

Enabled hydrodynamic simulations at finite μ

3D DYNAMICS BEYOND THE BJORKEN PARADIGM



- Geometry-Based initial conditions
C. Shen and S. Alzhvani, Phys. Rev. C 102, 014909 (2020)
- Classical string-based initial conditions
A. Bialas, A. Bzdak and V. Koch, Acta Phys. Polon. B49 (2018)
C. Shen and B. Schenke, Phys.Rev. C97 (2018) 024907
- Transport model based initial conditions
I. A. Karpenko, P. Huovinen, H. Petersen and M. Bleicher, Phys. Rev. C91 (2015) 064901
L. Du, U. Heinz and G. Vujanovic, Nucl. Phys. A982 (2019) 407-410
- Color Glass Condensate based models
M. Li and J. Kapusta, Phys. Rev. C 99, 014906 (2019)
L. D. McLerran, S. Schlichting and S. Sen, Phys. Rev. D 99, 074009 (2019)
M. Martinez, M. D. Sievert, D. E. Wertepny and J. Noronha-Hostler, arXiv:1911.10272 + arXiv:1911.12454 [nucl-th]
- Holographic approach at intermediate coupling
M. Attems, et al., Phys.Rev.Lett. 121 (2018), 261601

A MINIMUM EXTENSION TO 3D INITIAL CONDITIONS

C. Shen and S. Alzhirani, Phys. Rev. C 102, 014909 (2020)

- Impose energy and momentum conservation on the Glauber geometry
Assumption: All of the energy and momentum is deposited into the medium

$$\begin{aligned} E(x, y) &= [T_A(x, y) + T_B(x, y)] m_N \cosh(y_{\text{beam}}) \\ &\equiv M(x, y) \cosh(y_{\text{CM}}(x, y)) \\ P_z(x, y) &= [T_A(x, y) - T_B(x, y)] m_N \sinh(y_{\text{beam}}) \\ &\equiv M(x, y) \sinh(y_{\text{CM}}(x, y)). \end{aligned}$$

$$\begin{aligned} y_{\text{CM}}(x, y) &= \operatorname{arctanh} \left[\frac{T_A - T_B}{T_A + T_B} \tanh(y_{\text{beam}}) \right] \\ M(x, y) &= m_N \sqrt{T_A^2 + T_B^2 + 2T_A T_B \cosh(2y_{\text{beam}})} \end{aligned}$$

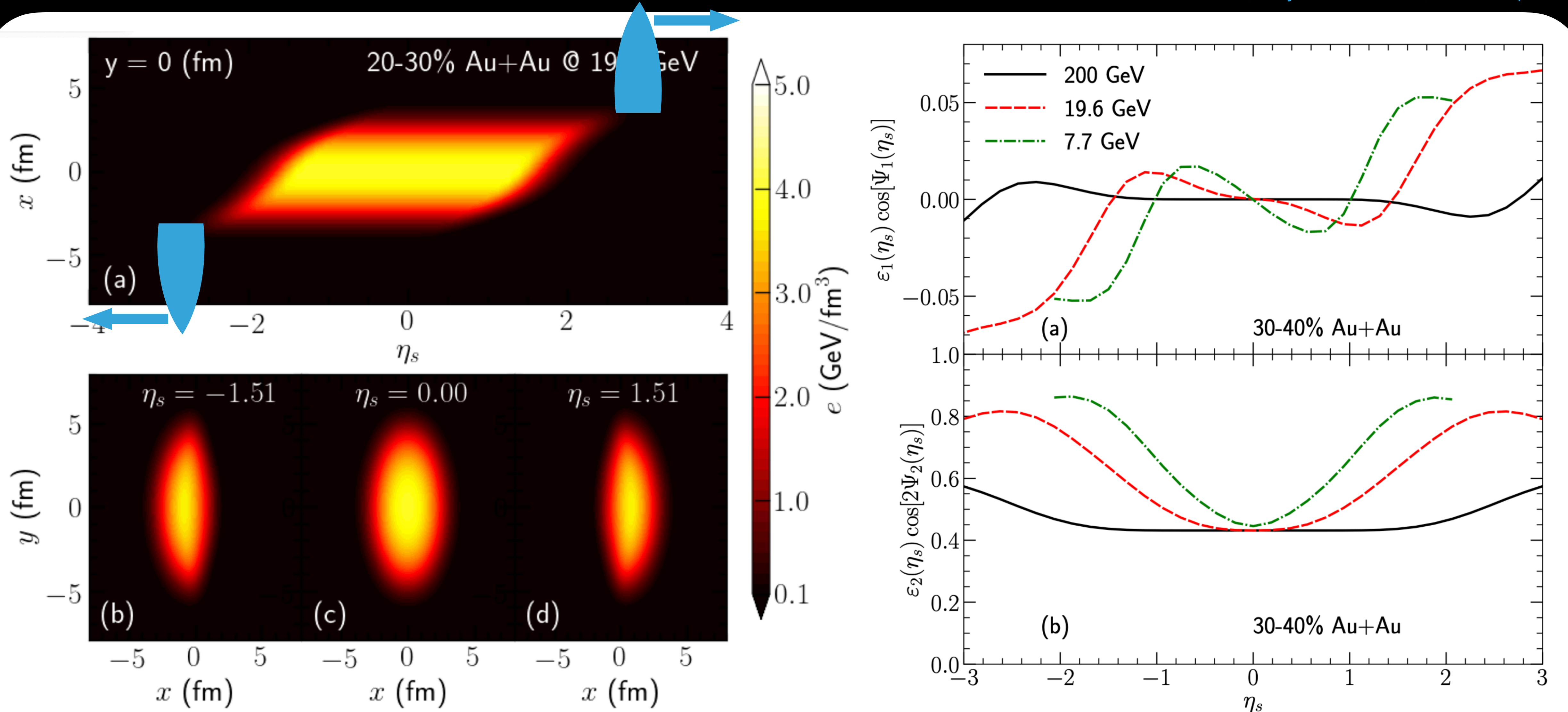
- Assume Bjorken flow for the velocity profile $u_{\text{init}}^\mu = (\cosh(\eta_s), 0, 0, \sinh(\eta_s))$
- Energy density given by a longitudinal flux-tube profile

$$\begin{aligned} e(x, y, \eta_s; y_{\text{CM}}) &= \mathcal{N}_e(x, y) \\ &\times \exp \left[-\frac{(|\eta_s - y_{\text{CM}}| - \eta_0)^2}{2\sigma_\eta^2} \theta(|\eta_s - y_{\text{CM}}| - \eta_0) \right] \end{aligned} \quad \text{where } \mathcal{N}_e(x, y) \propto M(x, y)$$

- For $\sqrt{s} \geq 5 \text{ GeV}$, the local energy density $e(x, y) \propto \sqrt{T_A T_B}$

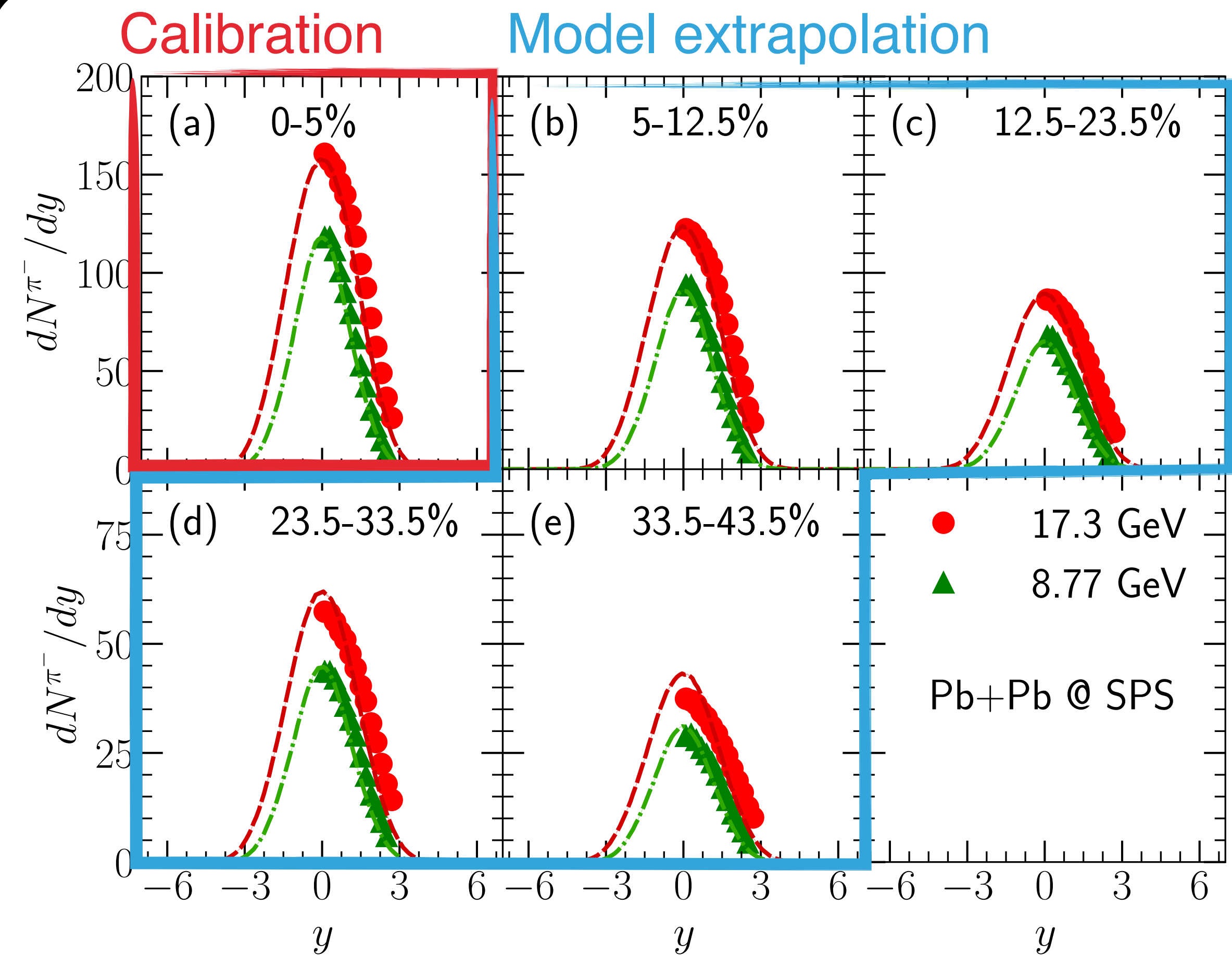
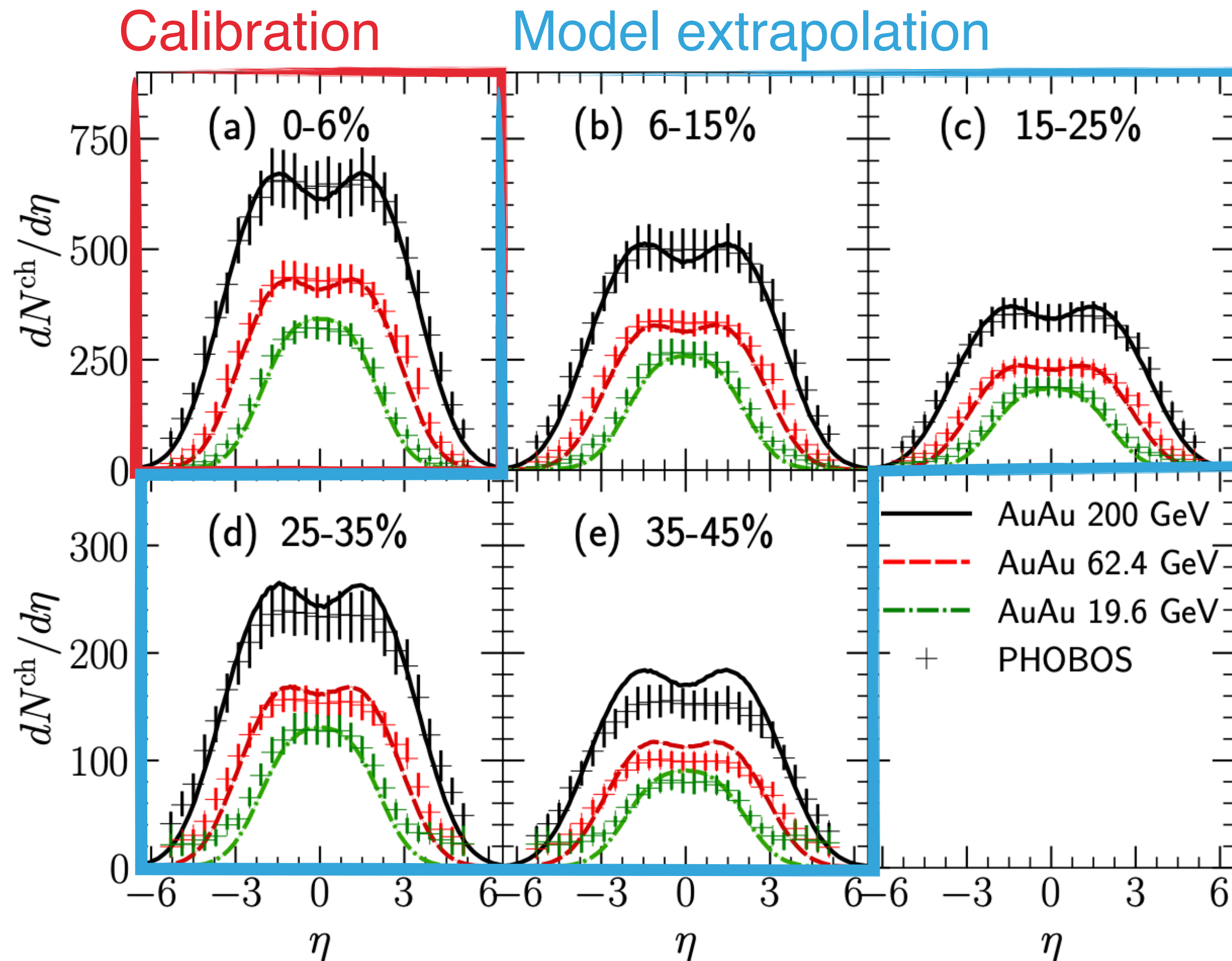
A MINIMUM EXTENSION TO 3D INITIAL CONDITIONS

C. Shen and S. Alzhrani, Phys. Rev. C 102, 014909 (2020)



PARTICLE PRODUCTIONS AT RHIC BES AND SPS

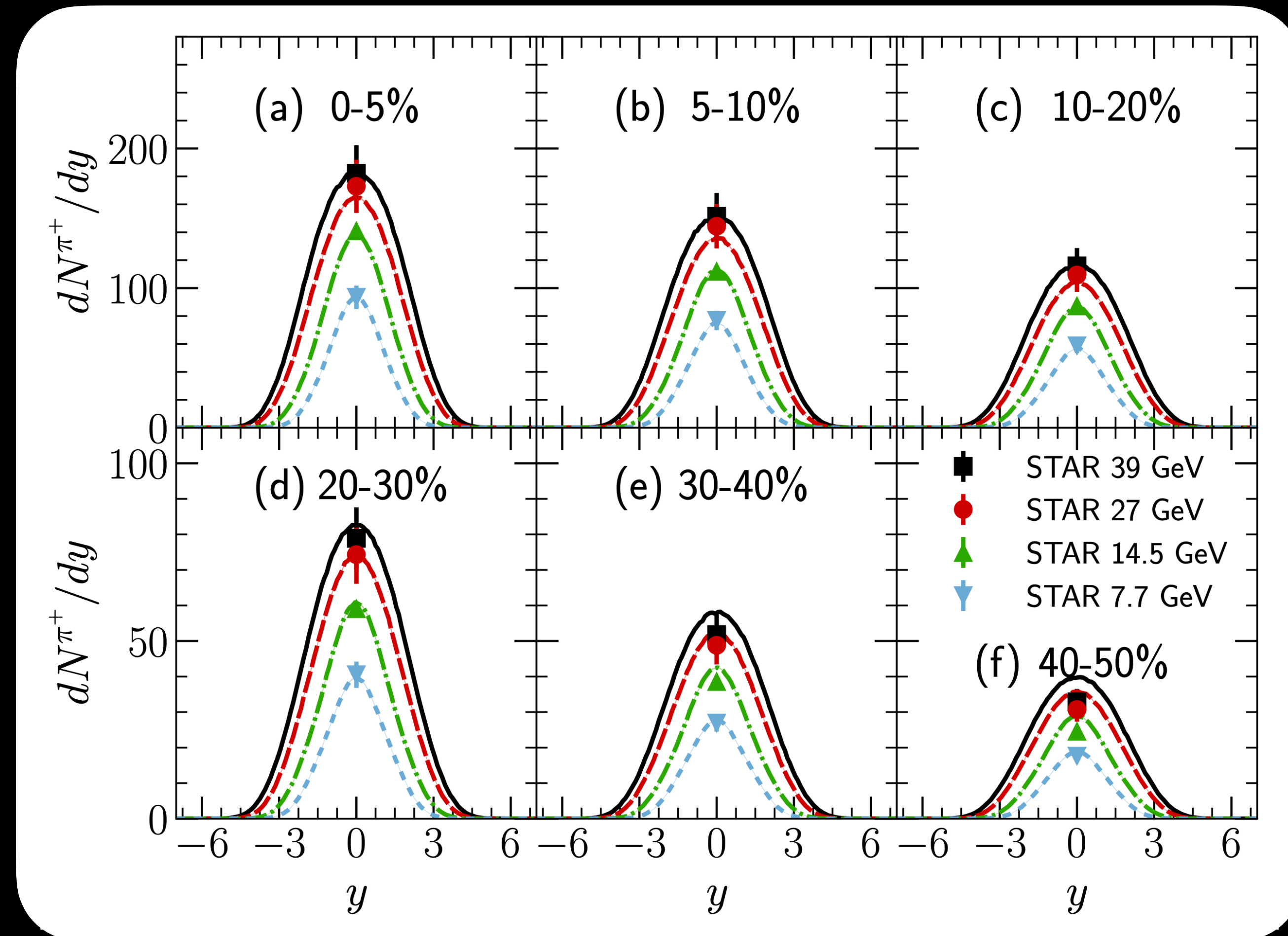
C. Shen and S. Alzhrani, Phys. Rev. C 102, 014909 (2020)



- Centrality dependence of particle production can be well reproduced

PARTICLE RAPIDITY DISTRIBUTION AT RHIC BES

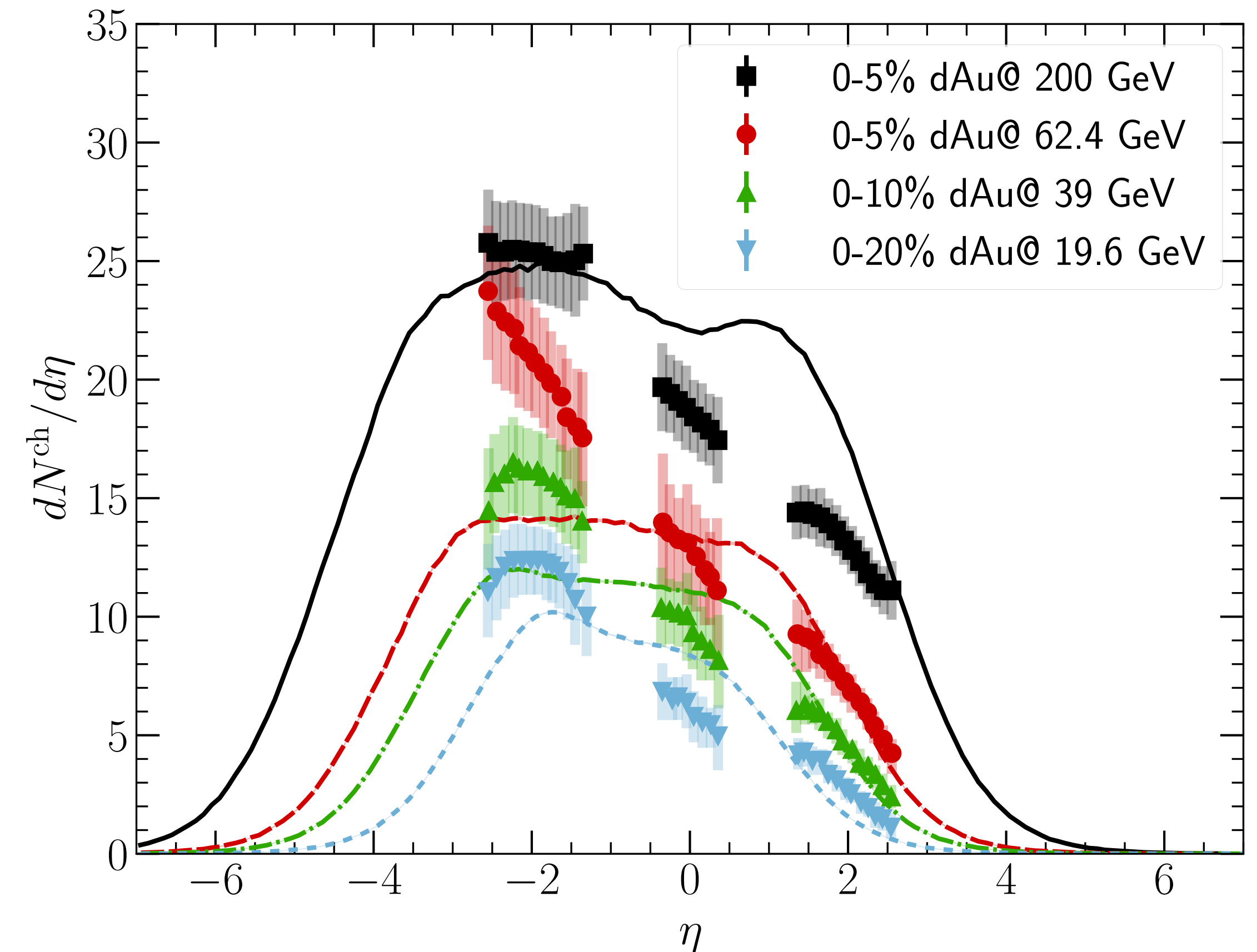
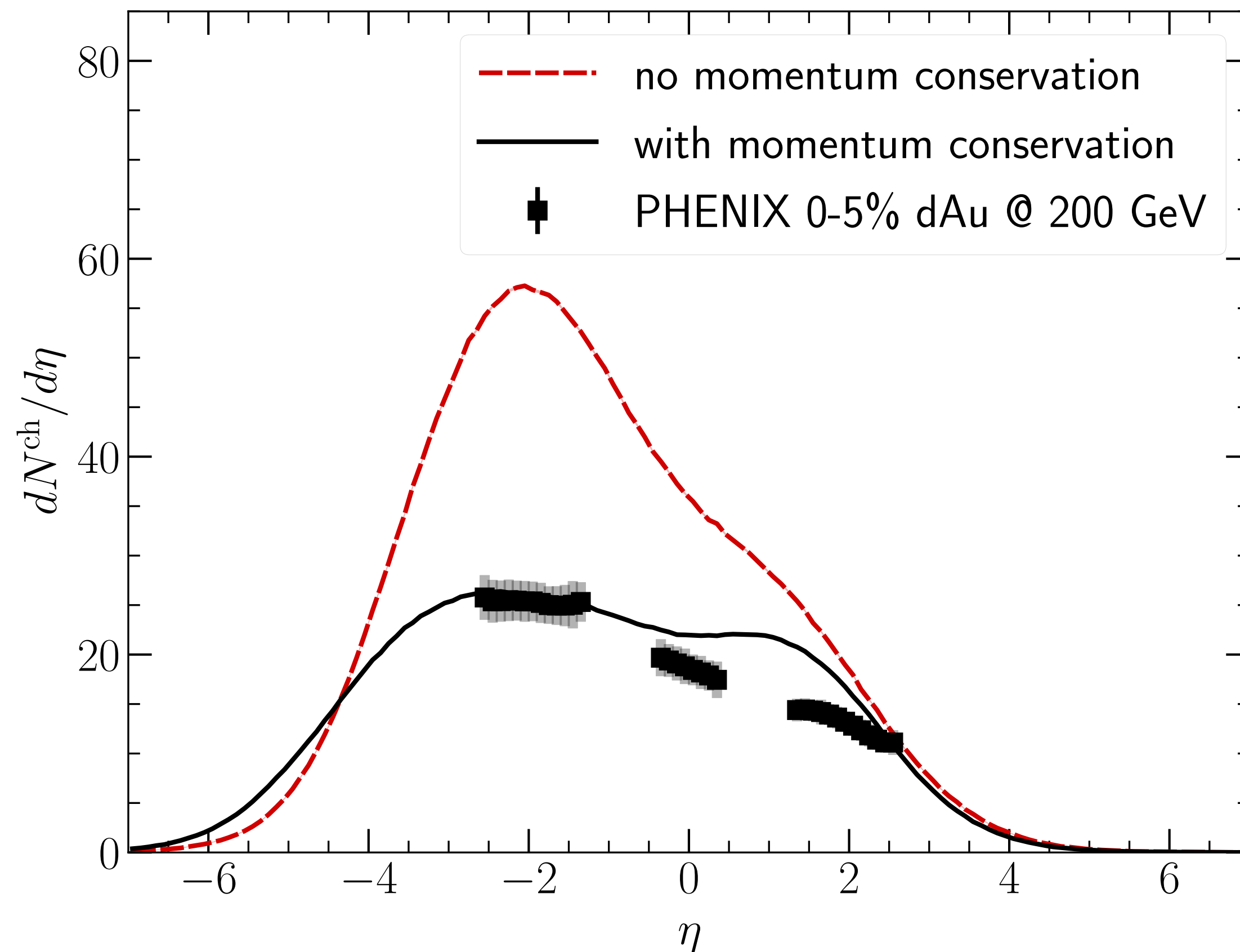
C. Shen and S. Alzhvani, Phys. Rev. C 102, 014909 (2020)



- With limited data from RHIC BES I, we make predictions for the rapidity dependence of particle productions

PARTICLE PRODUCTIONS AT RHIC BES AND SPS

C. Shen and S. Alzhvani, Phys. Rev. C 102, 014909 (2020)

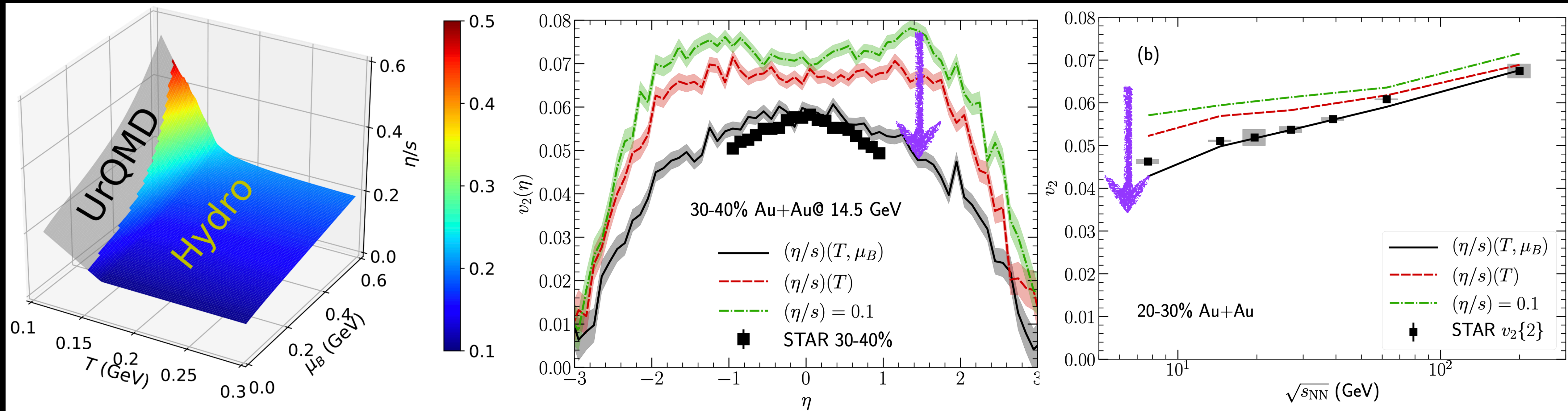


- Imposing energy-momentum conservation is extremely important for making predictions for asymmetric d+Au collisions

ELLIPTIC FLOW AT RHIC BES AND SHEAR VISCOSITY

I. A. Karpenko, P. Huovinen, H. Petersen and M. Bleicher, Phys. Rev. C91 (2015) 064901

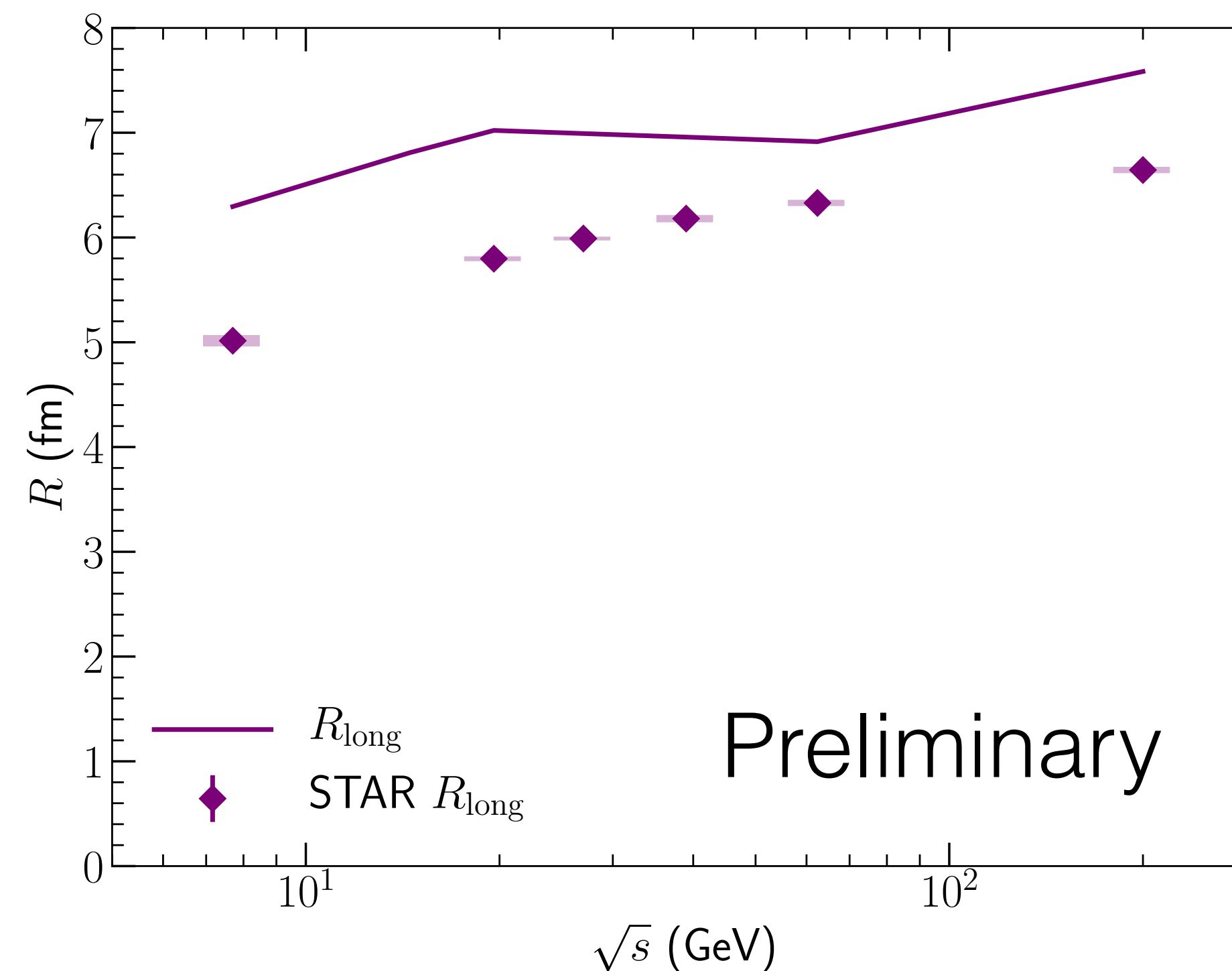
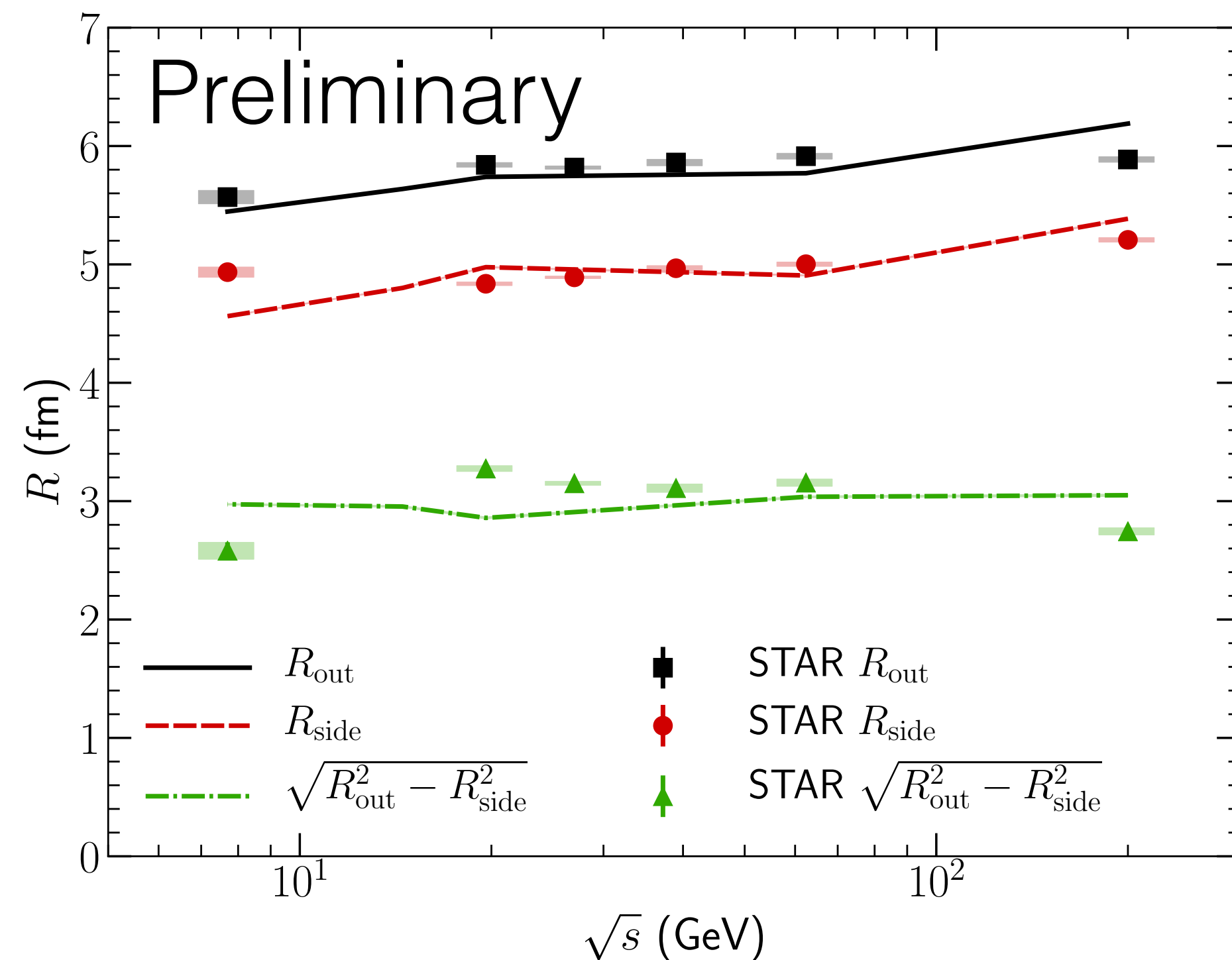
C. Shen and S. Alzhrani, Phys. Rev. C 102, 014909 (2020)



- The rapidity and centrality dependence of v_2 can set strong constraints on the $(\eta/s)(T, \mu_B)$

HBT RADII AT THE RHIC BES

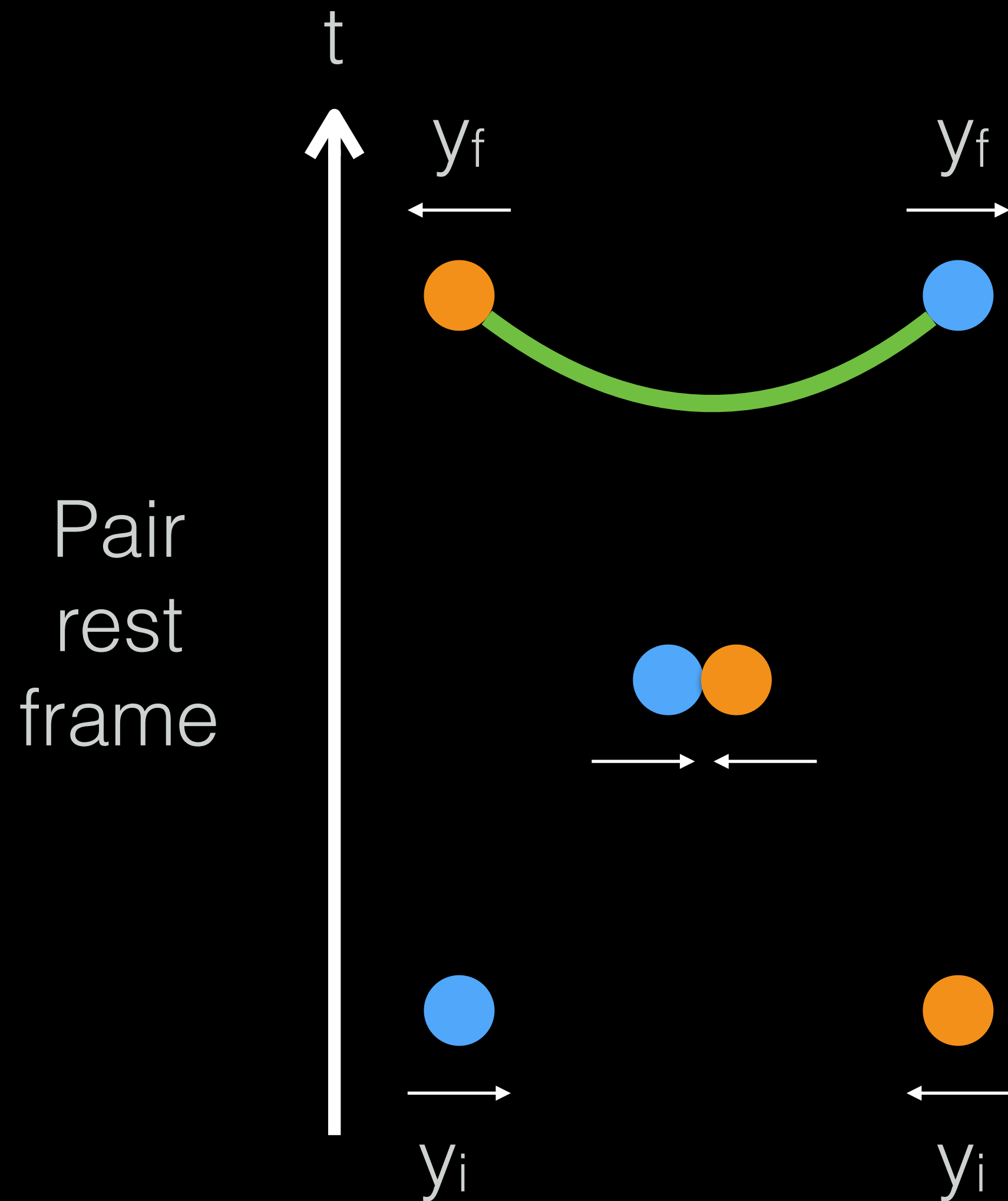
Based on C. Shen and S. Alzhrani, Phys. Rev. C 102, 014909 (2020)



- The model reasonably describe the collision energy dependence of R_{out} and R_{side} ; R_{long} is overestimated and need further investigation
- $\sqrt{R_{out}^2 - R_{side}^2}$ is flat vs. \sqrt{s}

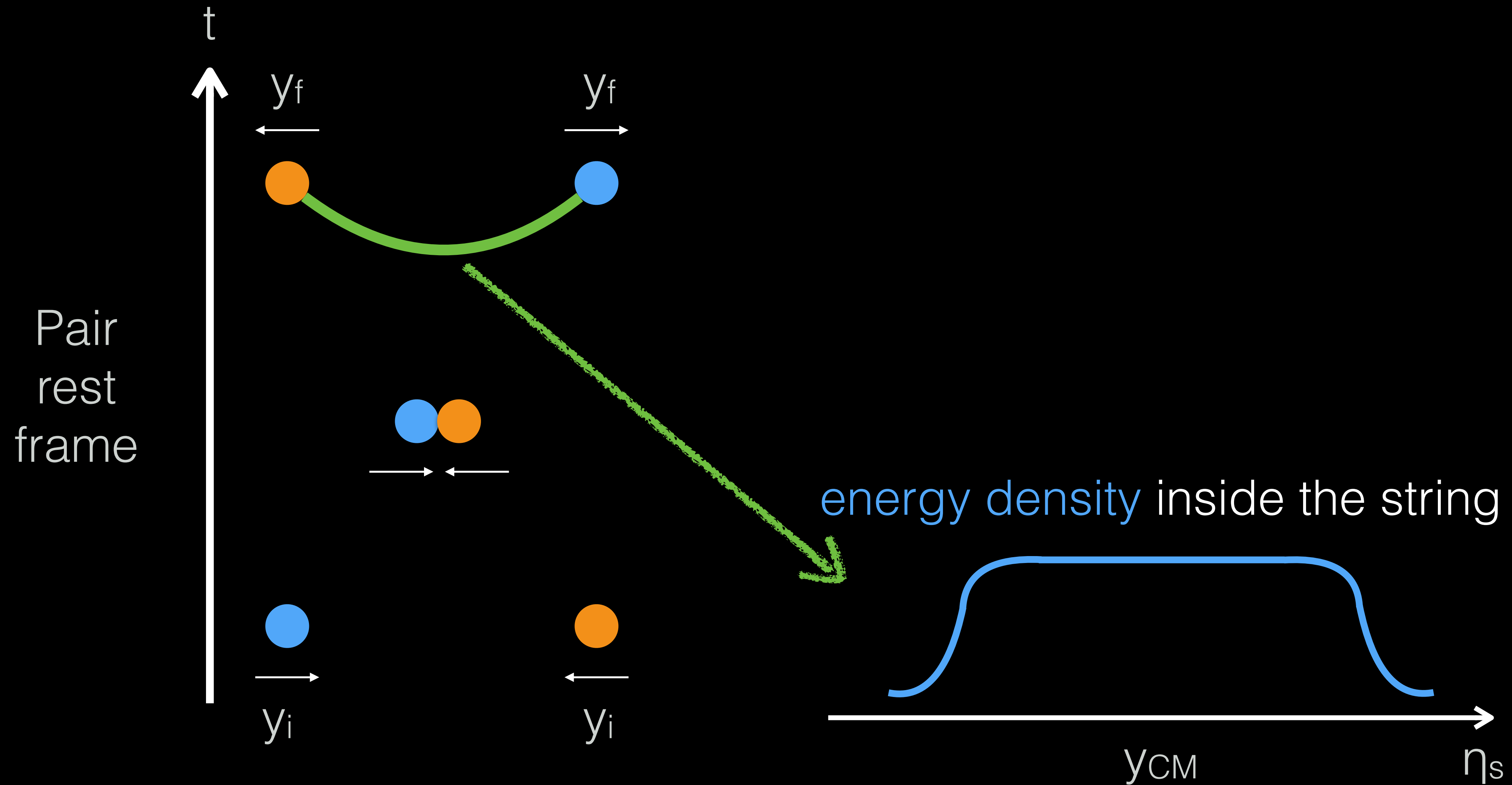
THE 3D MC-GLAUBER + STRING MODEL

C. Shen and B. Schenke, Phys.Rev. C97 (2018) 024907



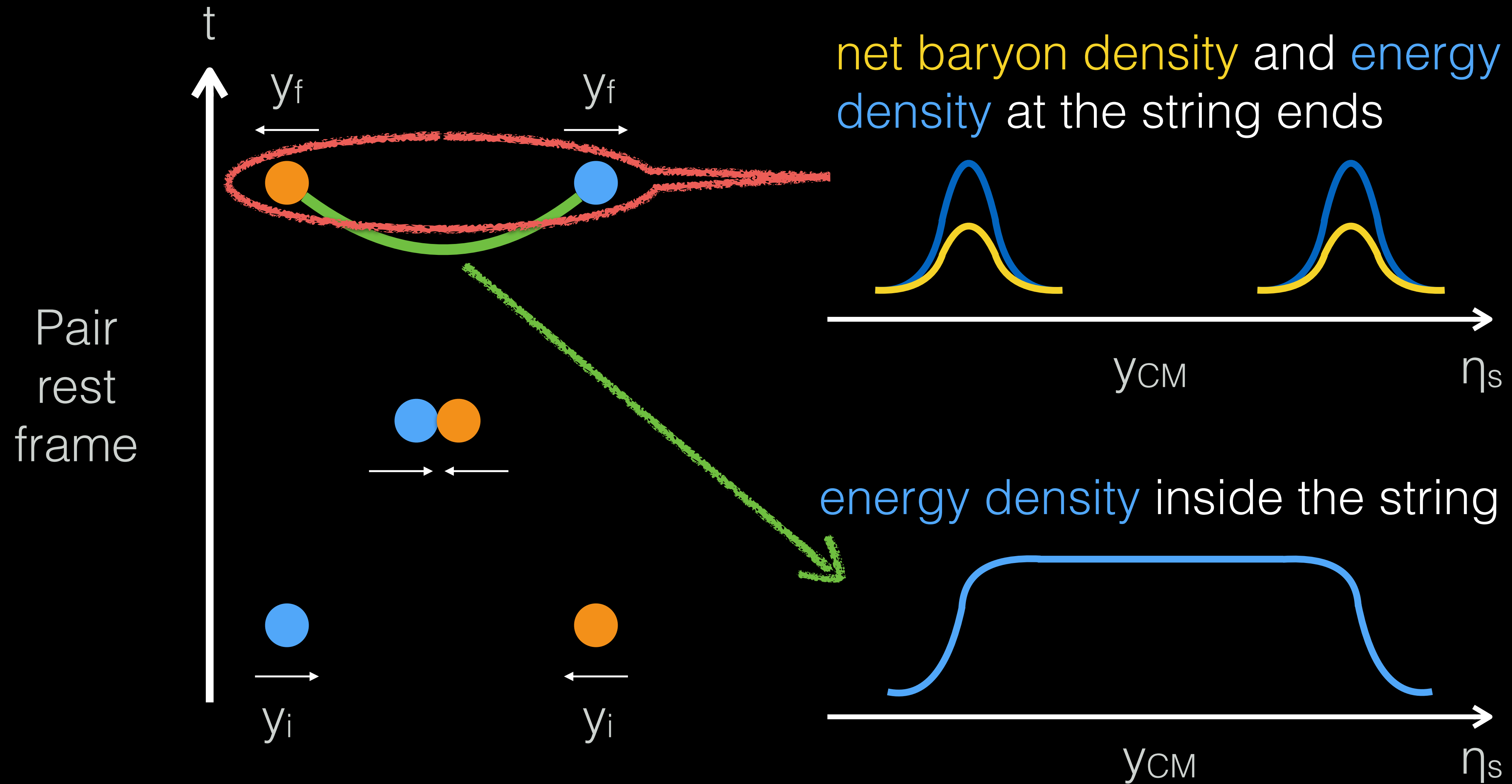
THE 3D MC-GLAUBER + STRING MODEL

C. Shen and B. Schenke, Phys.Rev. C97 (2018) 024907



THE 3D MC-GLAUBER + STRING MODEL

C. Shen and B. Schenke, Phys.Rev. C97 (2018) 024907

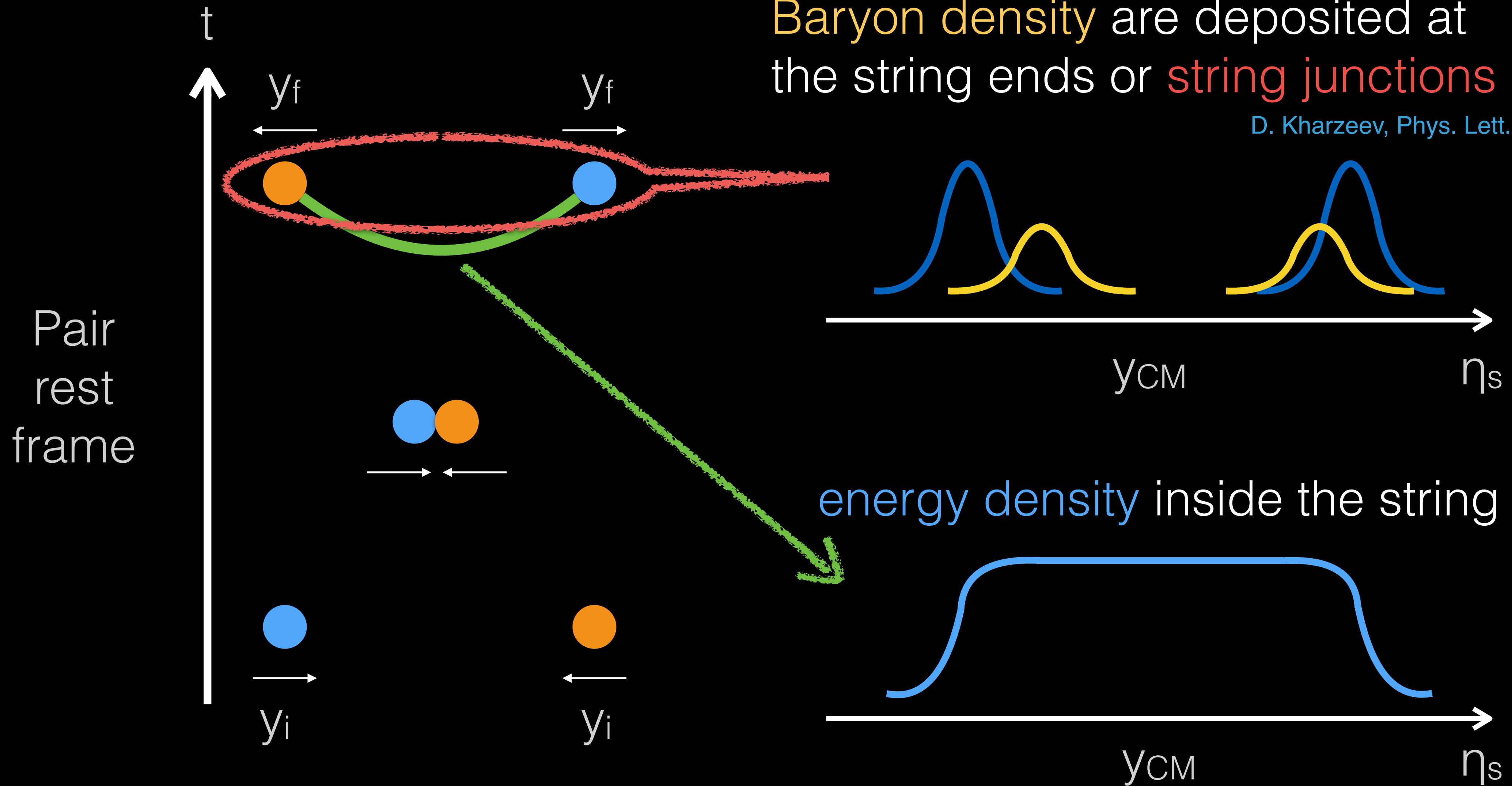


THE 3D MC-GLAUBER + STRING MODEL

C. Shen and B. Schenke, Phys.Rev. C97 (2018) 024907

Baryon density are deposited at the string ends or **string junctions**

D. Kharzeev, Phys. Lett. B 378, 238 (1996)

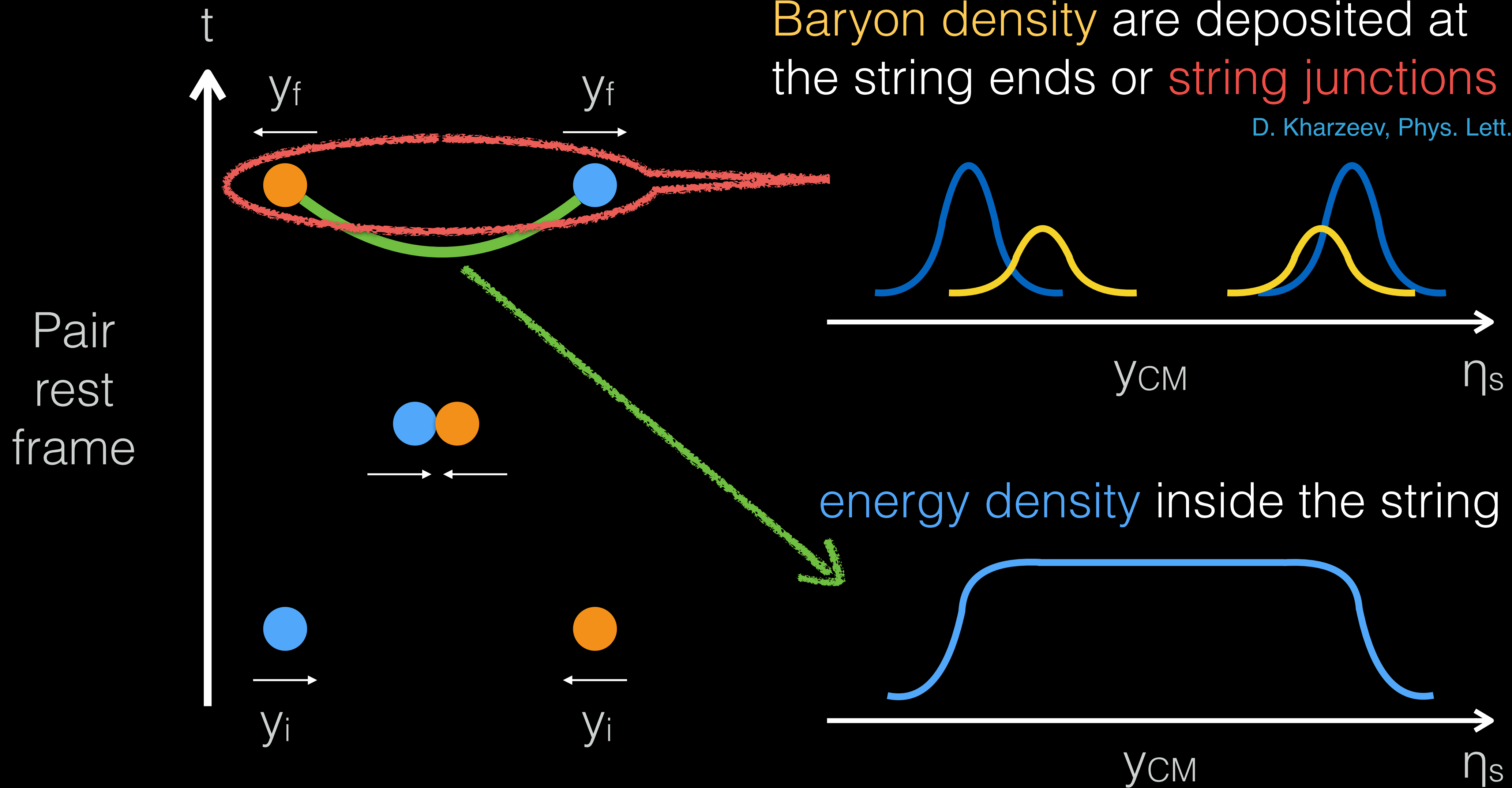


THE 3D MC-GLAUBER + STRING MODEL

C. Shen and B. Schenke, Phys.Rev. C97 (2018) 024907

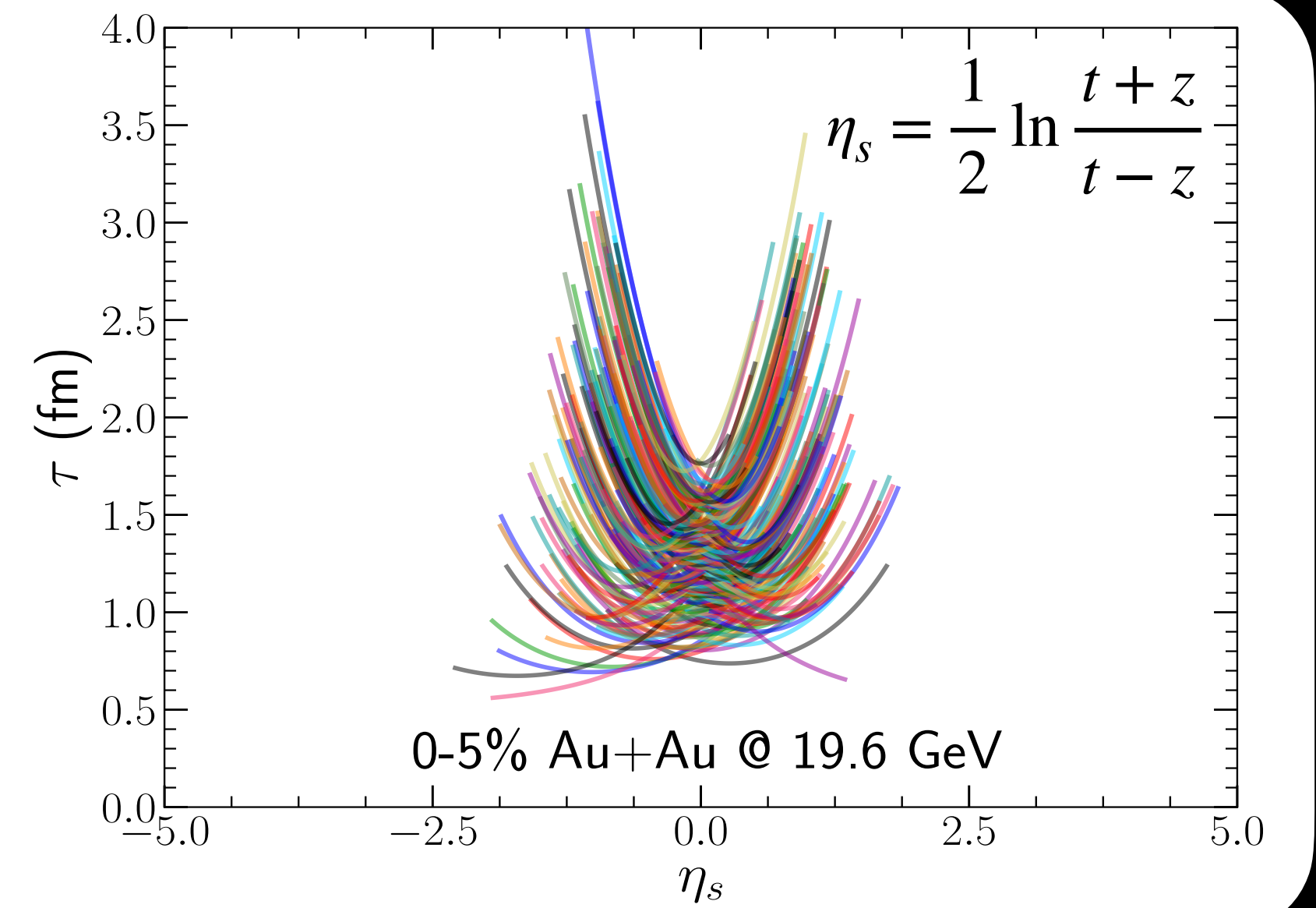
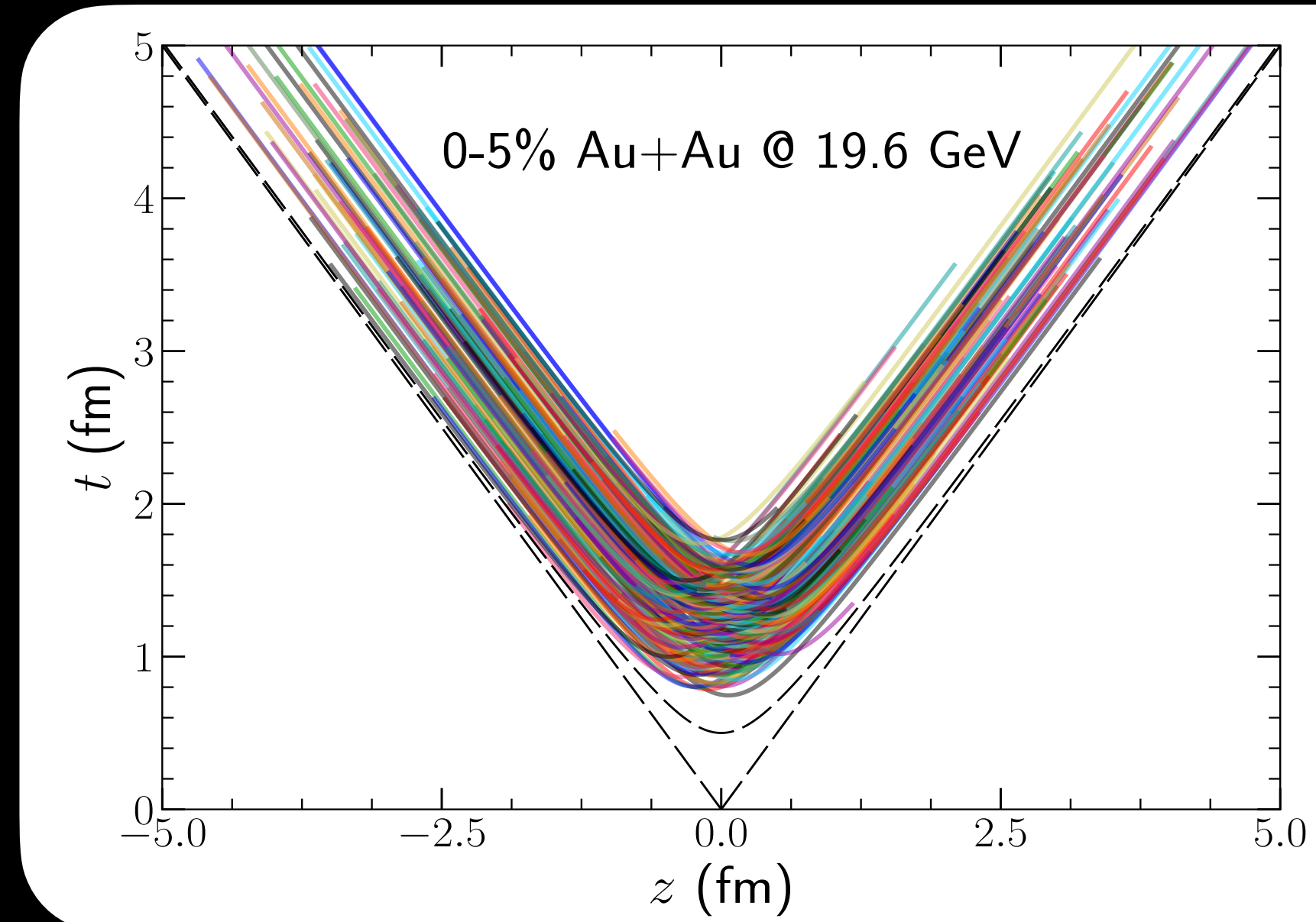
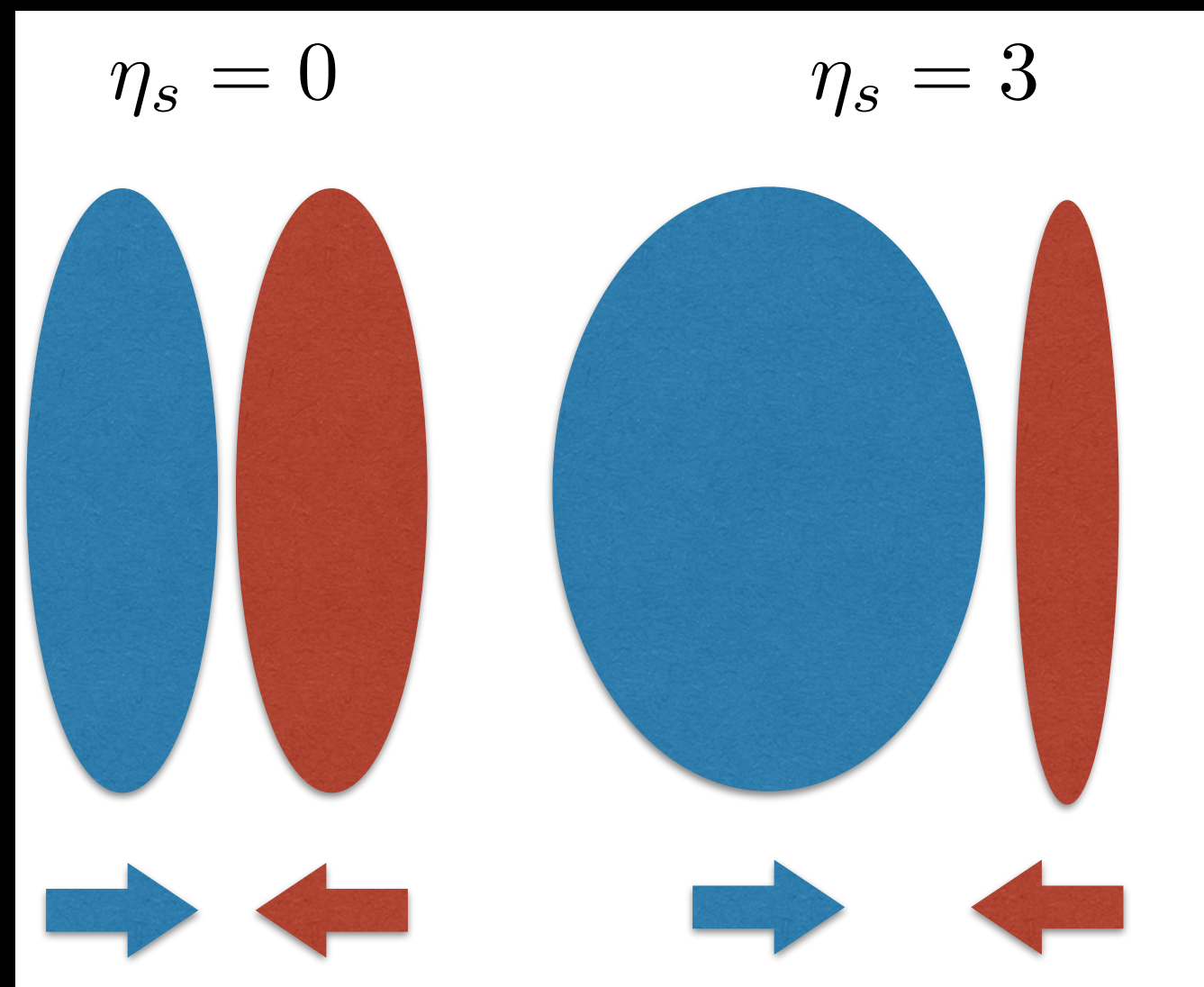
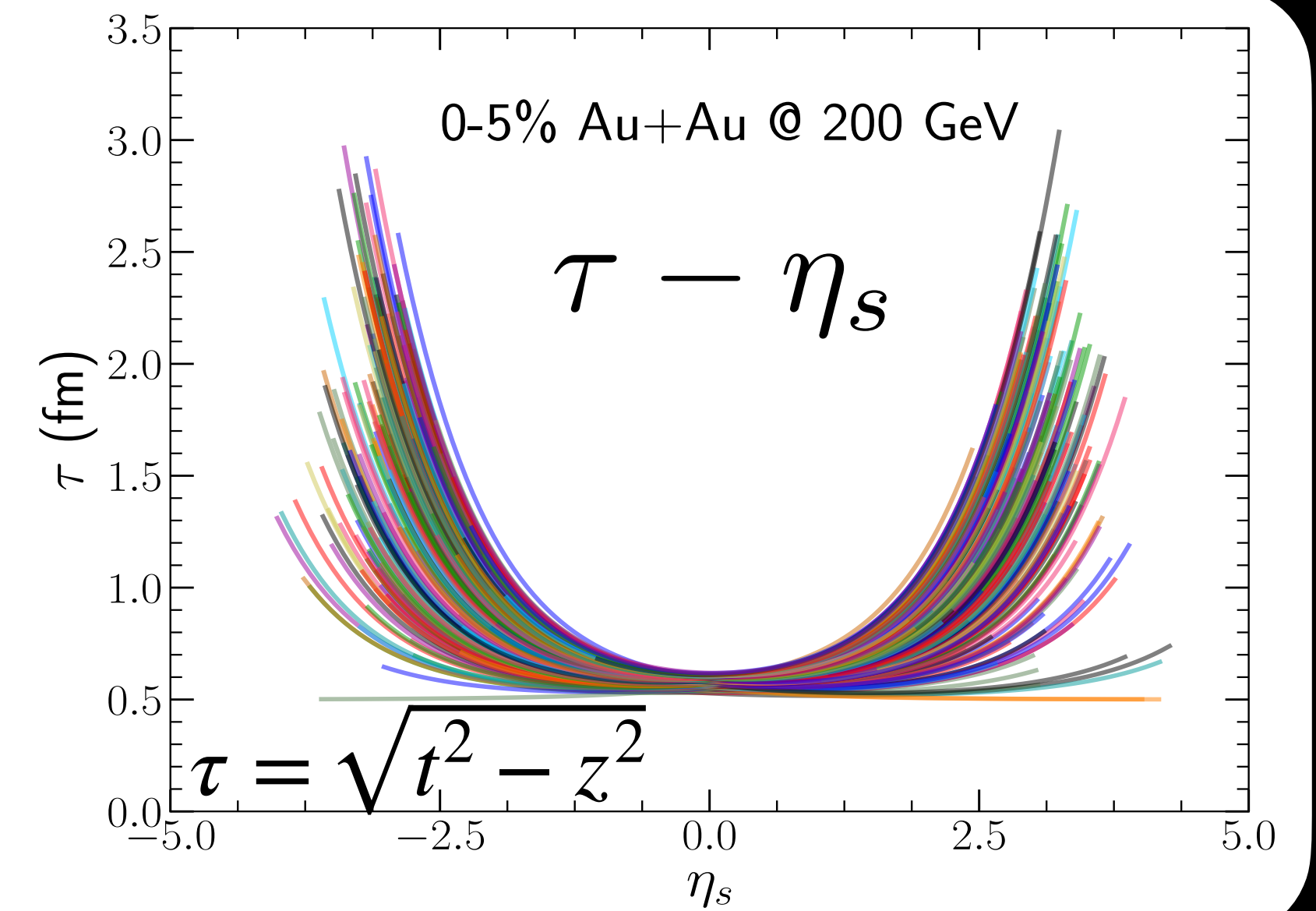
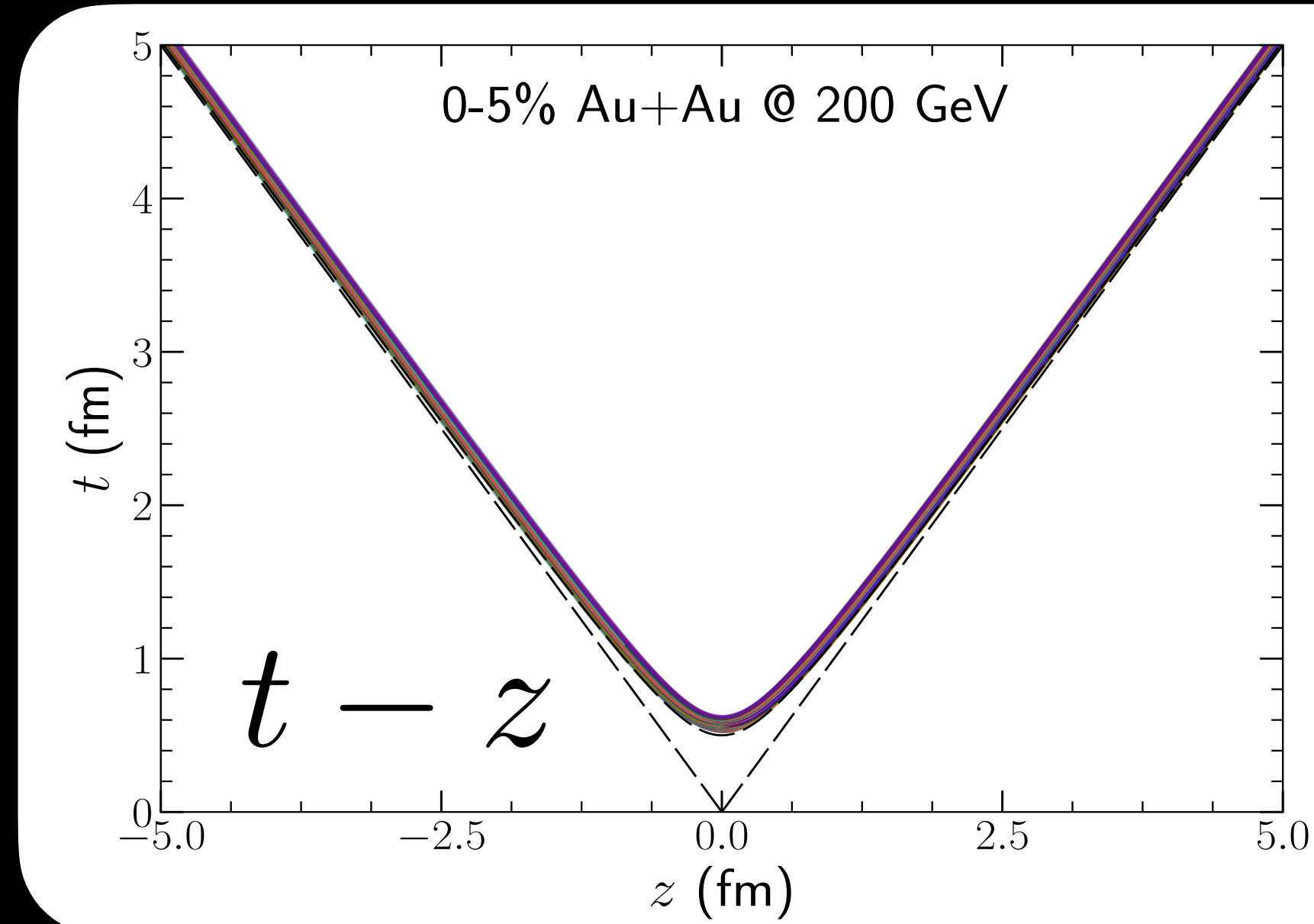
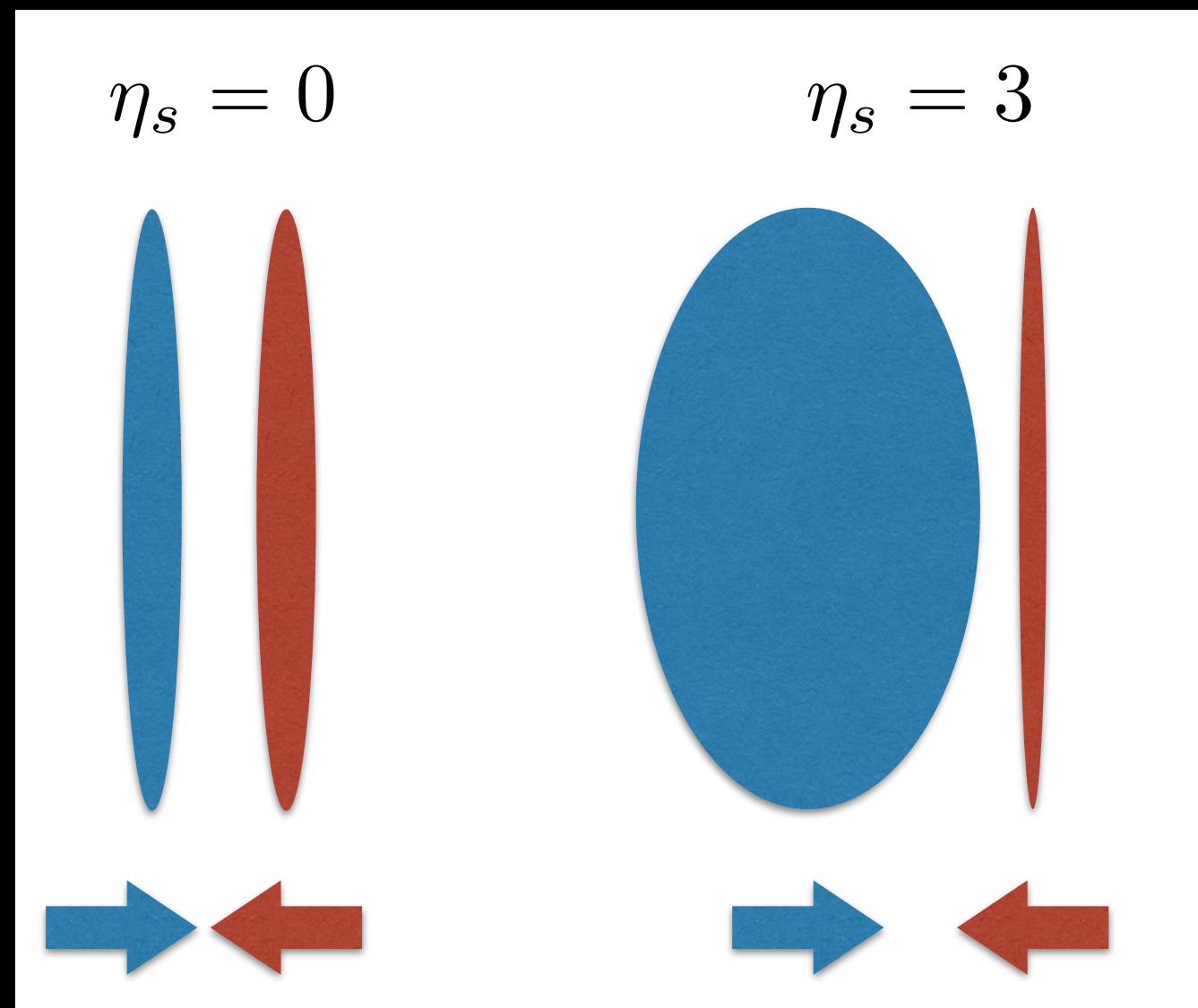
Baryon density are deposited at the string ends or **string junctions**

D. Kharzeev, Phys. Lett. B 378, 238 (1996)



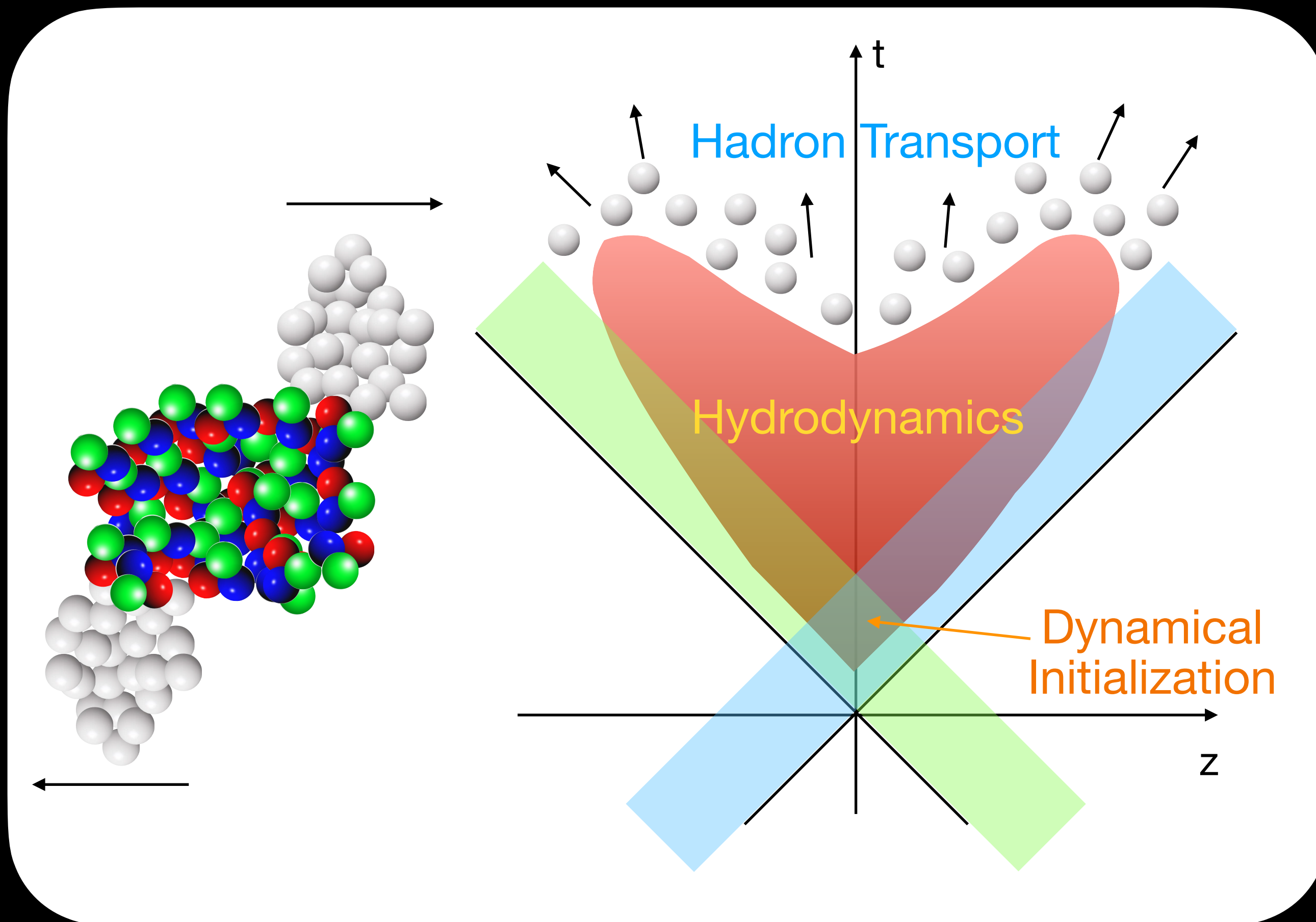
Imposed conservation for energy, momentum, and net baryon density

STRINGS' SPACE-TIME DISTRIBUTION



HYDRODYNAMICS WITH SOURCES

Energy-momentum current and net baryon density are fed into hydrodynamic simulation as source terms



$$\partial_{\mu} T^{\mu\nu} = J^{\nu}_{\text{source}}$$

$$\partial_{\mu} J^{\mu} = \rho_{\text{source}}$$

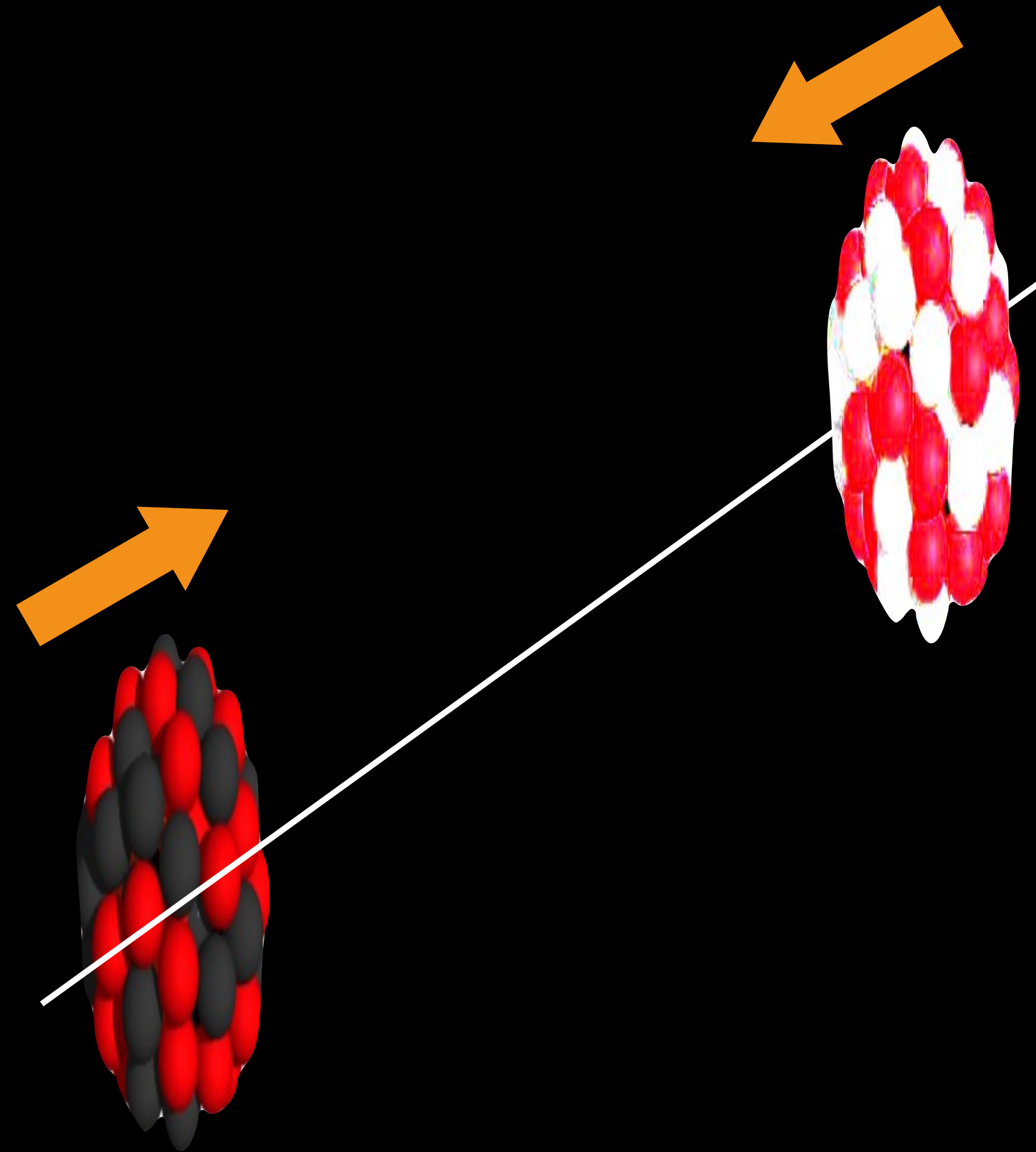
M. Okai, K. Kawaguchi, Y. Tachibana,
and T. Hirano, Phys. Rev. C95, 054914 (2017)

C. Shen and B. Schenke,
Phys. Rev. C97 (2018) 024907

L. Du, U. Heinz and G. Vujanovic,
Nucl. Phys. A982 (2019) 407-410

HYDRODYNAMICAL EVOLUTION WITH SOURCES

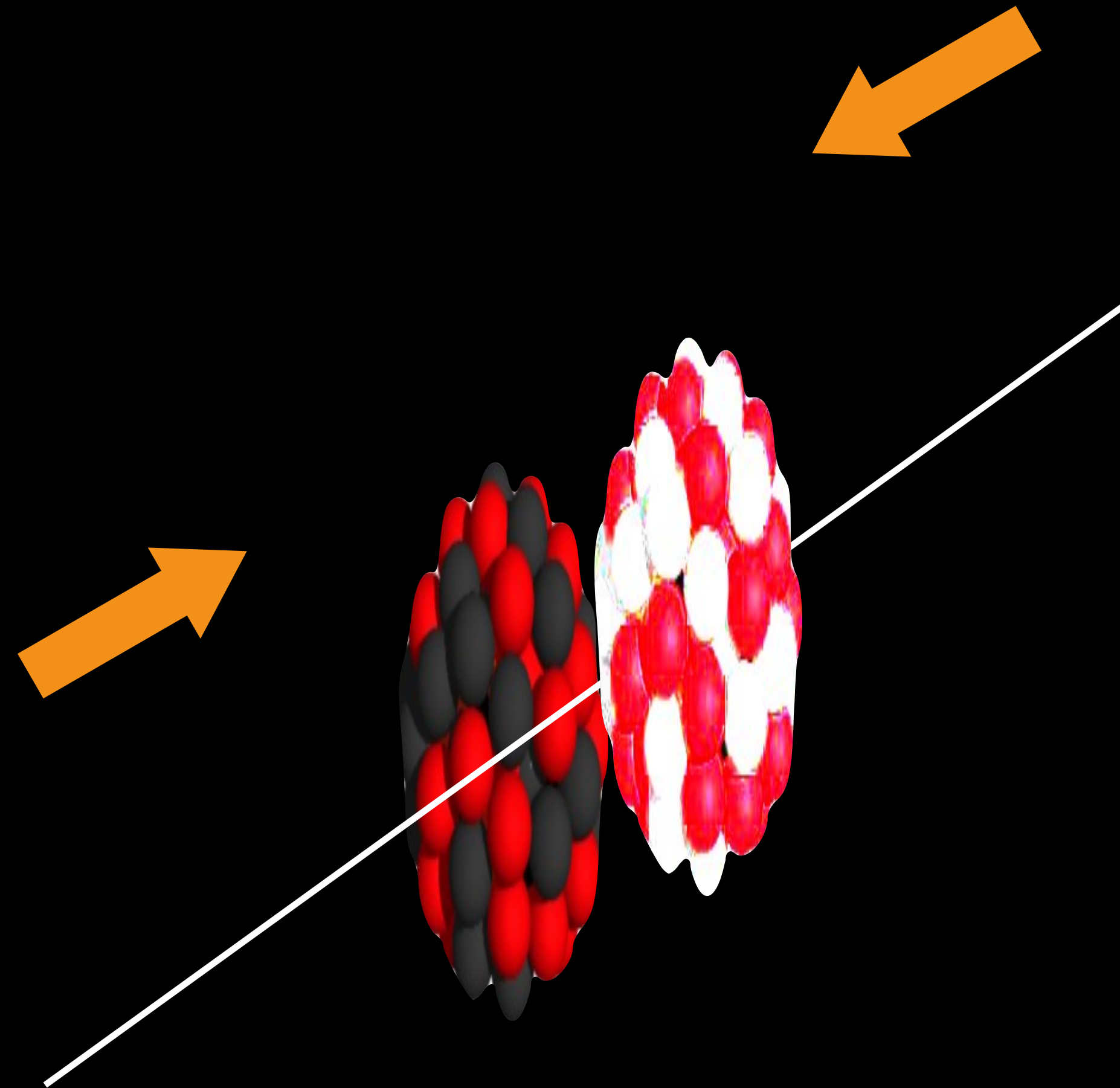
C. Shen and B. Schenke, Phys. Rev. C97 (2018) 024907



$$\sqrt{s_{NN}} = 19.6 \text{ GeV}$$

HYDRODYNAMICAL EVOLUTION WITH SOURCES

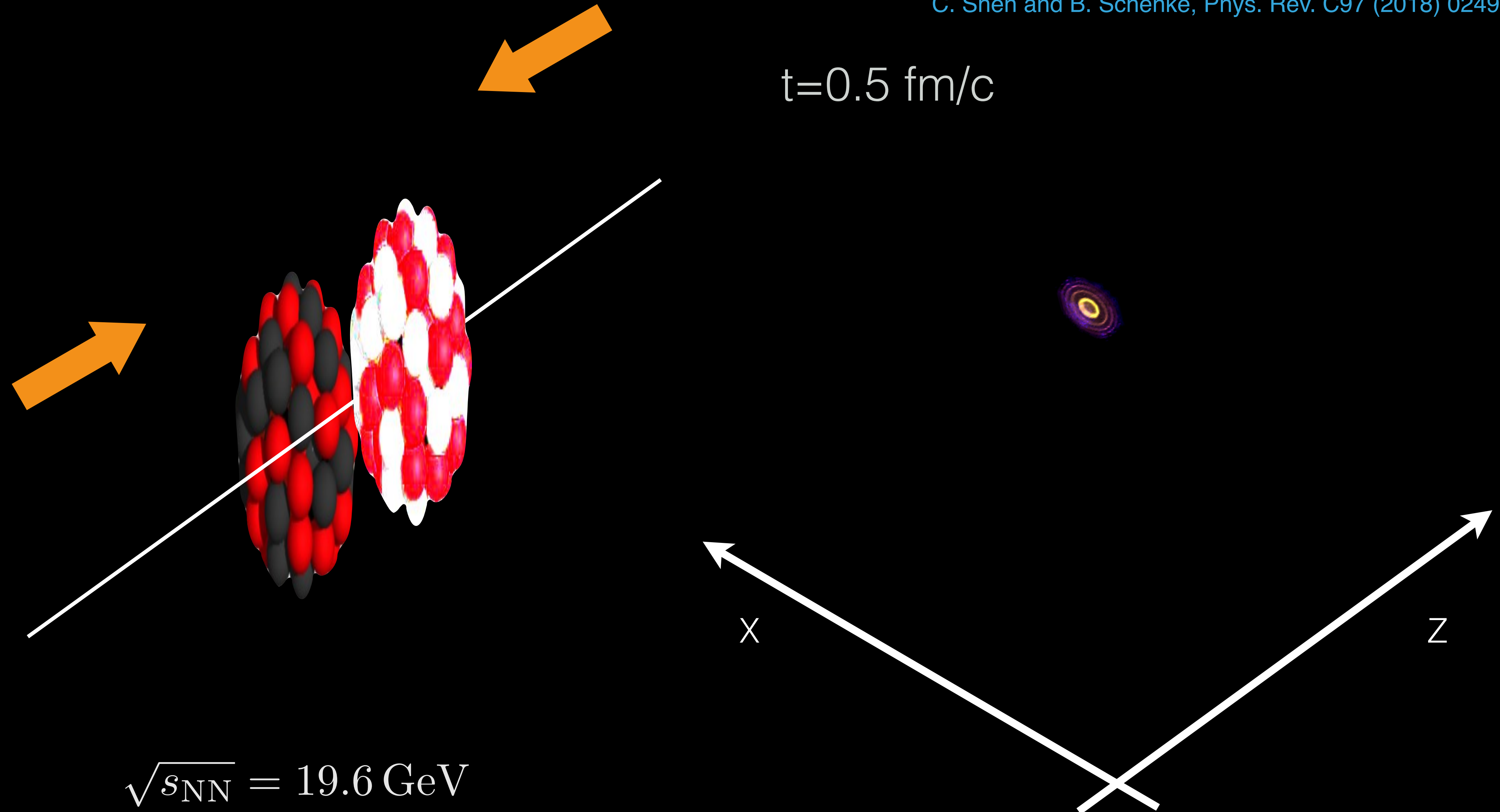
C. Shen and B. Schenke, Phys. Rev. C97 (2018) 024907



$$\sqrt{s_{\text{NN}}} = 19.6 \text{ GeV}$$

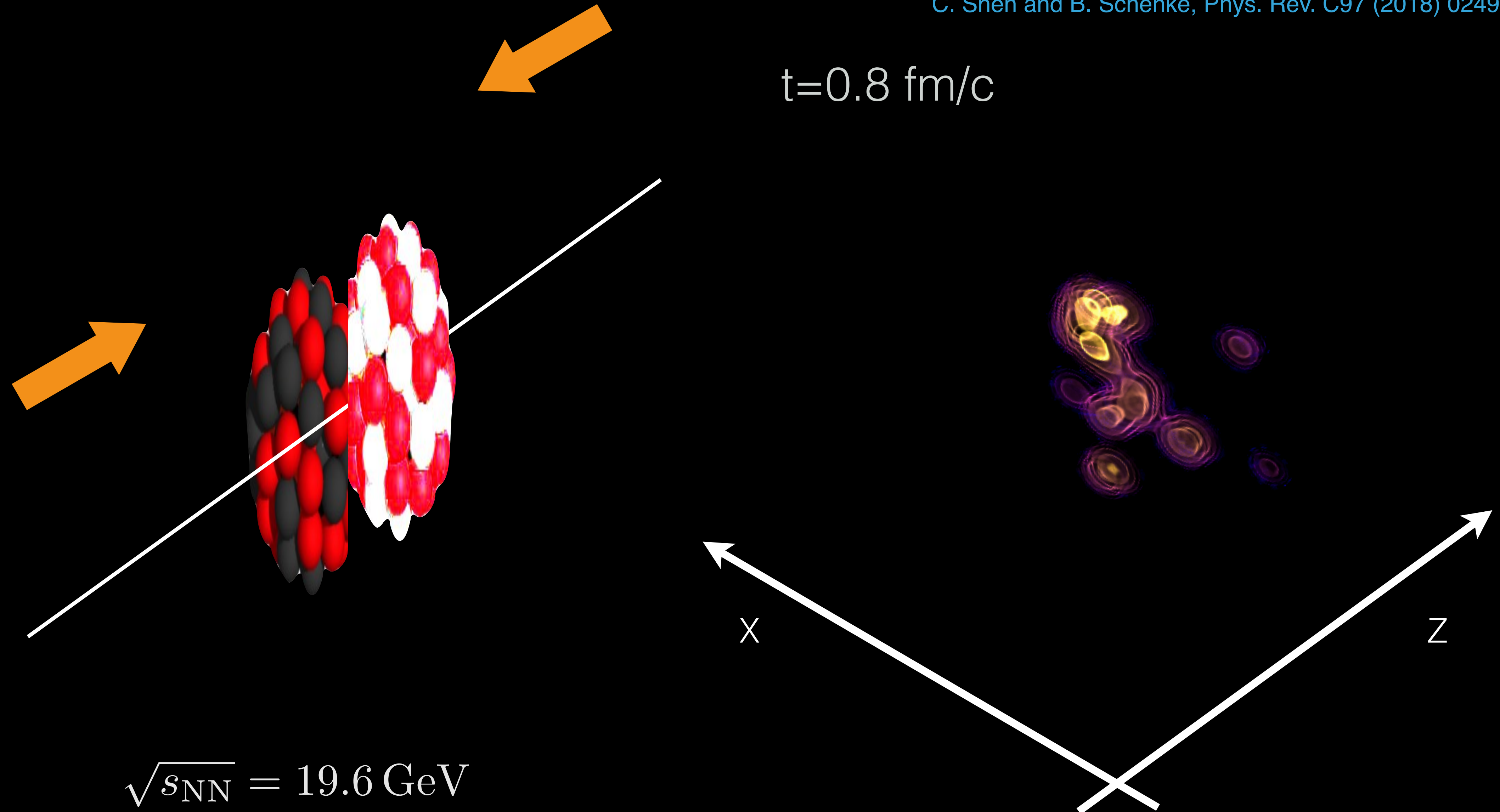
HYDRODYNAMICAL EVOLUTION WITH SOURCES

C. Shen and B. Schenke, Phys. Rev. C97 (2018) 024907



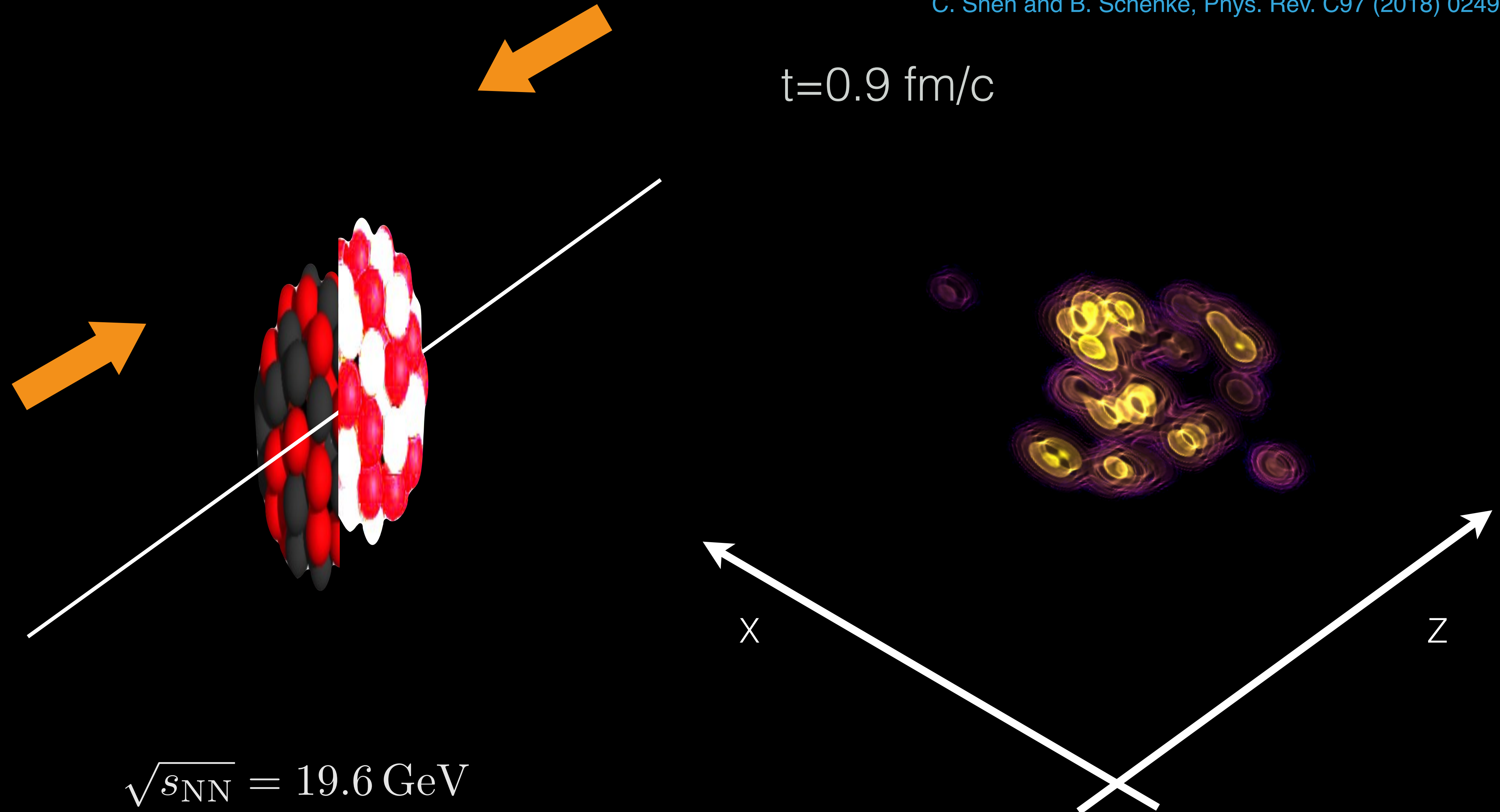
HYDRODYNAMICAL EVOLUTION WITH SOURCES

C. Shen and B. Schenke, Phys. Rev. C97 (2018) 024907



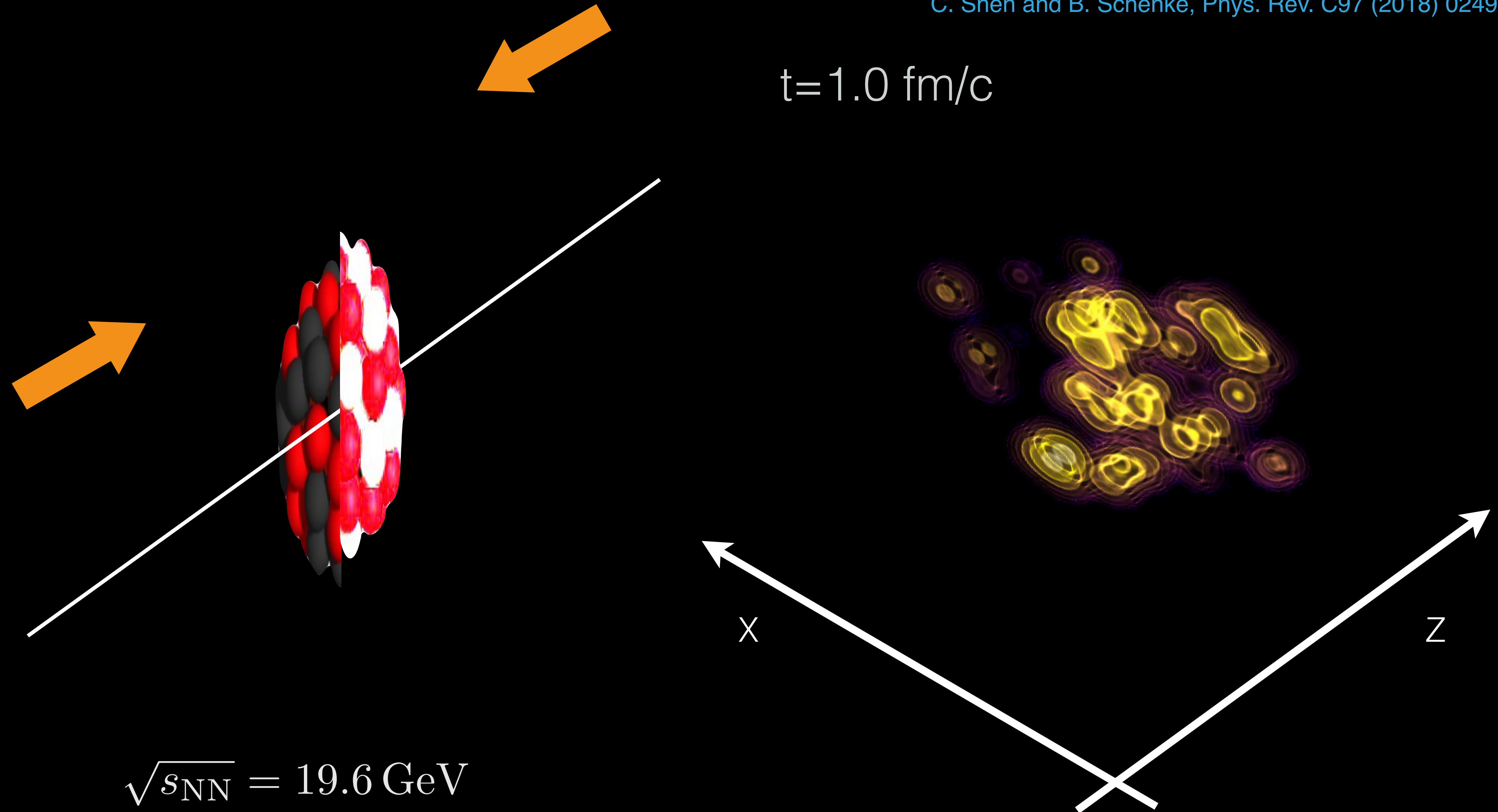
HYDRODYNAMICAL EVOLUTION WITH SOURCES

C. Shen and B. Schenke, Phys. Rev. C97 (2018) 024907



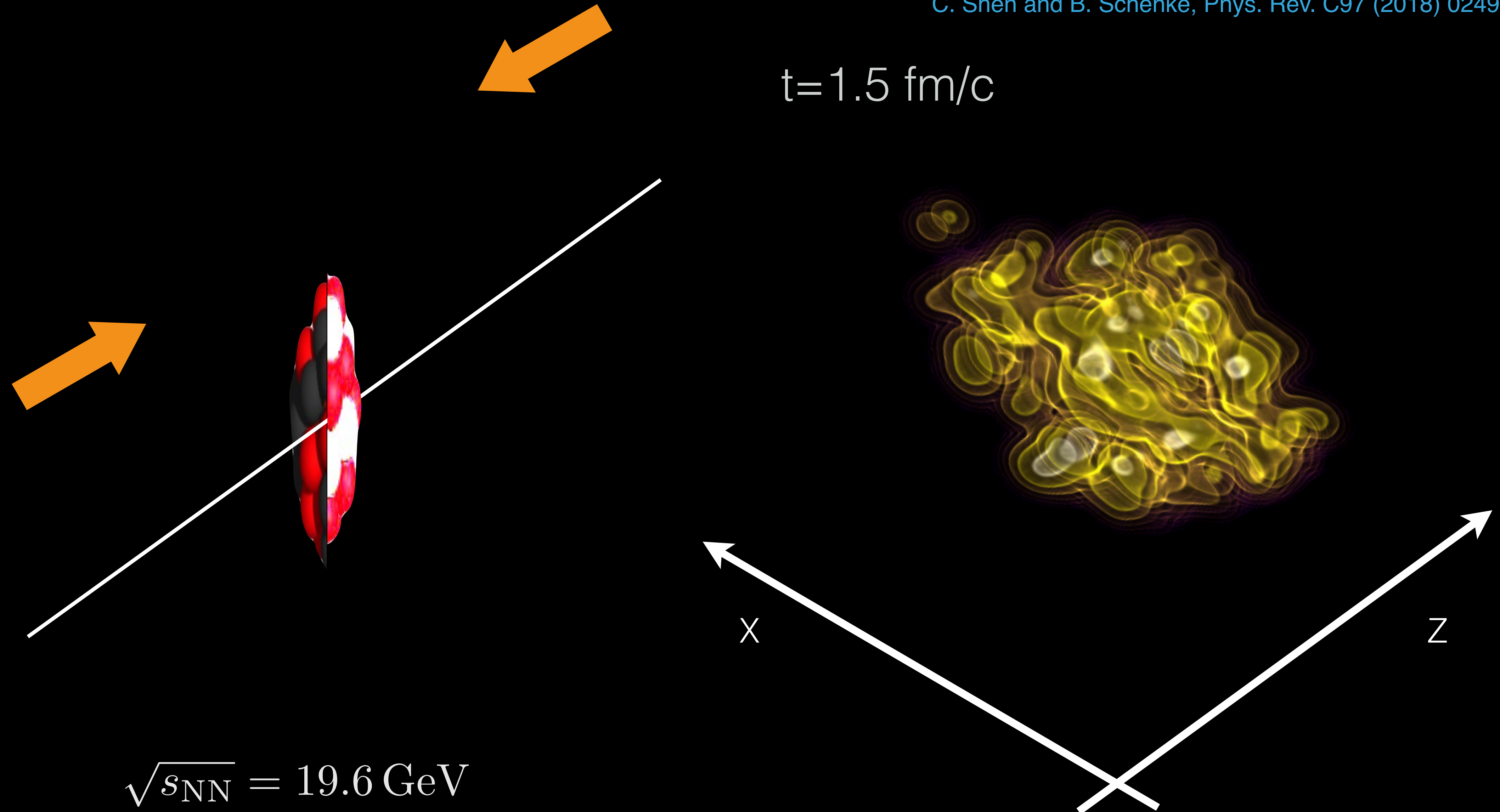
HYDRODYNAMICAL EVOLUTION WITH SOURCES

C. Shen and B. Schenke, Phys. Rev. C97 (2018) 024907



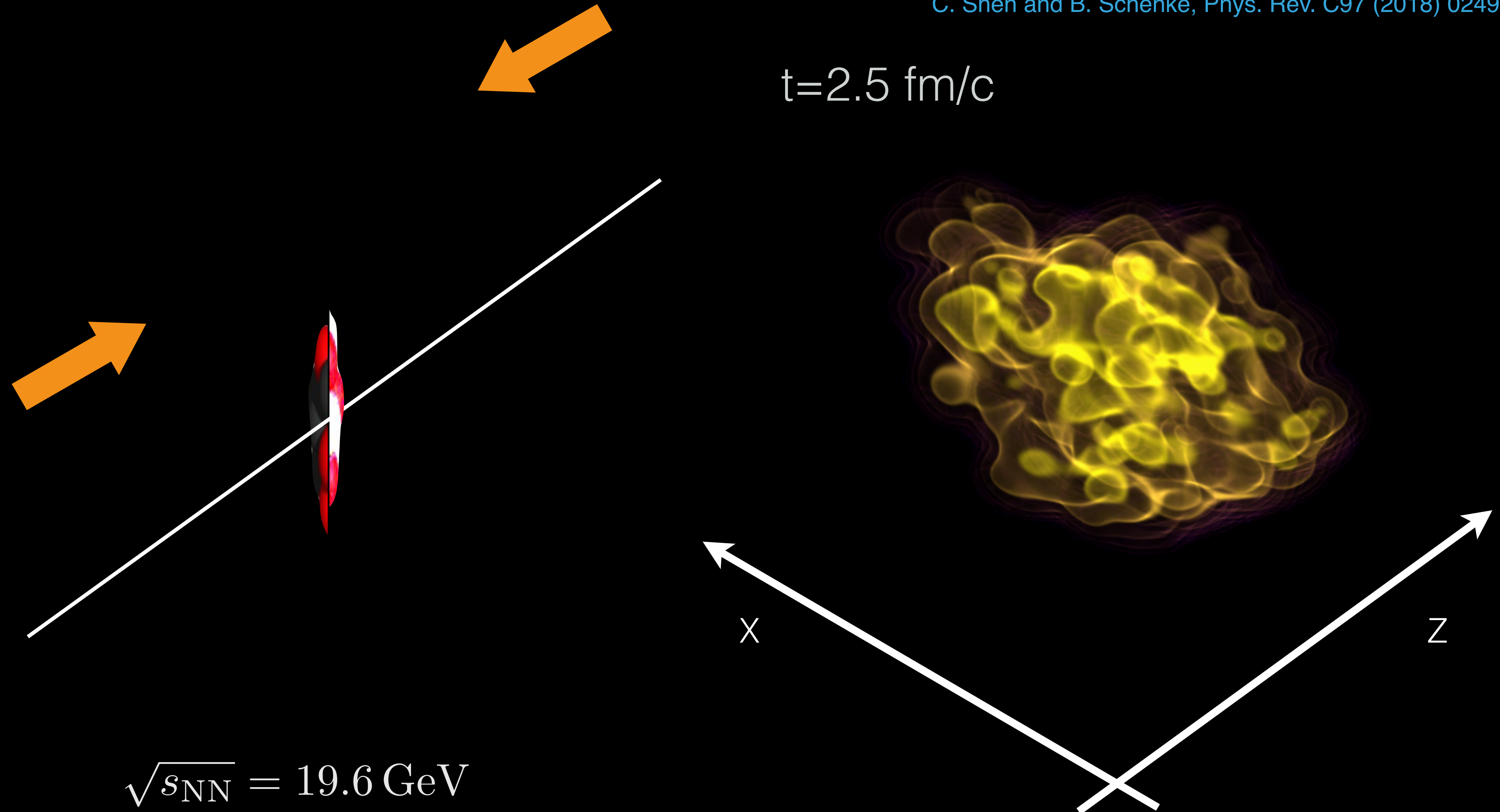
HYDRODYNAMICAL EVOLUTION WITH SOURCES

C. Shen and B. Schenke, Phys. Rev. C97 (2018) 024907



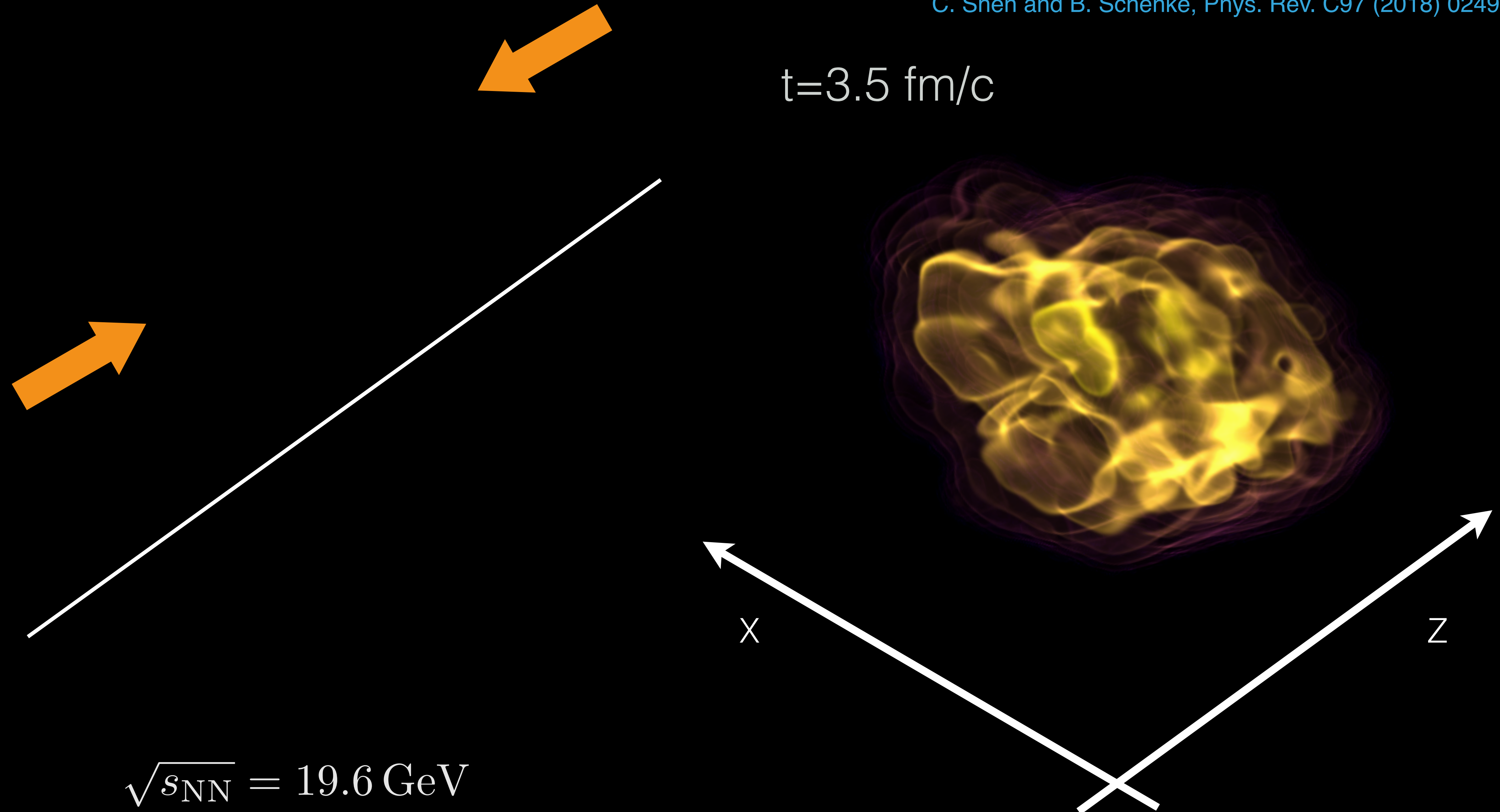
HYDRODYNAMICAL EVOLUTION WITH SOURCES

C. Shen and B. Schenke, Phys. Rev. C97 (2018) 024907



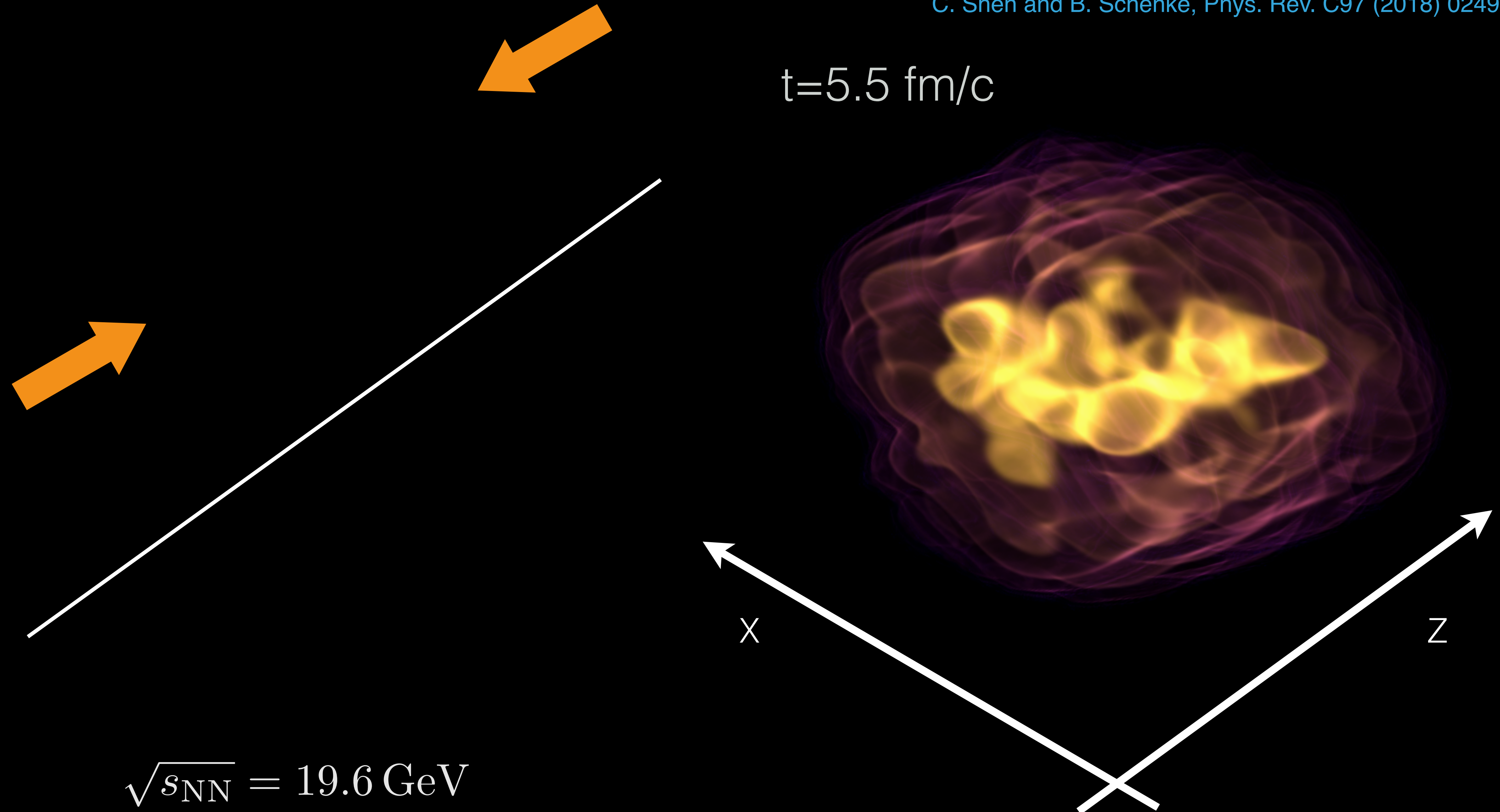
HYDRODYNAMICAL EVOLUTION WITH SOURCES

C. Shen and B. Schenke, Phys. Rev. C97 (2018) 024907



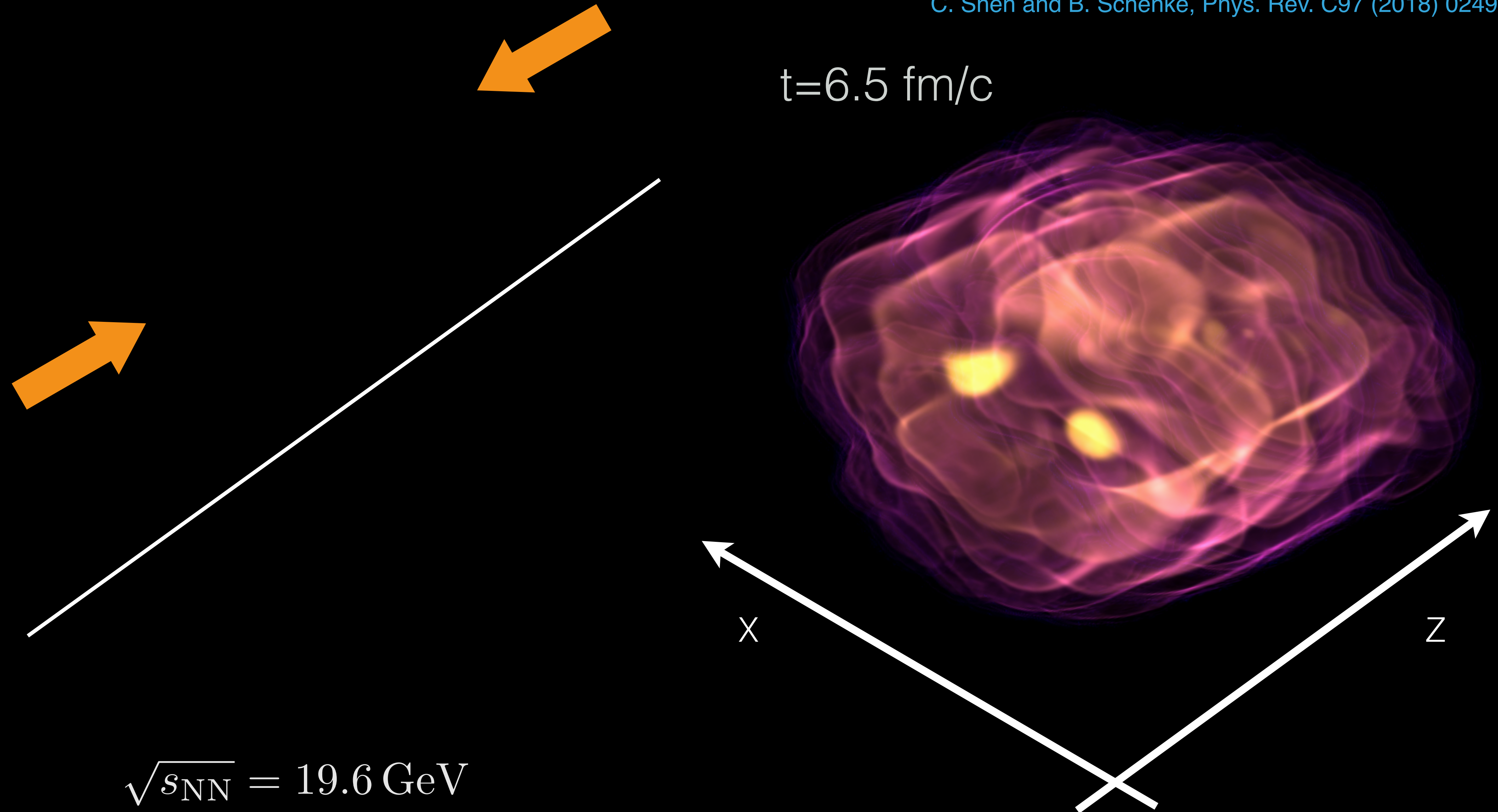
HYDRODYNAMICAL EVOLUTION WITH SOURCES

C. Shen and B. Schenke, Phys. Rev. C97 (2018) 024907



HYDRODYNAMICAL EVOLUTION WITH SOURCES

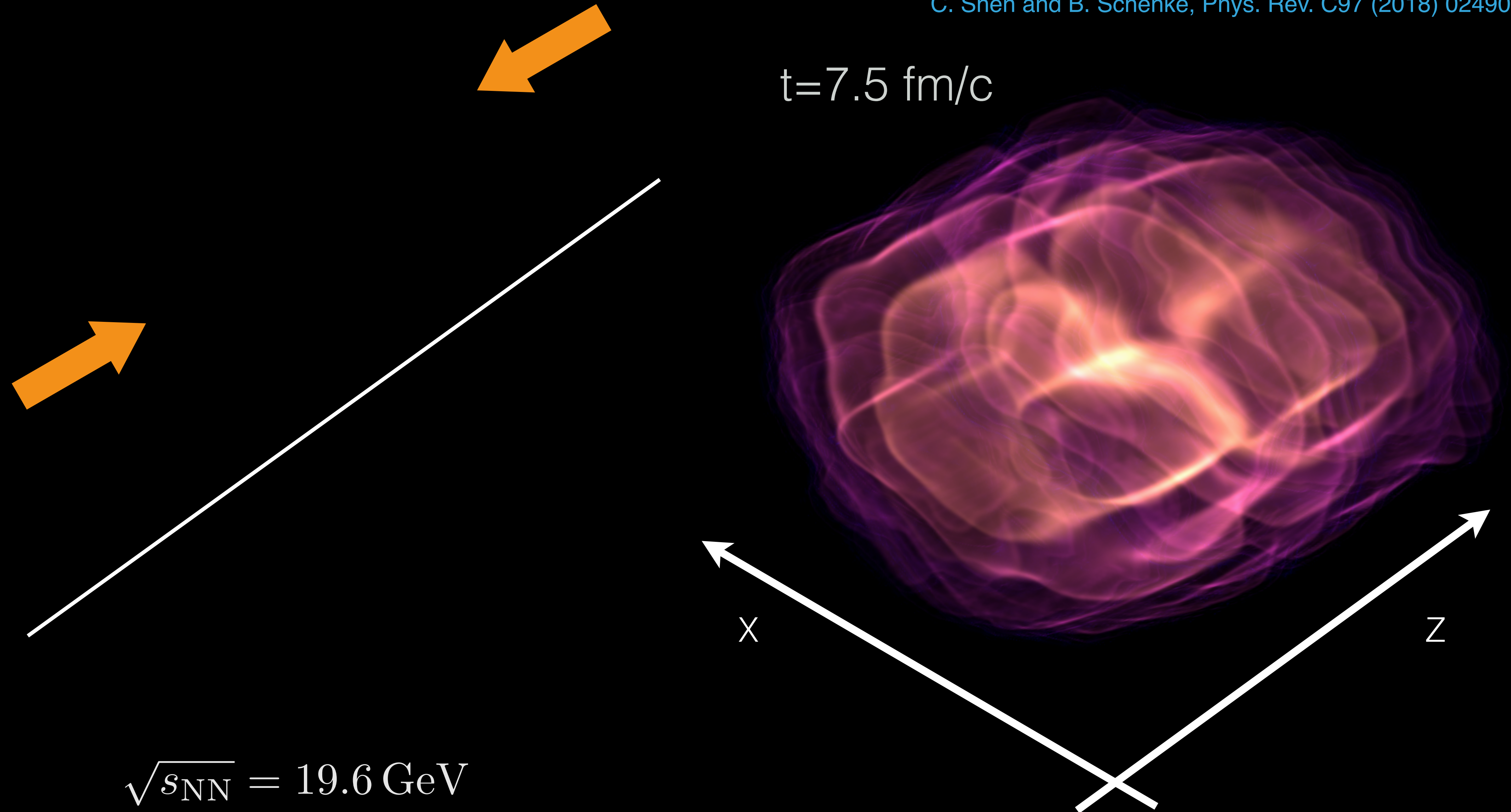
C. Shen and B. Schenke, Phys. Rev. C97 (2018) 024907



$$\sqrt{s_{NN}} = 19.6 \text{ GeV}$$

HYDRODYNAMICAL EVOLUTION WITH SOURCES

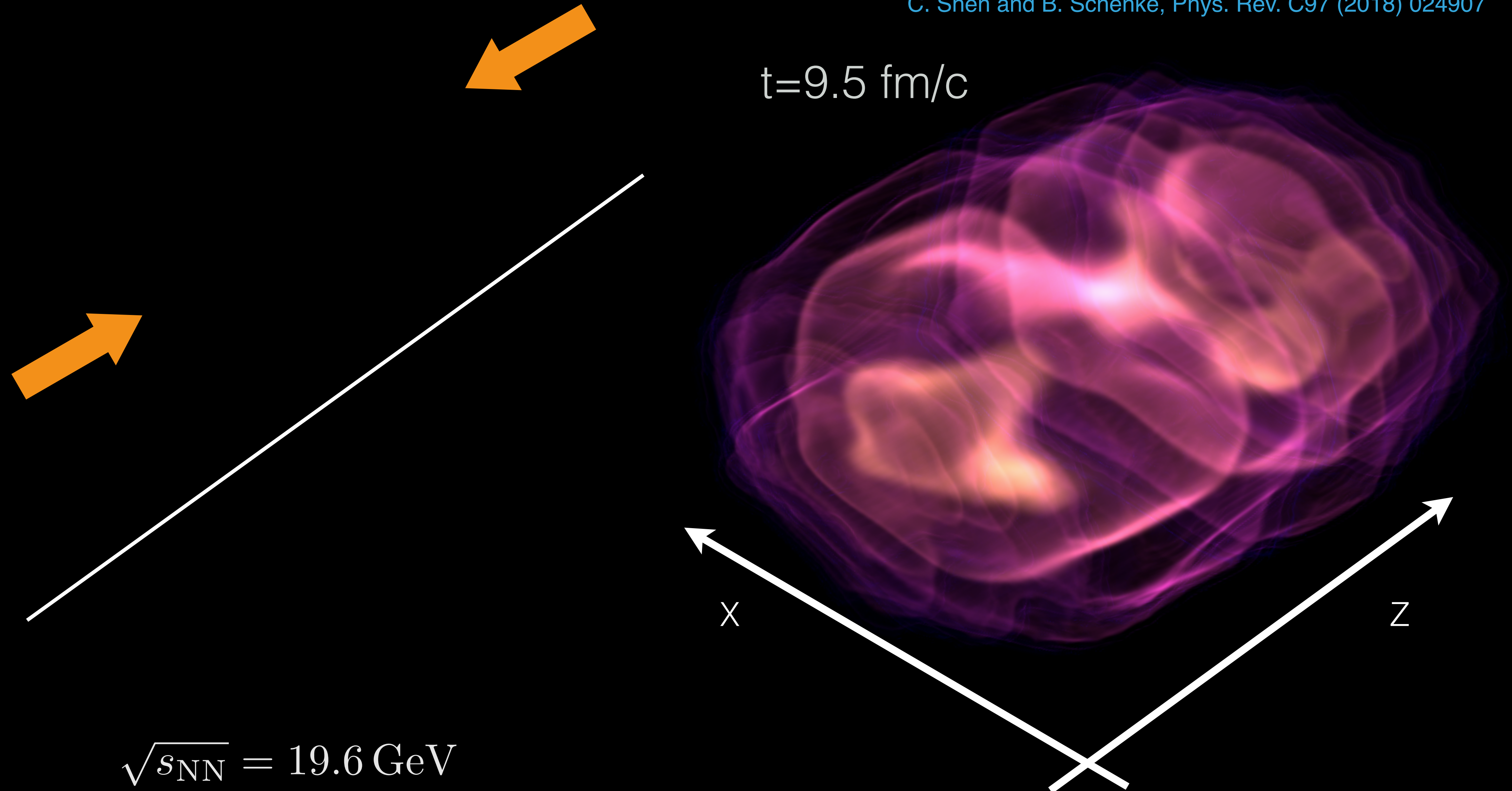
C. Shen and B. Schenke, Phys. Rev. C97 (2018) 024907



$$\sqrt{s_{\text{NN}}} = 19.6 \text{ GeV}$$

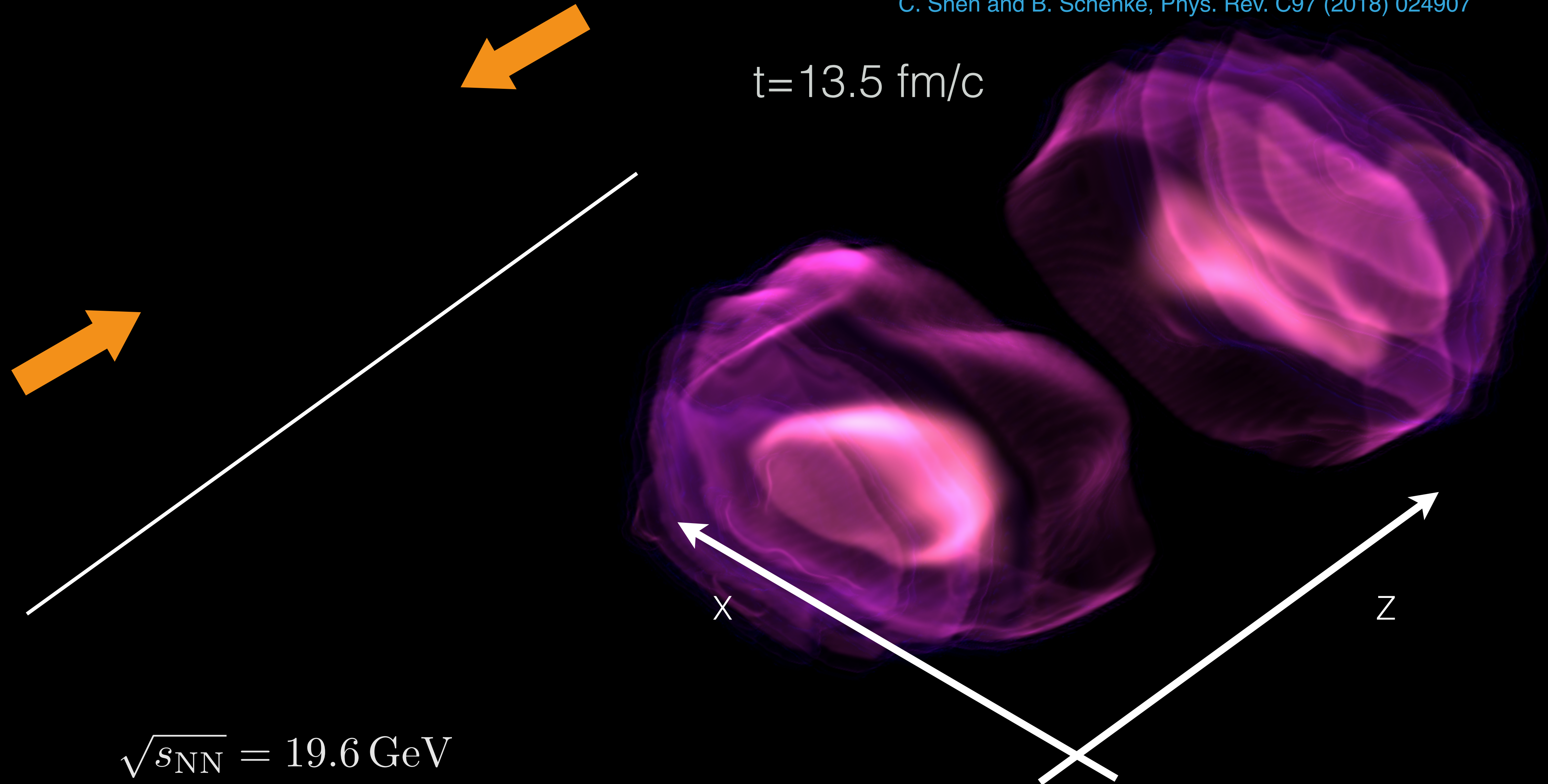
HYDRODYNAMICAL EVOLUTION WITH SOURCES

C. Shen and B. Schenke, Phys. Rev. C97 (2018) 024907



HYDRODYNAMICAL EVOLUTION WITH SOURCES

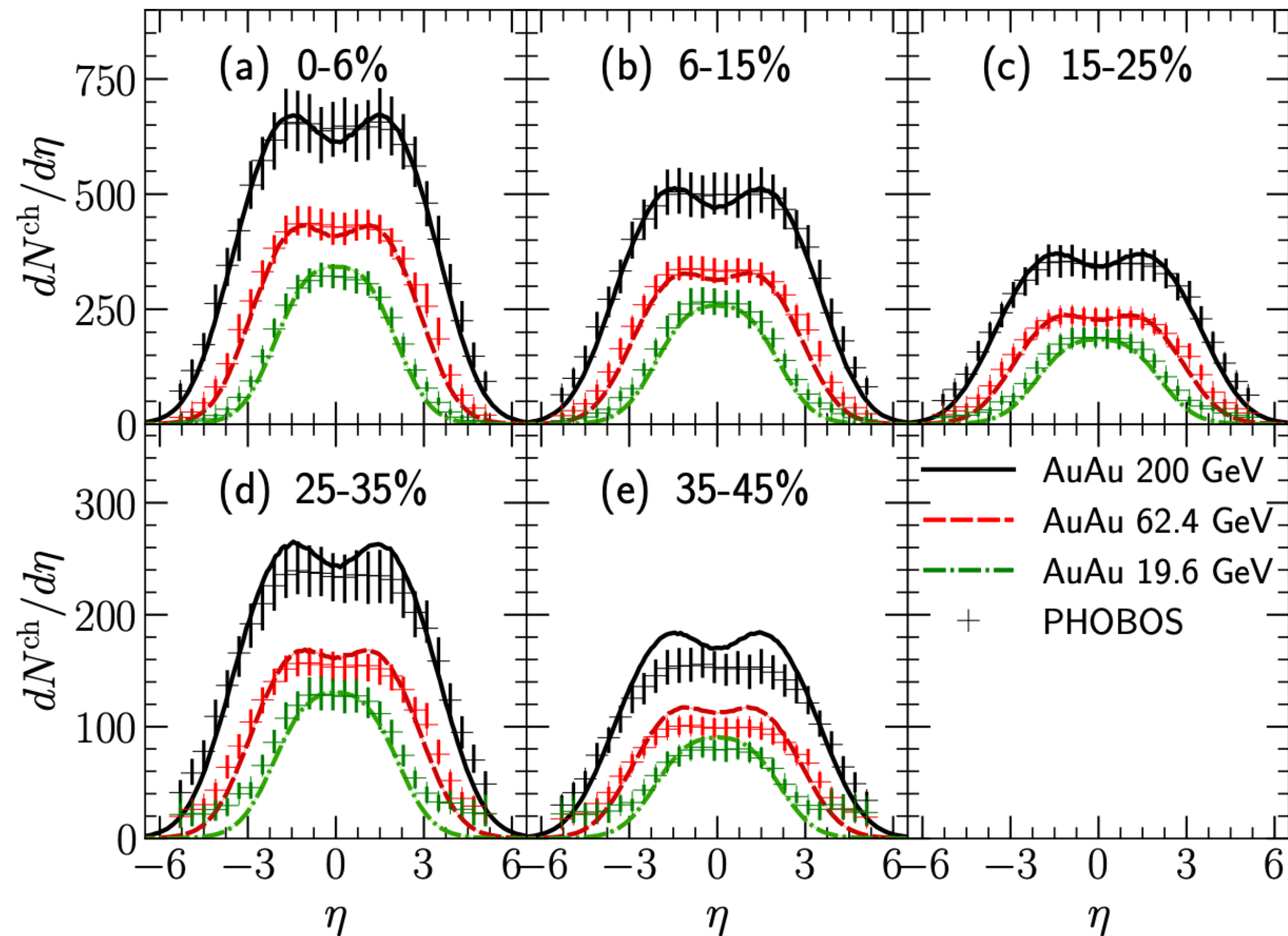
C. Shen and B. Schenke, Phys. Rev. C97 (2018) 024907



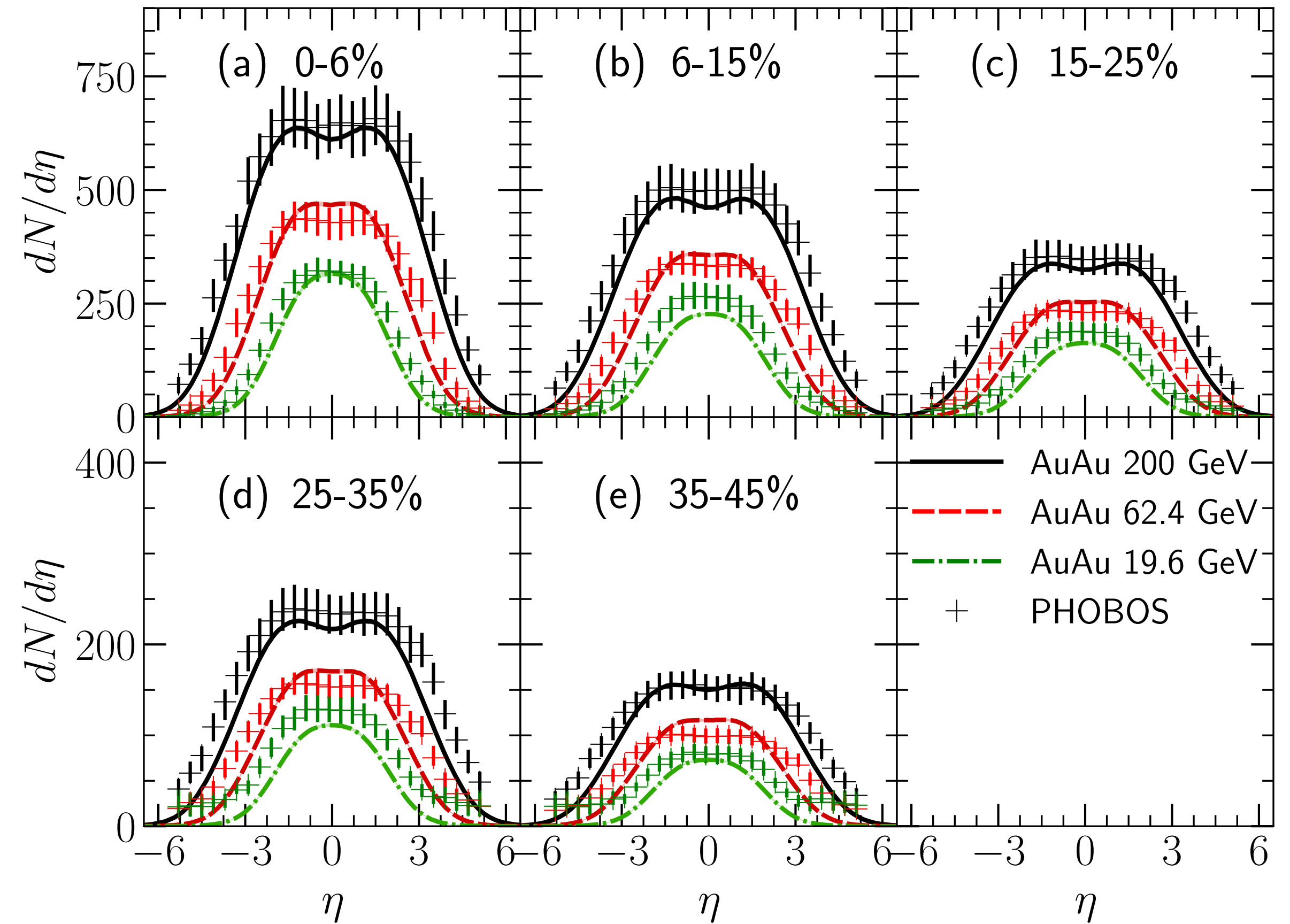
EVENT-BY-EVENT FLUCTUATIONS AT THE RHIC BES

B. Schenke and C. Shen, in preparation

Event-averaged simulations



Event-by-event with dynamical initialization

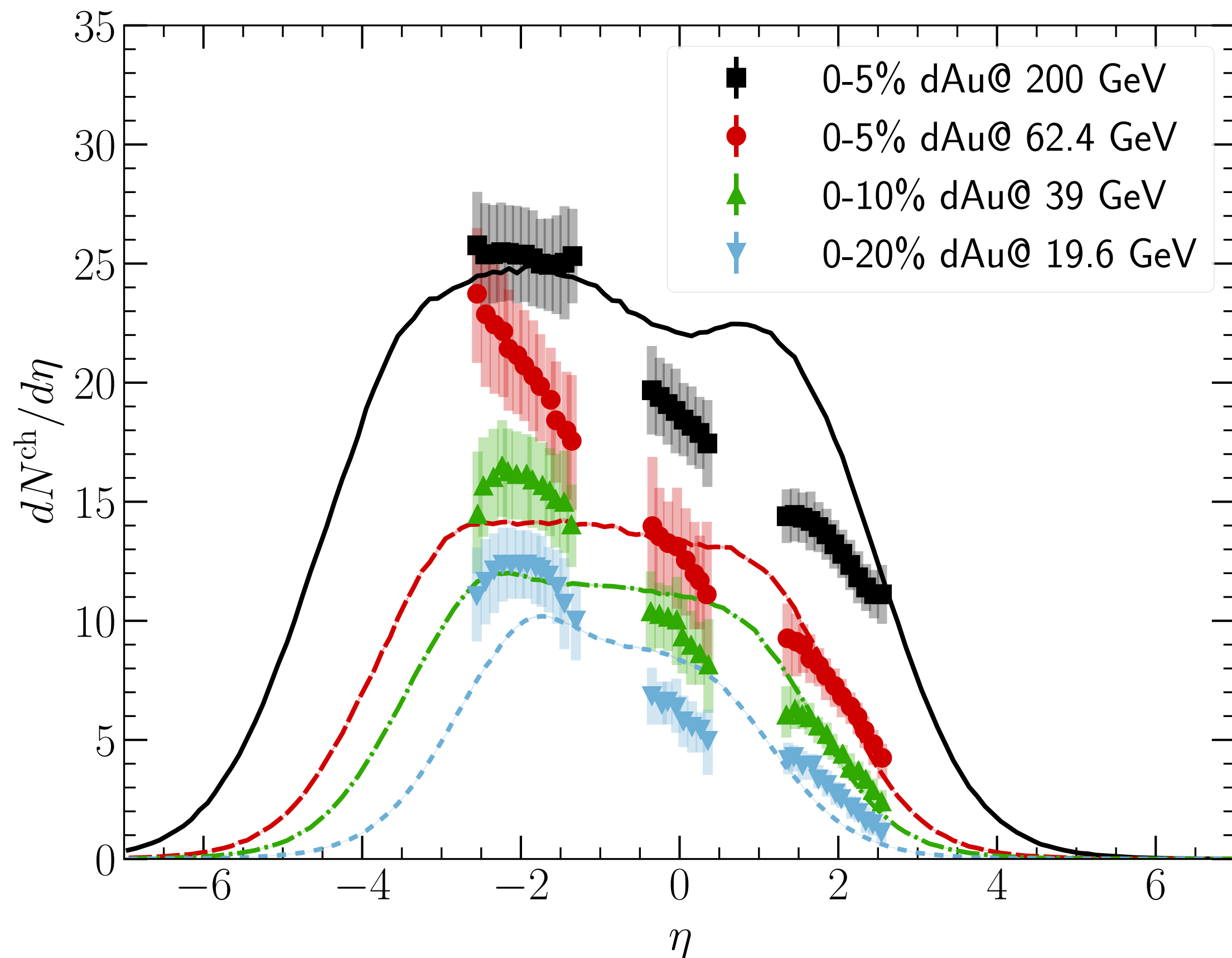


- A good description of particle productions in AuAu collisions

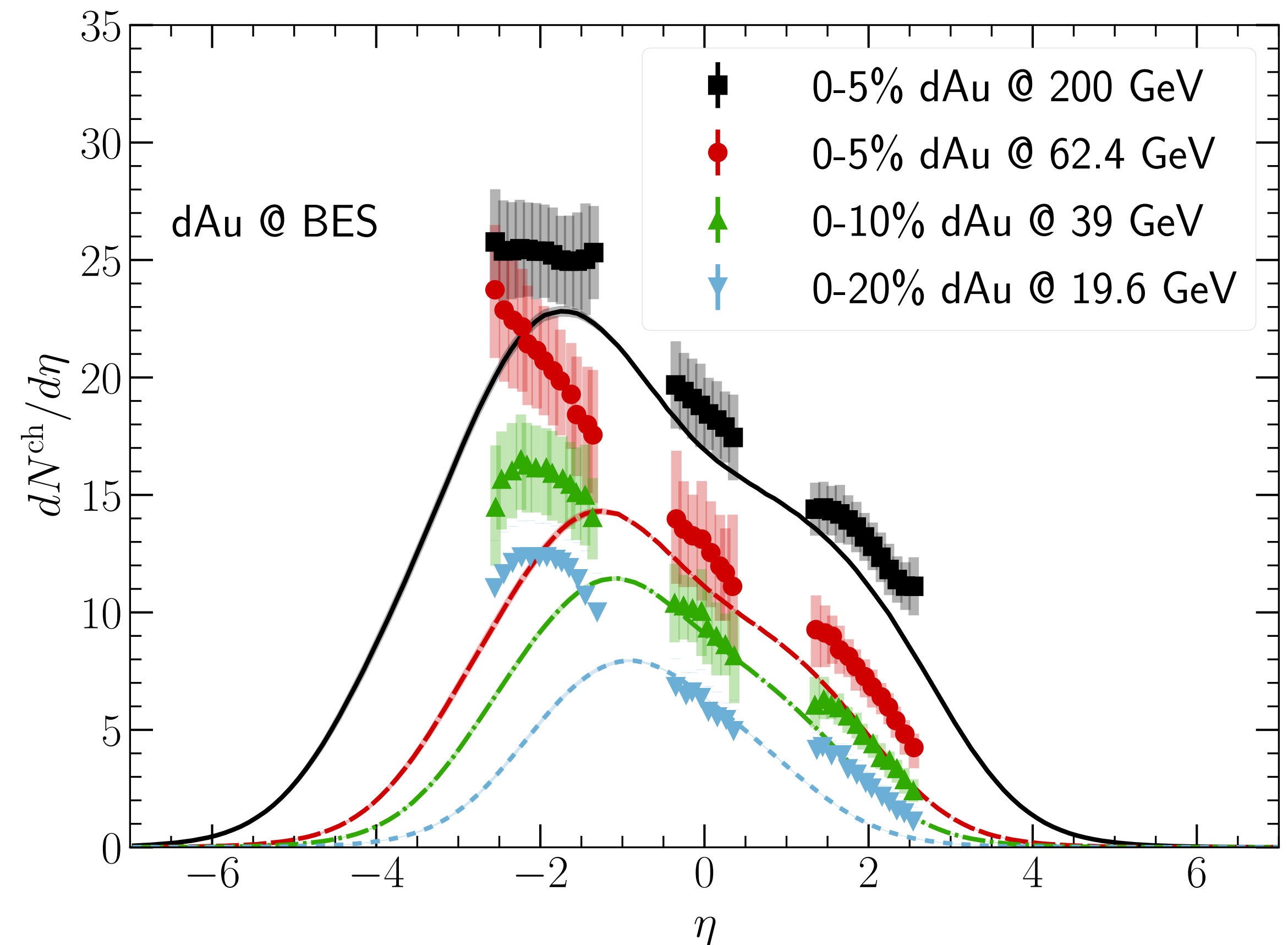
3D DESCRIPTION OF SMALL SYSTEMS AT THE RHIC BES

B. Schenke and C. Shen, in preparation

Event-averaged simulations



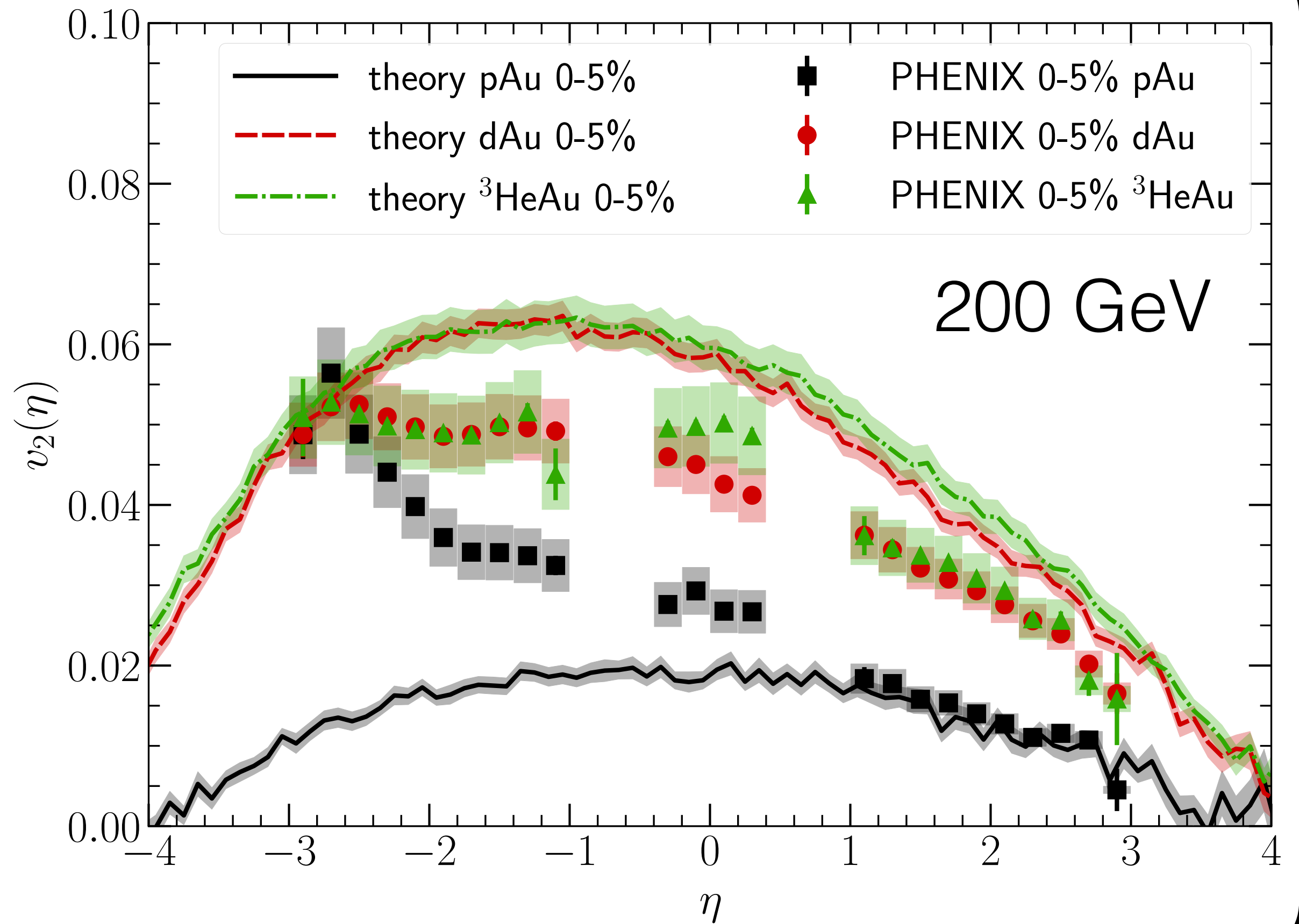
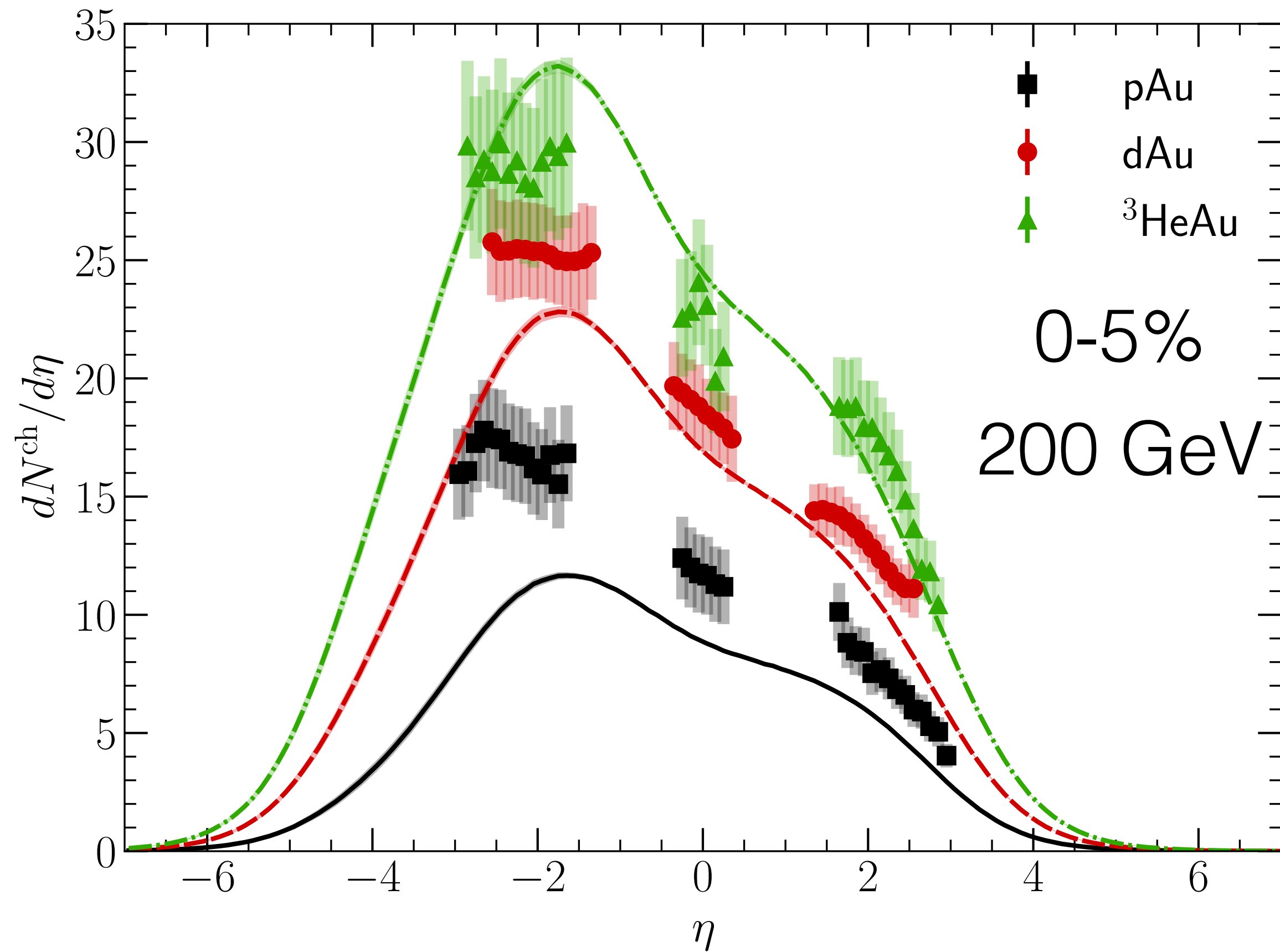
Event-by-event with dynamical initialization



- The event-by-event simulations give a better prediction for particle productions in d+Au collisions at RHIC BES

3D DESCRIPTION OF SMALL SYSTEMS AT THE RHIC BES

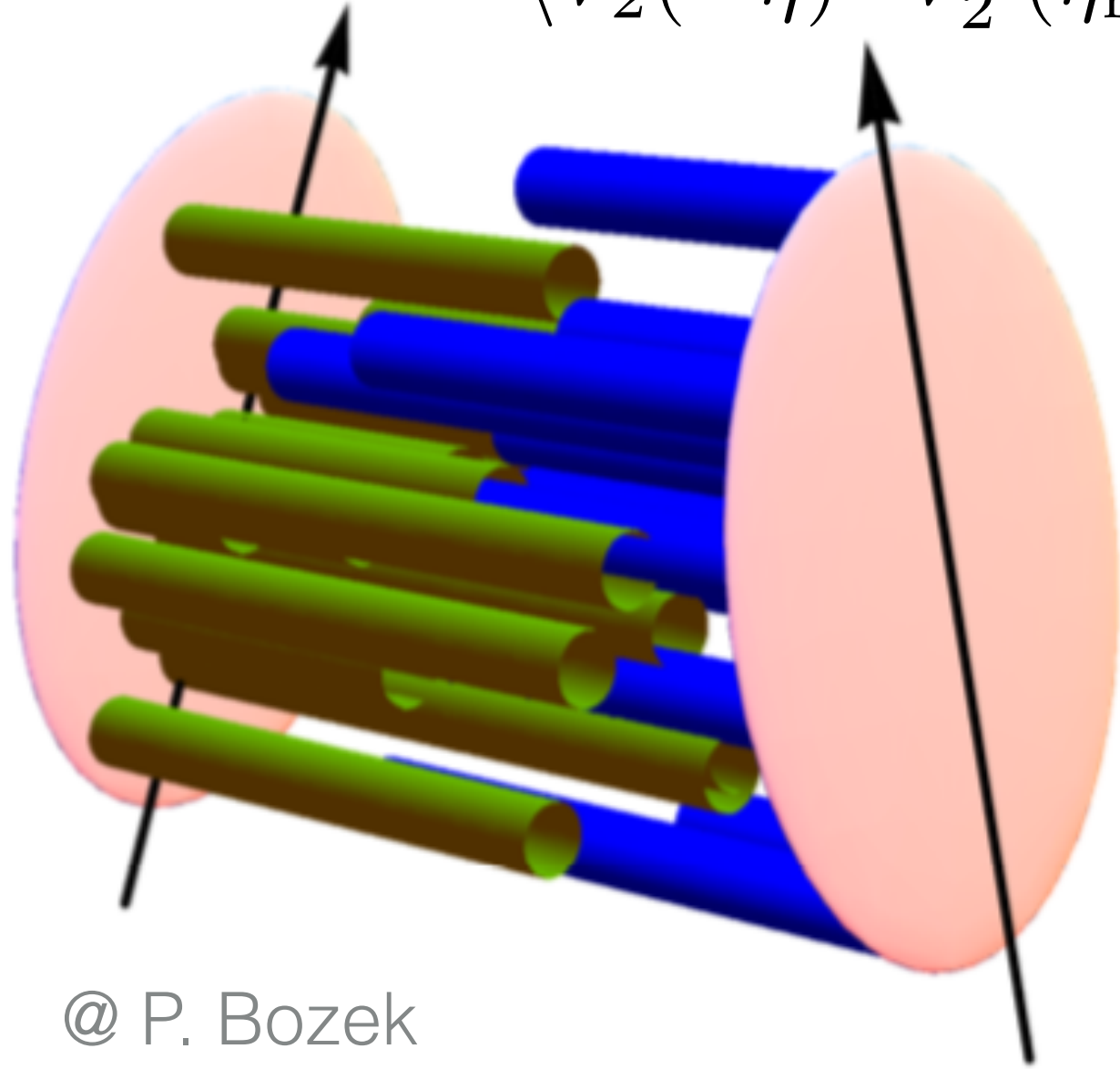
B. Schenke and C. Shen, in preparation



- A good starting point to study longitudinal fluctuations in asymmetric systems at RHIC

CONSTRAINING LONGITUDINAL FLUCTUATIONS

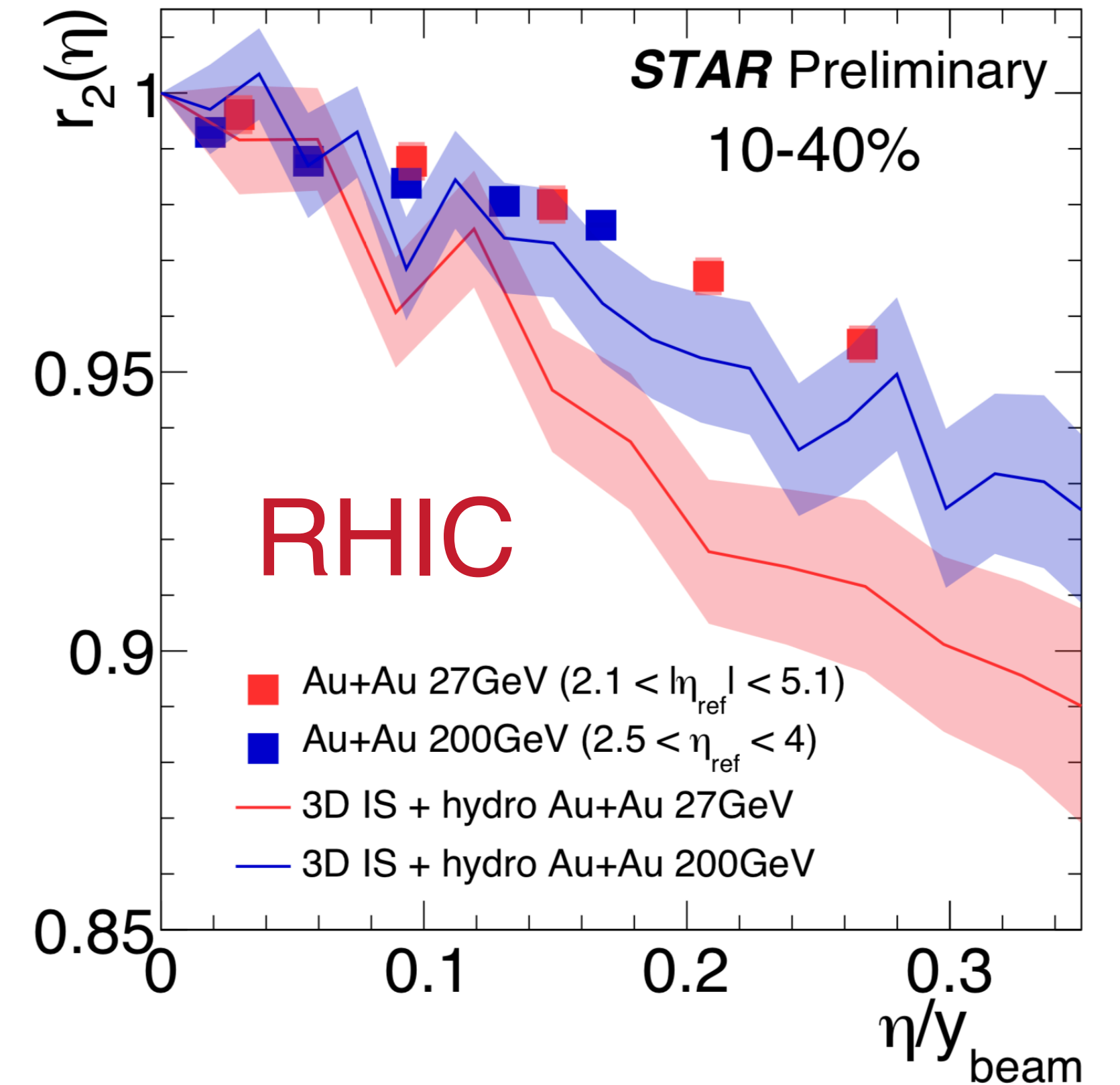
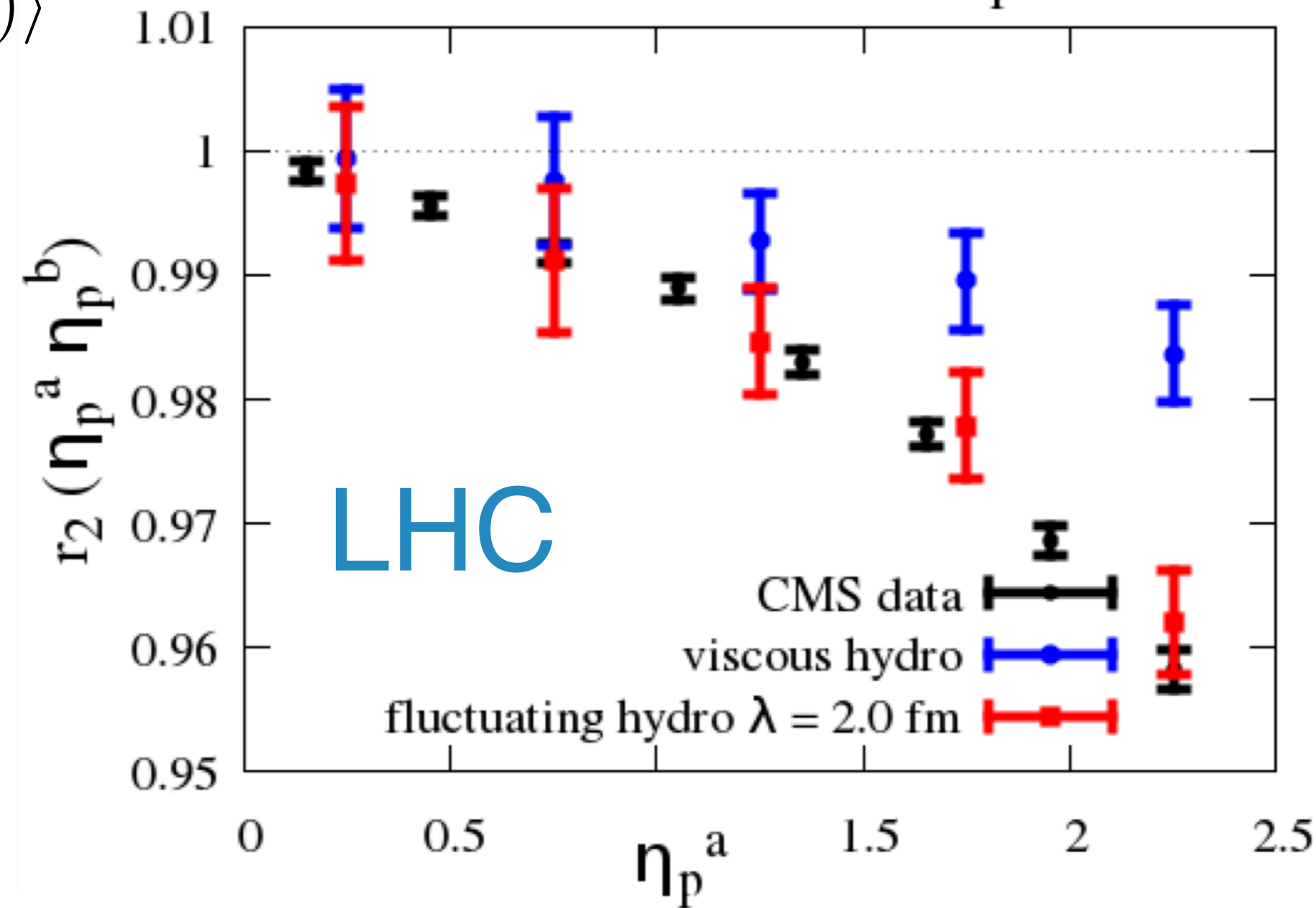
$$r_2(\eta, \eta_{\text{ref}}) = \frac{\langle V_2(\eta) \cdot V_2^*(\eta_{\text{ref}}) \rangle}{\langle V_2(-\eta) \cdot V_2^*(\eta_{\text{ref}}) \rangle}$$



@ P. Bozek

A. Sakai, K. Murase and T. Hirano,
arXiv:2003.13496 [nucl-th]

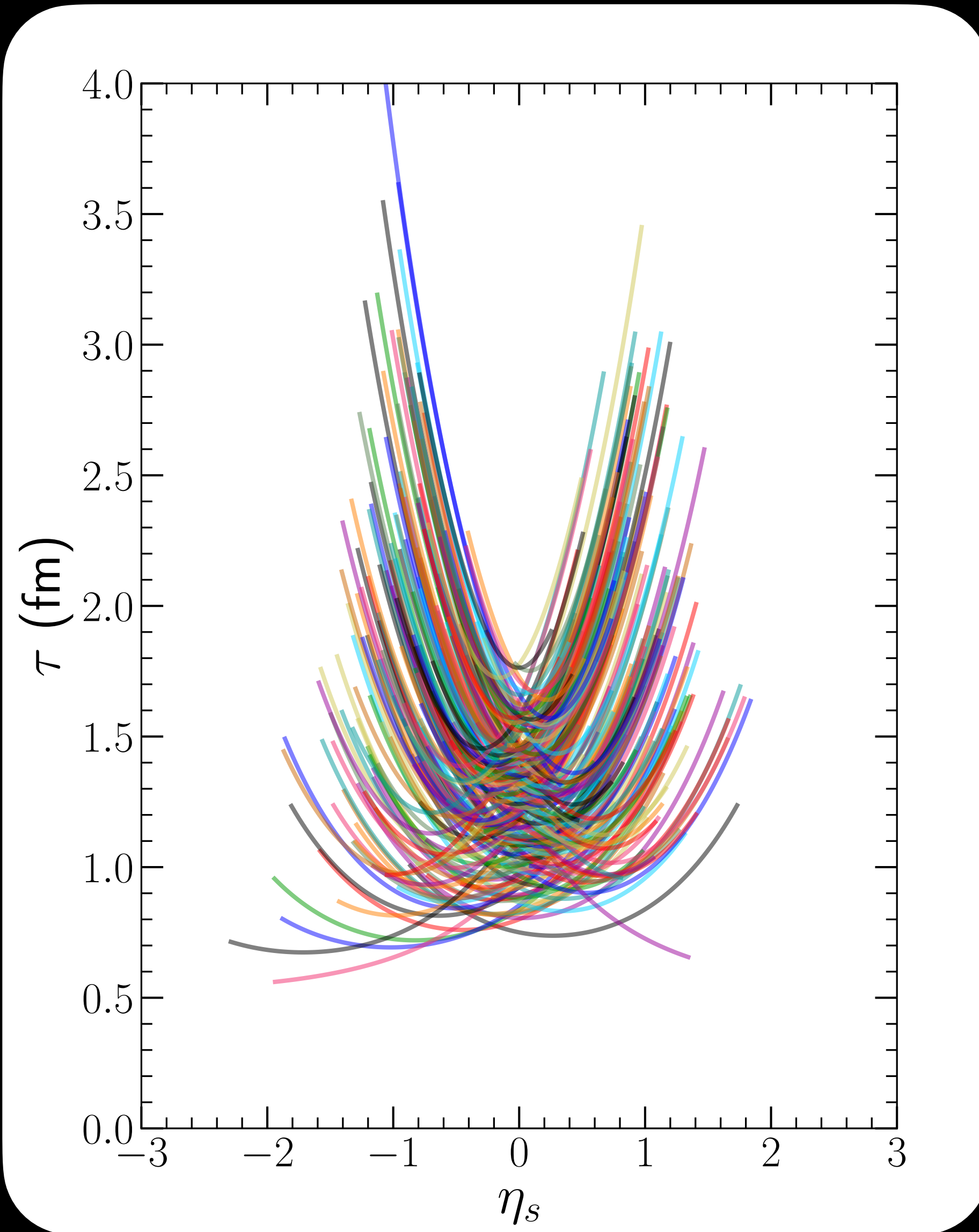
PbPb 20-30% $3.0 < \eta_p^b < 4.0$



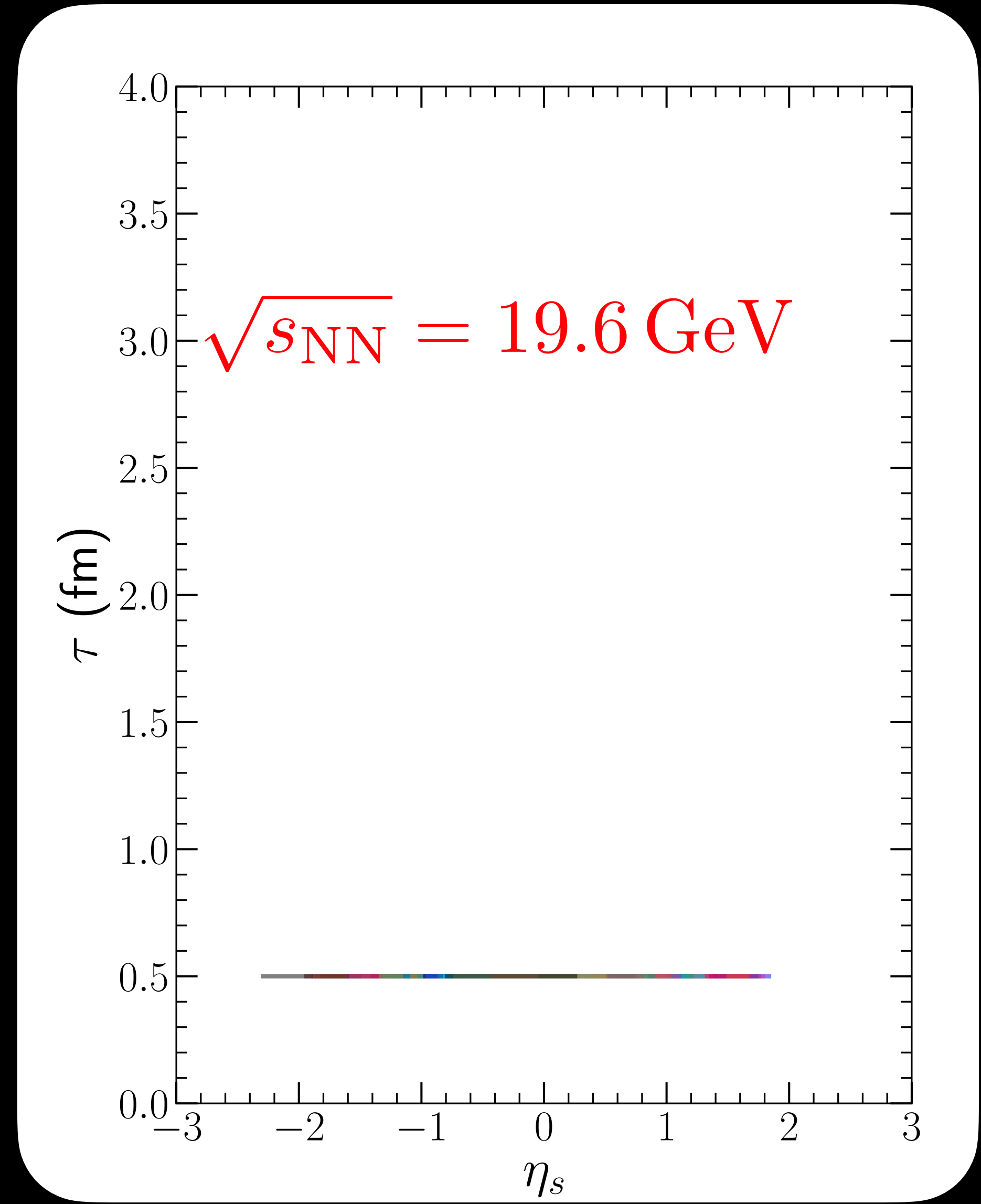
- Longitudinal flow decorrelation encodes the dynamical evolution of rapidity and thermal fluctuations

Strong constraining power on longitudinal dynamics

EARLY TIME DYNAMICS AT THE RHIC BES

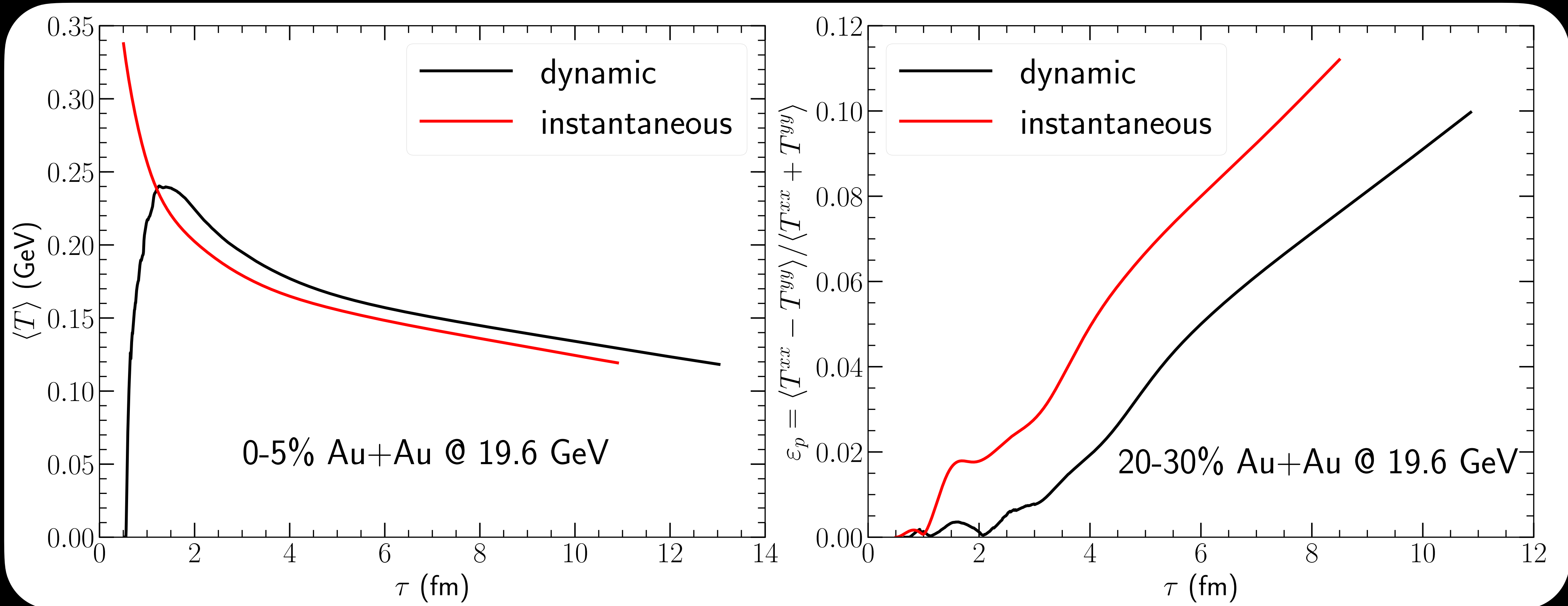


vs.



TRANSVERSE DYNAMICS WITH SOURCES

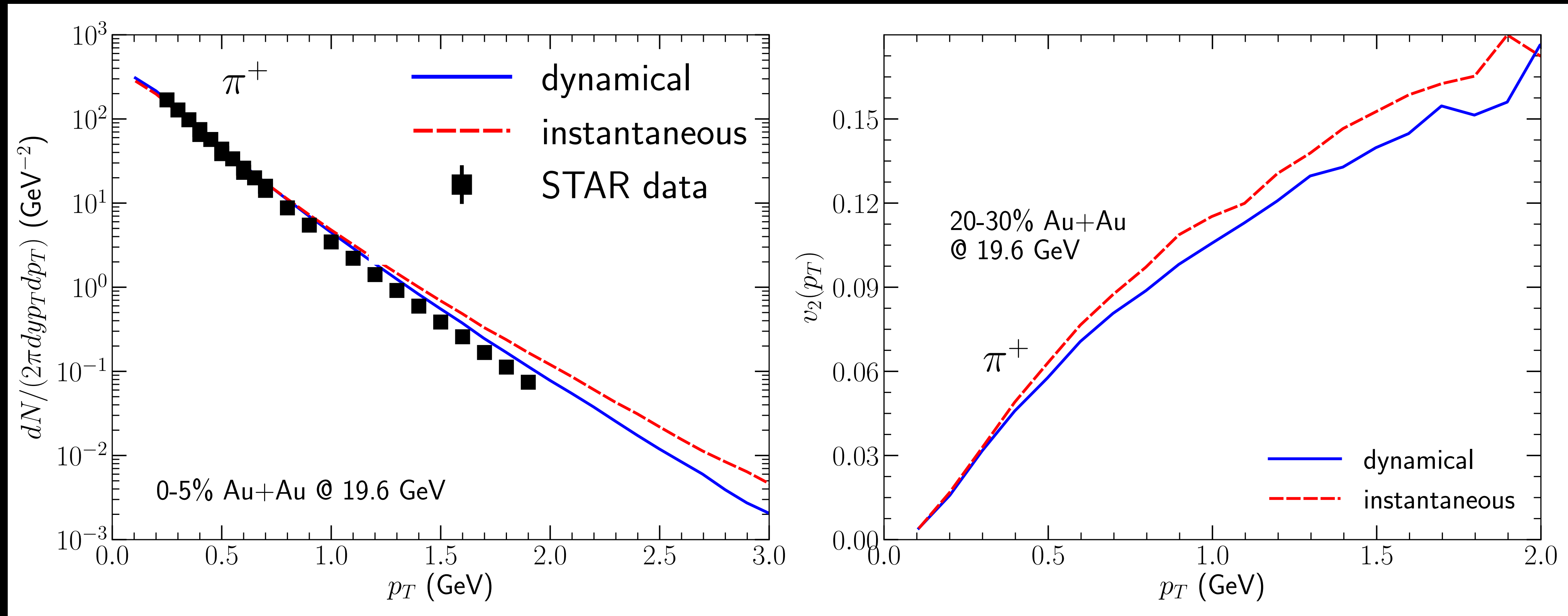
C. Shen and B. Schenke, Nucl. Phys. A 982, 411-414 (2019)



- Fireball lives ~ 2 fm longer with dynamical initialization compared to the instantaneous setup
- Hydrodynamic flow and its anisotropy develop slower with dynamical sources

DYNAMICAL VS INSTANTANEOUS INITIALIZATION

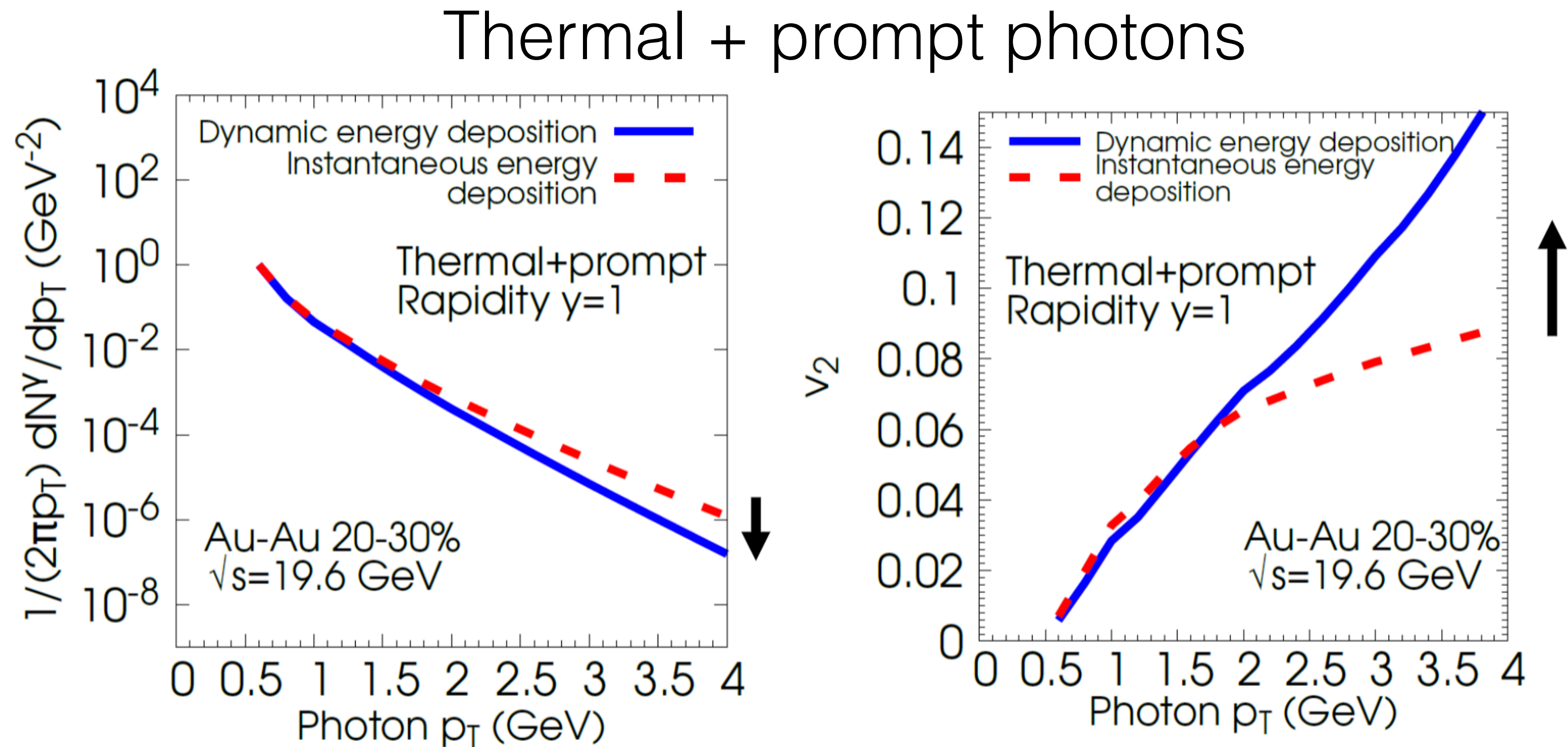
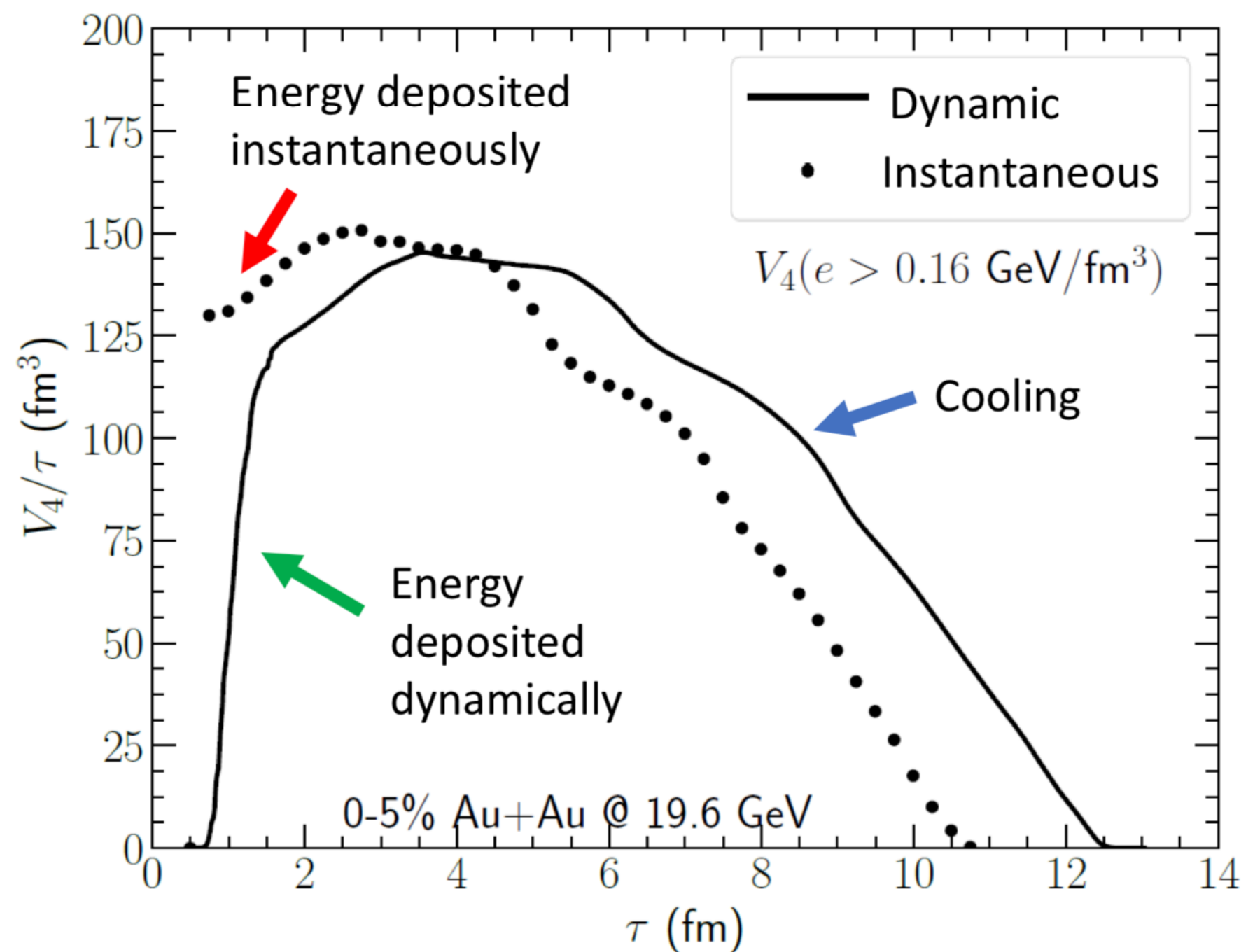
C. Shen and B. Schenke, Nucl. Phys. A 982, 411-414 (2019)



- Dynamical initialization results steeper particle spectra and smaller $v_2(p_T)$
5-10% less radial and elliptic flow

DYNAMICAL INITIALIZATION EFFECT ON EM PROBES

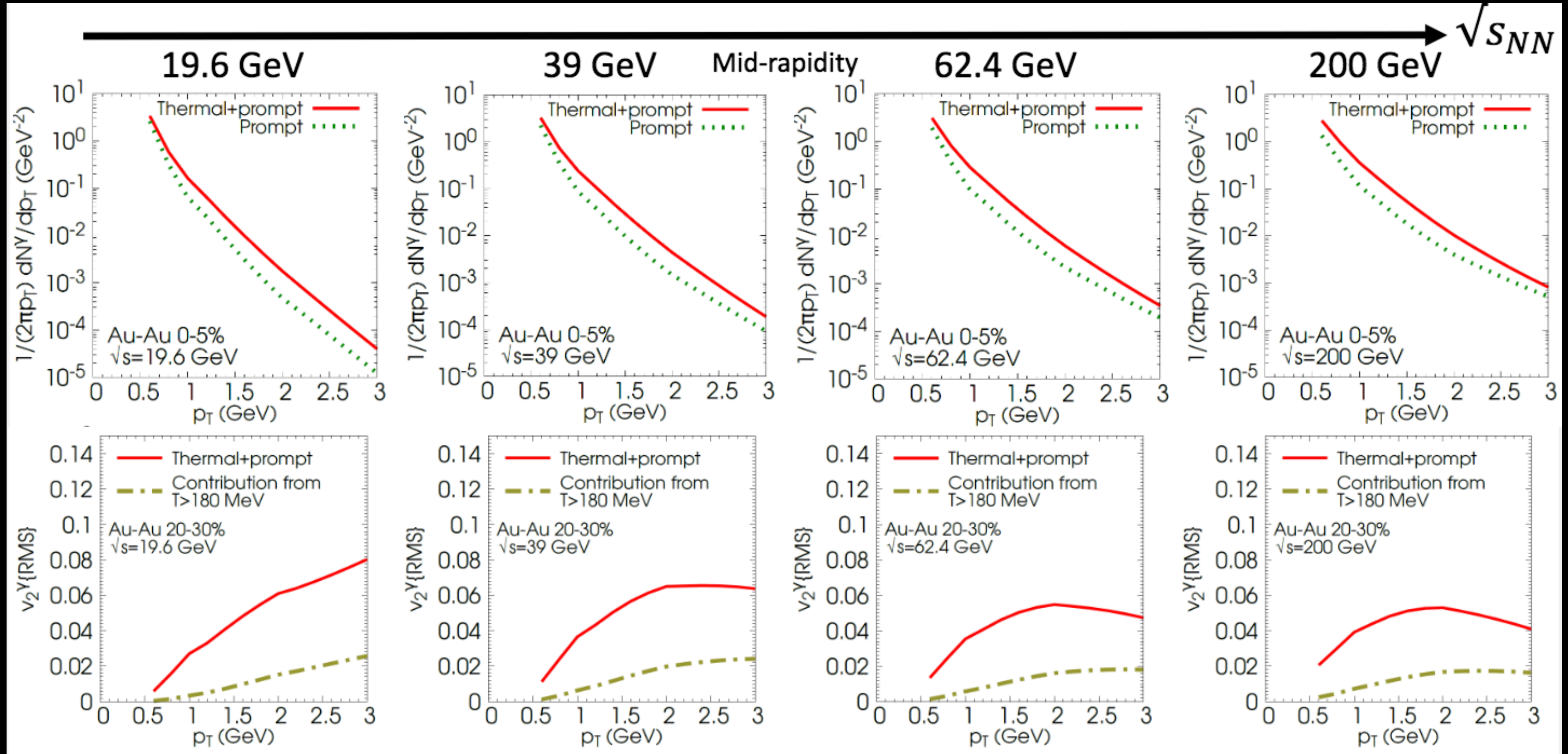
C. Gale, S. Jeon, S. McDonald, J.F. Paquet and C. Shen, Nucl. Phys. A982 (2019) 767-770



- Dynamical initialization results in large direct photon v_2 at high p_T
- EM probes show a large sensitivity to the early time dynamics**

EM TOMOGRAPHY AT RHIC BES ENERGIES

C. Gale, S. Jeon, S. McDonald, J.F. Paquet and C. Shen, Nucl. Phys. A982 (2019) 767-770



Photons are *unique* soft penetrating probes to early time dynamics

ACCESSING NEW QGP TRANSPORT PROPERTY

G. Denicol, C. Gale, S. Jeon, A. Monnai, B. Schenke and C. Shen, Phys. Rev. C98, 034916 (2018)
 L. Du and U. Heinz, arXiv:1906.11181 [nucl-th]
 M. Li and C. Shen, Phys. Rev. C 98, 064908 (2018)



$$T^{\mu\nu} = e u^\mu u^\nu - (P + \Pi) \Delta^{\mu\nu} + \pi^{\mu\nu}$$

$$J^\mu = n u^\mu + q^\mu$$

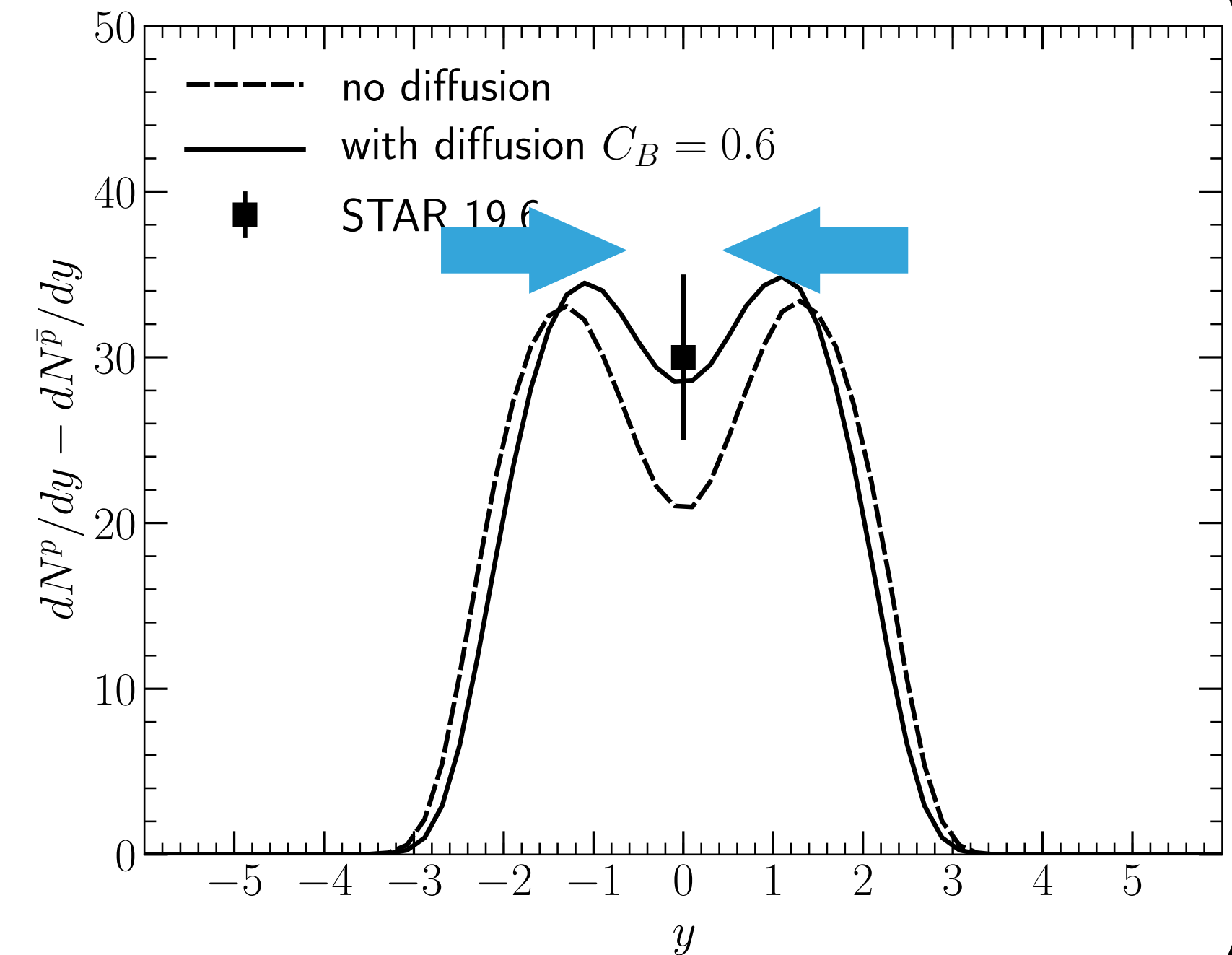
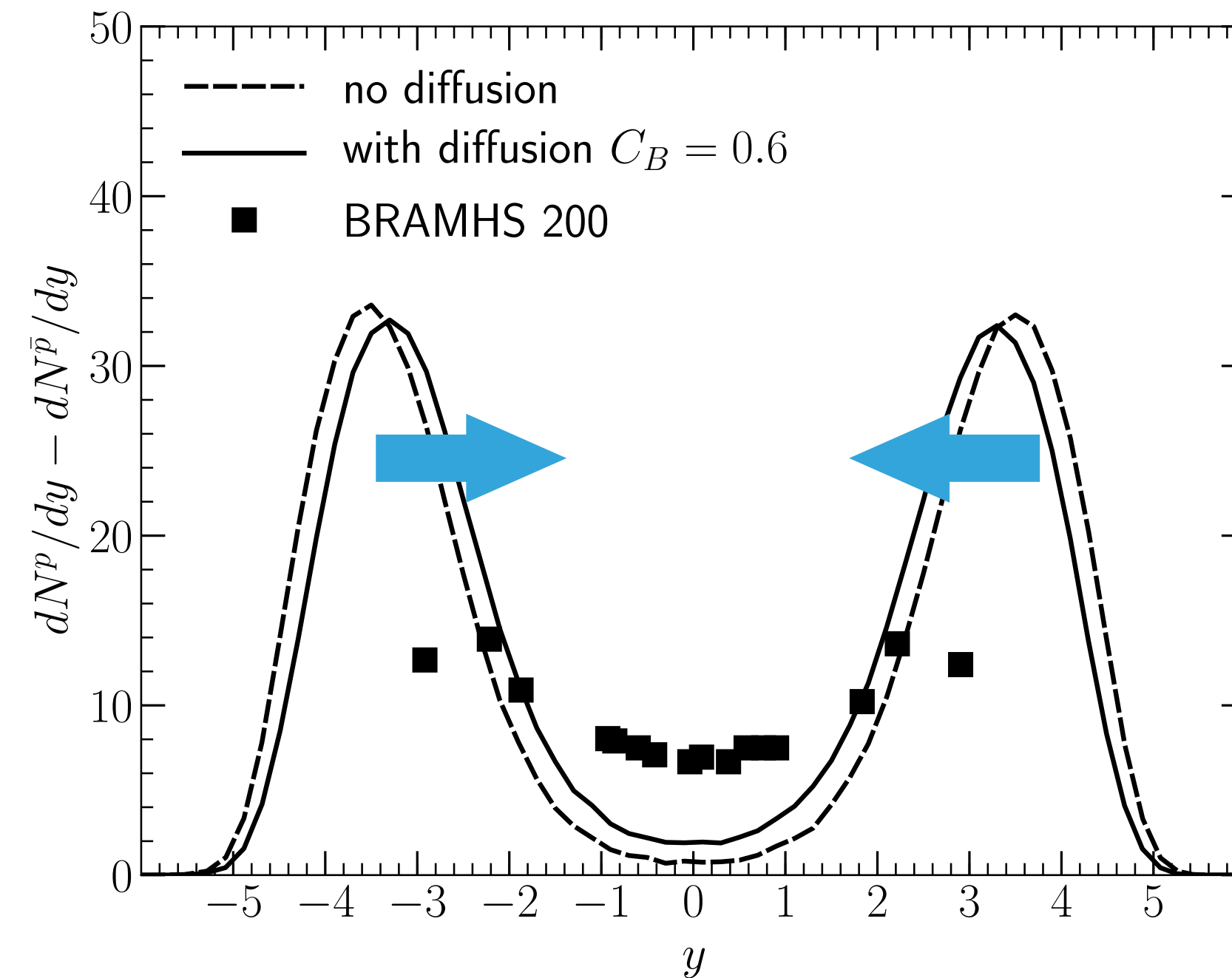
$$\begin{aligned} \partial_\mu T^{\mu\nu} &= 0 \\ \partial_\mu J^\mu &= 0 \end{aligned} \quad + \quad P(e, n)$$

$$\pi^{\mu\nu} \sim 2\eta \nabla^{\langle\mu} u^{\nu\rangle} \quad \Pi \sim -\zeta \partial_\mu u^\mu \quad q^\mu \sim \kappa \nabla^\mu \frac{\mu}{T}$$

- The charge diffusion current q^μ characterizes how conserved charges diffuse in and out of fluid cells
- The κ is the QGP charge diffusion coefficient [matrix]

ACCESSING NEW QGP TRANSPORT PROPERTY

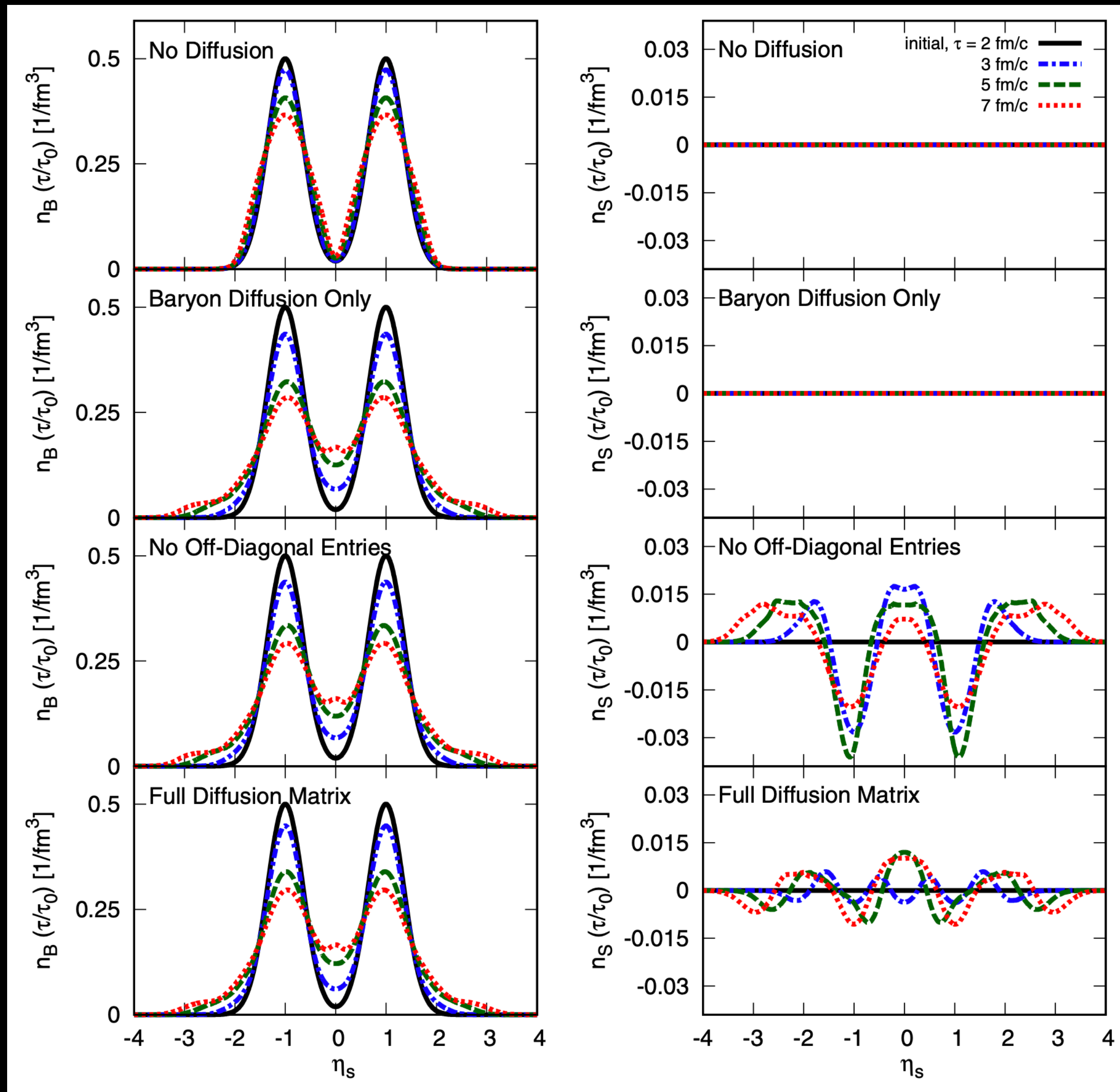
G. Denicol, C. Gale, S. Jeon, A. Monnai, B. Schenke and C. Shen, Phys. Rev. C98, 034916 (2018)
L. Du and U. Heinz, arXiv:1906.11181 [nucl-th]
M. Li and C. Shen, Phys. Rev. C 98, 064908 (2018)



- The net baryon diffusion current is driven by $\nabla^\mu \frac{\mu_B}{T}$; It transports more baryon charges to the mid-rapidity region

ACCESSING NEW QGP TRANSPORT PROPERTY

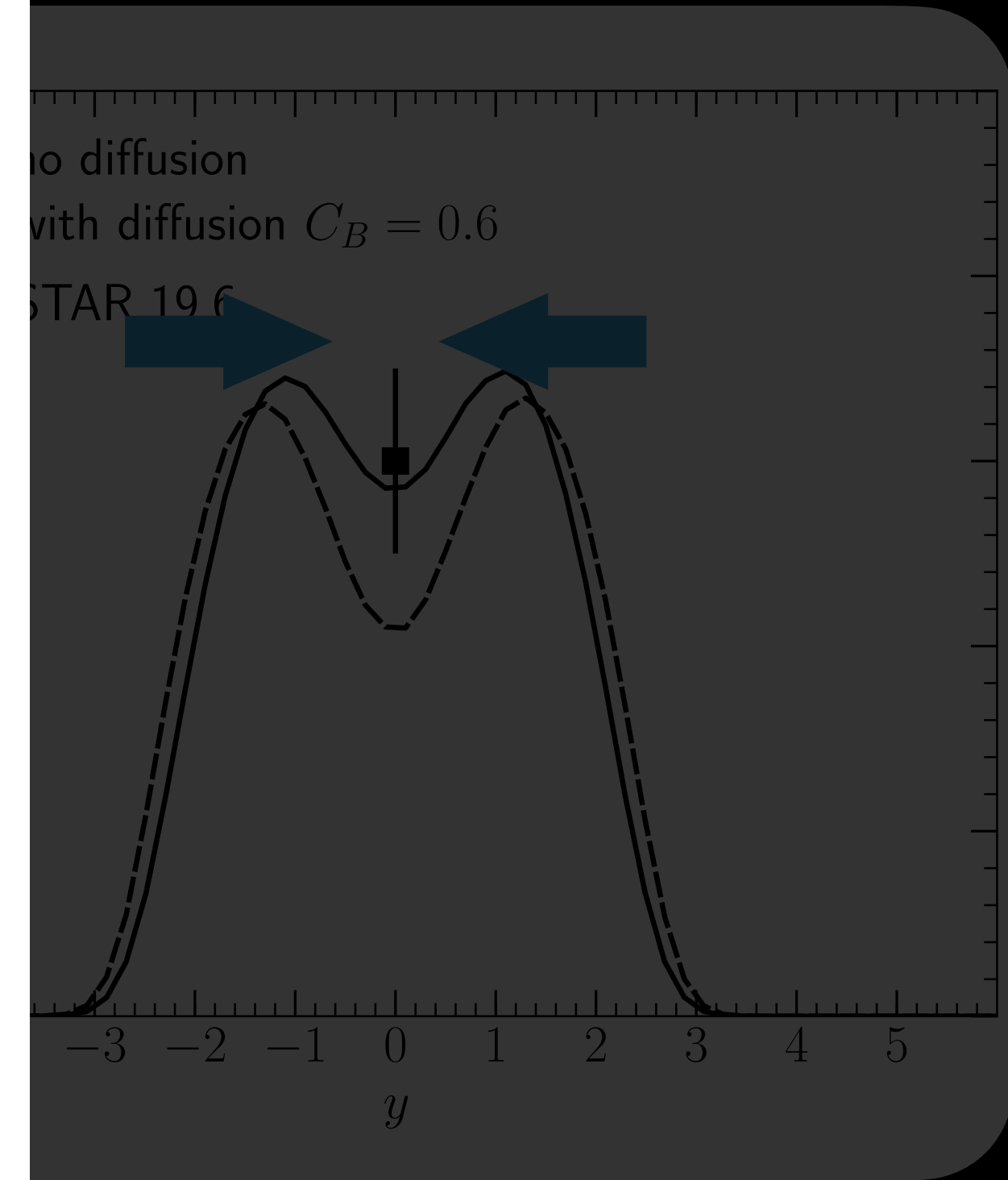
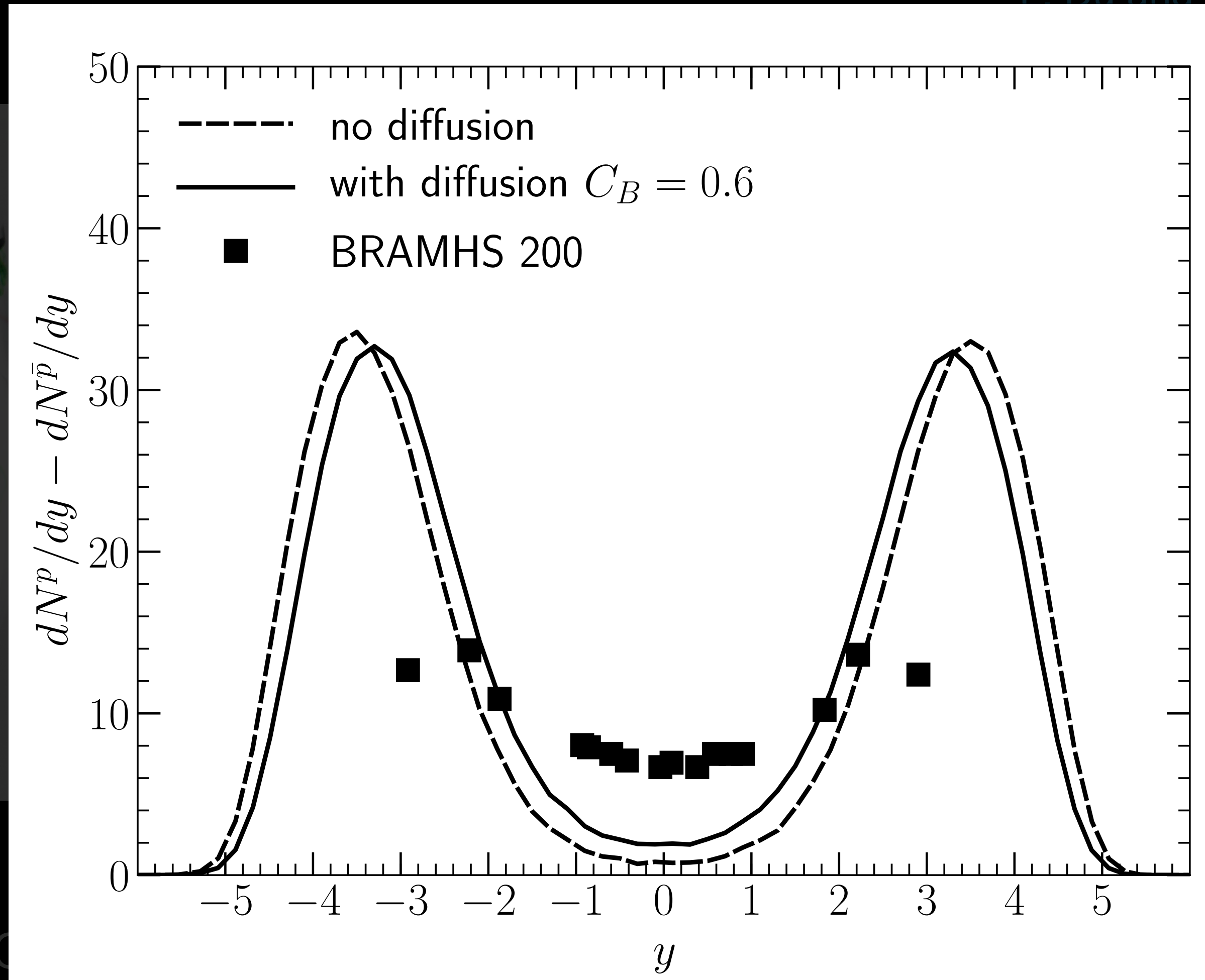
J. A. Fotakis, M. Greif, C. Greiner, G. S. Denicol, and H. Niemi,
 Phys. Rev. D 101, 076007 (2020)



- Heavy-ion collisions have at least three types conserved charges (B, Q, S)
- Their diffusion processes are mixed with each others
- For $n_S = 0$, the baryon diffusion dominates the evolution of the net baryon current
- The baryon diffusion can cross feed to the evolution of the net strangeness current

ACCESSING NEW QGP TRANSPORT PROPERTY

G. Denicol, C. Gale, S. Jeon, A. Monnai, B. Schenke and C. Shen, Phys. Rev. C98, 034916 (2018)
L. Du and U. Heinz, arXiv:1906.11181 [nucl-th]
S. Jeon, Phys. Rev. C 98, 064908 (2018)



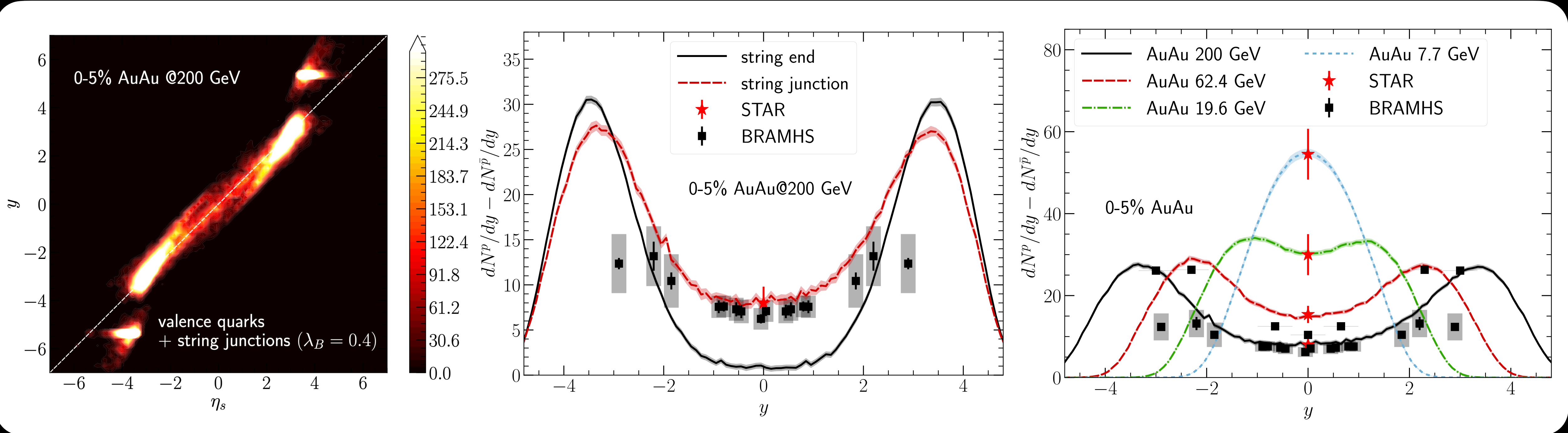
• Net charge diffusion
rapidity region

es to the mid-

Not enough in high energy collisions

INITIAL STATE BARYON STOPPING

C. Shen and B. Schenke, in preparation



- Allowing the initial baryon charges to fluctuate to string junctions improves description at high collision energies

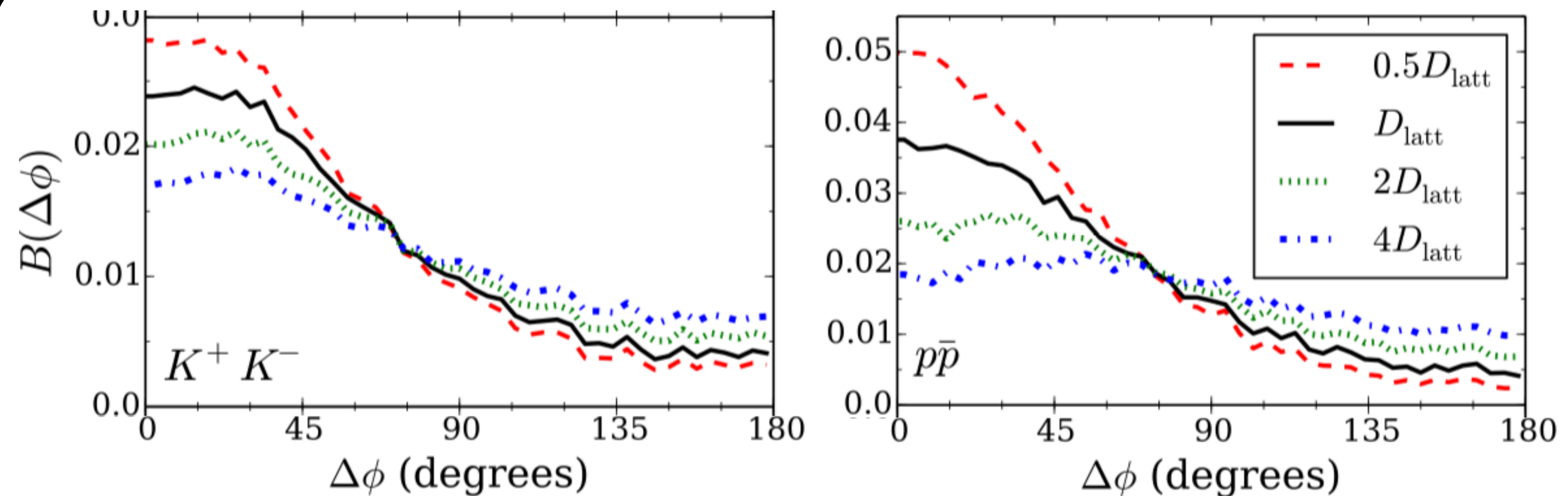
D. Kharzeev, Phys. Lett. B 378, 238 (1996)

Interplay between baryon diffusion and initial fluctuations

ACCESSING NEW QGP TRANSPORT PROPERTY

J. Kapusta and C. Plumberg, Phys. Rev. C97, 014906 (2018)

S. Pratt and C. Plumberg, arXiv:1904.11459 [nucl-th]



- A larger diffusion constant diffuse the charge pair more away from each other — widened the charge balance function in the azimuthal direction

An independent observable to constrain charge diffusion

SUMMARY

- Relativistic heavy-ion collisions over 3 orders of magnitude in collision energy map out the phase structure of hot QCD matter
 - Search for a critical point and the first-order phase transition
 - Build connections with neutron star/black hole mergers
- Full 3D hybrid framework starts to quantitatively describe bulk observables at the RHIC BES program
 - First principle inputs from **lattice QCD**
 - Elucidating the **initial baryon stopping**, **charge diffusion**, and **collectivity** of QGP in a baryon rich environment
 - Consistent 3D dynamical descriptions of pp, pA, and AA collisions